University of California Transportation Center
UCTC Dissertation UCTC-DISS-2011-03

Reliable GPS Integer Ambiguity Resolution

Anning Chen
University of California, Riverside
2011

UNIVERSITY OF CALIFORNIA
RIVERSIDE

Reliable GPS Integer Ambiguity Resolution

A Dissertation submitted in partial satisfaction
of the requirements for the degree of

Doctor of Philosophy

in

Electrical Engineering

by

Anning Chen

June 2011

Dissertation Committee:

Dr. Jay A. Farrell , Chairperson
Dr. Matthew J. Barth
Dr. Christian R. Shelton

The Dissertation of Anning Chen is approved:

Committee Chairperson

University of California, Riverside

Acknowledgments

First and foremost, I would like to express my thanks to Prof. Jay A. Farrell for his utmost guidance, support, encouragement, and patience during my journey towards a Ph.D. Professor Farrell helped me tremendously from the first day I joined his research group. He taught me much more than his extensive knowledge, but also enthusiasm and rigorous attitude towards research. I will be forever grateful, thankful, and honored for all the valuable learning and advices he has given me.

I would like to thank my dissertation committee members, Professor Matthew Barth and Professor Christian Shelton, for their helpful suggestions and comments for making this dissertation better. I'm honored to have chances working with Professor Barth on many cooperative projects. His superior talent of system-level thinking helps me a lot in my research. I'm grateful to Professor Christian Shelton's sharp insight and helpful suggestions during my oral proposal exam which helped me to make this dissertation better.

I am grateful to other professors that I met in the University of California, Riverside, especially Professor Anastasios Mourikis, Professor Gerardo Beni, Professor Ertem Tuncel and Professor Jie Chen, for the fabulous courses they offered. Knowledge I learned in those classes well prepared me working on my Ph.D. research and this dissertation.

I would like to give my appreciation to my coworkers Arvind Ramanandan, Anh Vu, Dongfang Zheng, Behlul Sutarwala, Sarath Suvanah and Sheng Zhao, for all the help, suggestions and discussions I got during our cooperative work on several research projects. I am happy to have worked with Arvind Ramanandan for the past five years. His enthusiasm towards research, sense of humor were great encouragements to me in our darkest days

working on the projects. Our tough experience working on the projects will always be beneficial to me.

I am indebt to the former students work on the GPS/INS project, namely Dr. Yunchun Yang, Dr. Jingrong Cheng and Dr. Yu Lu, for making a nice starting platform for us to work on, and for their continuous suggestions and help during us working on this project.

I would also like to thank the former and current student members at the Control and Robotic lab, including Dr. Yuanyuan Zhao, Dr. Wenjie Dong, Dr. Yiqian Li, Dr. Vladmir Djapic, Akshay Morye, Yiming Chen, Mingyang Li, Haiyu Zhang, Tue Cuong (Kenny) Dong Si, Rathavut (Biggie) Vanitsthian, Jeffe Herrera, and Ajurn Prabhakaran, for making the lab a wonderful and memorable place to learn and work.

Finally, thanks to my husband, my parents and my son, for their endless and unconditional love, encouragement and support that they have always given me. Their supports are essential to my research study and finally finishing my dissertation. I dedicate this dissertation to them.

ABSTRACT OF THE DISSERTATION

Reliable GPS Integer Ambiguity Resolution

by

Anning Chen

Doctor of Philosophy, Graduate Program in Electrical Engineering
University of California, Riverside, June 2011
Dr. Jay A. Farrell , Chairperson

To operate, guide and control vehicles in low visibility conditions, it is critical that the states of the vehicle are accurately estimated, which includes the three dimensional position, velocity, and attitude. This can be accomplished by GPS (Global Positioning System) aided encoder or GPS aided inertial approaches. The overall positioning accuracy of either approach will be determined by the GPS performance. Real-time centimeter accuracy GPS positioning can be achieved using carrier phase measurements. This requires fast and reliable on-the-fly integer ambiguity resolution.

In this dissertation, we focus on resolving GPS ambiguity problem, including both integer ambiguity estimation and integer ambiguity validation. For integer ambiguity estimation, a brief overview of pervious work on integer ambiguity resolution is first presented. Then, an improved integer ambiguity resolution method is proposed. Subsequently, simulations and real-world data are presented to demonstrate the effectiveness of the method. We also present integer ambiguity algorithms with auxiliary measurements and algorithms with multiple epoch measurements, both of which are useful in GPS challenging areas. For integer ambiguity validation, a brief overview is first presented, and then analytic discussion

and test results on several popular validations methods are studied. Finally we discuss GPS modernization and its effect on integer estimation and validation.

Contents

List of Figures

List of Tables

Chapter 1

Introduction

1.1 Motivation

To operate, guide and control vehicles in low visibility conditions, it is critical that the states of the vehicle are accurately estimated, which includes the three dimensional position, velocity, and attitude. This can be accomplished by GPS (Global Positioning System) aided encoder or GPS aided inertial approaches [14]. The overall positioning accuracy of either approach is determined by the GPS performance.

The GPS is based on time-of-arrival ranging. The GPS offers two kinds of signals that can be used to estimate antenna position: code measurement, which is also referred to as pseudorange, and the carrier phase measurement. The pseudorange is calculated from the apparent transit time of the signal from a satellite to the receiver, which is determined by the receiver clock and the transmission time at the satellite marked in the signal code. This measurement is biased due to the fact that the satellite and receiver clocks are not synchronized, and therefore is referred as pseudorange.

A measurement much more precise than that of code is the phase of the carrier received from a satellite, which is the difference between the phase of the receiver-generated carrier signal and the carrier received from a satellite at the instant of the measurement. In case that a satellite is locked-on, the receiver will measure the initial fractional phase difference between the received and receiver-generated signals and from then on tracks the change in this measurement counting full carrier cycles and keeping track of the fractional cycle at each epoch. It does not require the actual information being transmitted, but the fractional part phase of the carrier signal. As long as the connection between the receiver and the satellite is not broken, the number of full carrier cycles remains constant while the fractional beat phase changes over time. The loss of signal lock between a GPS satellite and the receiver is referred to as "cycle slip". If the signal lock is re-established, a new ambiguity will exist and must be solved for separately from the original ambiguity. In carrier phase measurement, the number of full carrier cycles is typically not known and varies for every receiver-satellite combination. Because of its ambiguous nature, this number of full carrier cycles is referred to as the integer ambiguity and need to be estimated before we can use carrier phase measurement for position estimate.

By using different kind of GPS signals, GPS can work in three modes: for civilian non-differential GPS, the position estimation accuracy will be in the order of 10 meters; with differential GPS (DGPS), which will be introduced in Chapter 2, the positioning accuracy will be of few meters; and for carrier phase DGPS (CPDGPS), the accuracy will be in the order of centimeters. This CPDGPS accuracy enables various lane level vehicle control and guidance applications. The comparison is shown in Fig. 1.1, in which : non-differential GPS is presented on the left, DGPS is presented in the center and CPDGPS is presented

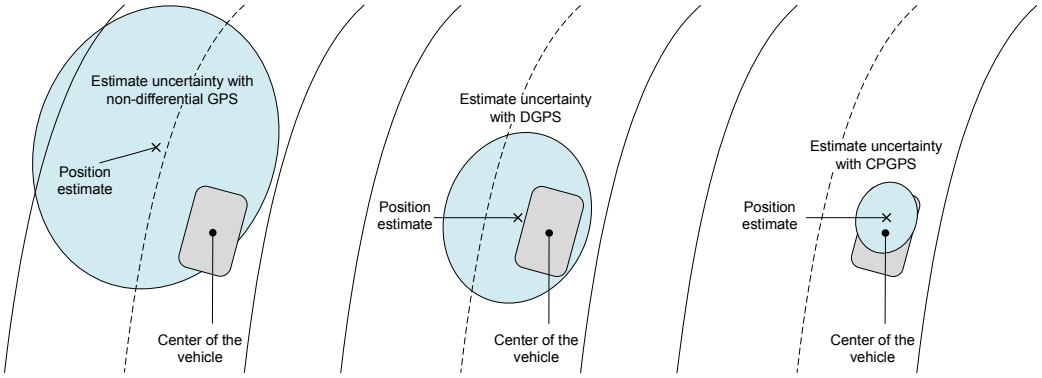

Figure 1.1: Position estimate uncertainty with different GPS modes.

on the right. In each subplot, the gray box represents a vehicle in a lane, the 'x' represents the estimated vehicle center position, the ellipse represents the estimate uncertainty.

A key issue for CPDGPS is to solve the integer ambiguities in the GPS carrier phase measurements efficiently and reliably. Such solutions draw much interest both in theoretical study and practical implementation.

1.2 Thesis Outline

The thesis is organized as follows: In Chapter 2, we review the background of GPS carrier phase signals, propose the GPS integer ambiguity problem, review existing algorithms and introduce a new integer ambiguity estimation algorithm by combing the advantages of two of the leading algorithms, GPS integer ambiguity searching strategies are also discussed. In chapter 3, we study GPS integer ambiguity estimation algorithms with auxiliary measurements from INS, and in chapter 4, we investigate ambiguity estimation method by using GPS measurements from multiple epoches. In Chapter 5, GPS integer ambiguity validation problem is studied, various methods are reviewed and analytically discussed,

and the effect of GPS modernization, specifically, the launch of L5 signals, to GPS integer ambiguity validation problem is presented.

Chapter 2

Integer Ambiguity Resolution

2.1 GPS Measurements

2.1.1 Single GPS Measurements

The GPS code and carrier phase measurements for satellite i can be modeled as

$$\rho^{(i)} = R^{(i)} + c\delta t_r - c\delta t^{(i)} + I^{(i)} + T^{(i)} + E^{(i)} + MP^{(i)} + \epsilon^{(i)} \quad (2.1)$$

$$\lambda\phi^{(i)} = R^{(i)} + c\delta t_r - c\delta t^{(i)} - I^{(i)} + T^{(i)} + E^{(i)} + \lambda N^{(i)} + mp^{(i)} + \eta^{(i)} \quad (2.2)$$

where $R^{(i)} = \|\mathbf{p}^{(i)} - \mathbf{p}\|$ is the geometric distance between the satellite i position $\mathbf{p}^{(i)}$ and receiver antenna position $\mathbf{p}$. The symbol $c\delta t_r$ is the receiver clock bias and $c\delta t^{(i)}$ is the error caused by satellite clock error of satellite i. The symbol $I^{(i)}$ represents the ionospheric error of satellite i. The symbol $E^{(i)}$ represents the error caused by satellite ephemeris error. The symbol $T^{(i)}$ represents the tropospheric error of satellite i. The symbols $MP^{(i)}$ and $mp^{(i)}$ represents the error caused by multipath effects in the code and phase measurements. The symbols $\epsilon^{(i)}$ and $\eta^{(i)}$ represents the error caused by receiver noise in the code and phase

measurements. The symbol λ represents the signal wavelength. The symbol $N^{(i)}$ represents the unknown integer ambiguity to be determined. The index $i = 1, \cdots, K$, for K satellite measurements.

2.1.2 Differential GPS

Several of the error terms (satellite ephemeris error, satellite clock bias, ionospheric error and tropospheric error) in Eqns. (2.1) and (2.2), referred as common mode errors, are highly spatially correlated. Therefore, if we have a base station at known position $\mathbf{p}_b$, then the errors can be estimated and broadcast to other roving receivers in the local area (at the range of about 20 miles). By doing this, the GPS positioning accuracy at each of these roving receivers could be highly improved.

The ideal correction for code and phase measurements would be

$$C_\rho^{(i)} = -\left(-c\delta t^{(i)} + I^{(i)} + T^{(i)} + E^{(i)}\right) \tag{2.3}$$

$$C_\phi^{(i)} = -\left(-c\delta t^{(i)} - I^{(i)} + T^{(i)} + E^{(i)}\right)\frac{1}{\lambda} \tag{2.4}$$

We should note that the multipath and receiver noise directly affect the computed corrections. The corrections will also be affected by the residual of ionospheric error and tropospheric error between the base and roving receivers. Assume the code and phase measurements of the base station are $\rho_b^{(i)}$ and $\lambda\phi_b^{(i)}$, respectively, then the common mode

errors estimated as

$$\begin{aligned}
\hat{C}_{\rho}^{(i)} &= R_b^{(i)} + c\delta\hat{t}_b^{(i)} - \rho_b^{(i)} \\
&= -\left(-c\delta t^{(i)} + I_b^{(i)} + T_b^{(i)} + E^{(i)}\right) - c\delta\tilde{t}_b^{(i)} - MP_b^{(i)} - \epsilon_b^{(i)}, \qquad (2.5) \\
\hat{C}_{\phi}^{(i)} &= \frac{1}{\lambda}\left(R_b^{(i)} + c\delta\hat{t}_b^{(i)} + \lambda N_b^{(i)}\right) - \phi_b^{(i)} \\
&= -\left(-c\delta t^{(i)} - I_b^{(i)} + T_b^{(i)} + E^{(i)}\right) - c\delta\tilde{t}_b^{(i)} - mp_b^{(i)} - \eta_b^{(i)}, \qquad (2.6)
\end{aligned}$$

where $R_b^{(i)} = \|\mathbf{p}^{(i)} - \mathbf{p}_b\|$ is the geometric distance between the satellite i position $\mathbf{p}^{(i)}$ and receiver antenna position $\mathbf{p}$. The symbol $c\delta\hat{t}_b^{(i)}$ denotes an estimate of the base receiver bias. The symbol $I_b^{(i)}$ represents the ionospheric error of satellite i at the base. The symbol $T_b^{(i)}$ represents the tropospheric error at the base. The symbol $c\delta\tilde{t}_b^{(i)} = c\delta t_b^{(i)} - c\delta\hat{t}_b^{(i)}$ represents the residual of the base receiver clock bias. The symbol $N_b^{(i)}$ represents the integer ambiguity at the base. The symbol $MP^{(i)}$ and $mp^{(i)}$ represents the error caused by multipath effects in the code and phase measurements at the base. The symbols $\epsilon_b^{(i)}$ and $\eta_b^{(i)}$ represents the error caused by the base receiver noise in the code and phase measurements.

The differential GPS measurement is computed as

$$\begin{aligned}
\Delta\rho^{(i)} &= \rho^{(i)} + C_{\rho}^{(i)} \\
&= R^{(i)} + c\delta t_r - c\delta\tilde{t}_b^{(i)} + \delta I^{(i)} + \delta T^{(i)} + MP^{(i)} + \epsilon^{(i)} + MP_b^{(i)} + \epsilon_b^{(i)} \\
&= R^{(i)} + c\delta\bar{t}_r + \bar{\epsilon}^{(i)}, \qquad (2.7) \\
\lambda\Delta\phi^{(i)} &= \lambda\left(\phi^{(i)} + C_{\phi}^{(i)}\right) \\
&= R^{(i)} + c\delta t_r - c\delta\tilde{t}_b^{(i)} - \delta I^{(i)} + \delta T^{(i)} + \lambda N^{(i)} + mp^{(i)} + \eta^{(i)} + mp_b^{(i)} + \eta_b^{(i)} \\
&= R^{(i)} + c\delta\bar{t}_r + \lambda N^{(i)} + \bar{\eta}^{(i)} \qquad (2.8)
\end{aligned}$$

where $\delta I^{(i)} = I^{(i)} - I_b^{(i)}$, $\delta T^{(i)} = T^{(i)} - T_b^{(i)}$, $c\delta\bar{t}_r = c\delta t_r - c\delta\tilde{t}_b^{(i)}$, $\bar{\epsilon}^{(i)} = \delta I^{(i)} + \delta T^{(i)} + MP^{(i)} +$

$\epsilon^{(i)} + MP_b^{(i)} + \epsilon_b^{(i)}$ and $\bar{\eta}^{(i)} = -\delta I^{(i)} + \delta T^{(i)} + \lambda N^{(i)} + mp^{(i)} + \eta^{(i)} + mp_b^{(i)} + \eta_b^{(i)}$. Throughout the thesis, $\delta I^{(i)}$ and $\delta T^{(i)}$ are assumed to be small enough so that they can be neglected.

2.1.3 Residual Measurements

This thesis will work with residual measurements computed relative to a position $\mathbf{p}_0$ which is assumed to be sufficiently accurate to the roving receiver so that the high order terms (i.e., *h.o.t*s) are neglectable after linearization. The residual measurements are

$$\delta\Delta\rho^{(i)} = \Delta\rho^{(i)} - \|\mathbf{p}^{(i)} - \mathbf{p}_0\| \tag{2.9}$$

$$\lambda\delta\Delta\phi^{(i)} = \lambda\Delta\phi^{(i)} - \|\mathbf{p}^{(i)} - \mathbf{p}_0\|. \tag{2.10}$$

The linearized residual measurements are modeled as

$$\delta\Delta\rho^{(i)} = h^{(i)}\delta\mathbf{p} + c\delta\bar{t}_r + \bar{\epsilon}^{(i)} \tag{2.11}$$

$$\lambda\delta\Delta\phi^{(i)} = h^{(i)}\delta\mathbf{p} + c\delta\bar{t}_r + \lambda N^{(i)} + \bar{\eta}^{(i)} \tag{2.12}$$

where $\delta\mathbf{p} = (\mathbf{p} - \mathbf{p}_0)^\top \in \mathbb{R}^3$ and $h^{(i)} = \frac{\mathbf{p}-\mathbf{p}_0}{\|\mathbf{p}-\mathbf{p}_0\|} \in \mathbb{R}^3$. We assume that $\bar{\epsilon}^{(i)} \sim \mathcal{N}\left(0, \sigma_{\rho_i}^2\right)$ and $\bar{\eta}^{(i)} \sim \mathcal{N}\left(0, \sigma_{\Phi_i}^2\right)$. In typical GPS applications, the magnitude of σ_{ρ_i} is in the order of meters and the magnitude of σ_{Φ_i} is in the order of centimeters. All the noise terms are uncorrelated with each other.

Assuming that there are K satellites in view, the phase residual measurements from these K satellites can be put in matrix form as

$$\lambda\delta\Delta\boldsymbol{\phi} = \mathbf{H}\mathbf{x} + \lambda\mathbf{N} + \bar{\boldsymbol{\eta}} \tag{2.13}$$

where $\delta\Delta\boldsymbol{\phi} = \begin{bmatrix} \delta\Delta\phi^{(1)} & \dots & \delta\Delta\phi^{(K)} \end{bmatrix}^\top \in \mathbb{R}^K$, $\mathbf{x} = \begin{bmatrix} \delta\mathbf{p}^\top & c\delta\bar{t}_r \end{bmatrix}^\top \in \mathbb{R}^n$, $n = 4$, $\mathbf{H} = \begin{bmatrix} h^{(1)} & 1 \\ \vdots & \vdots \\ h^{(K)} & 1 \end{bmatrix} \in \mathbb{R}^{K\times n}$, $\bar{\boldsymbol{\eta}} = \begin{bmatrix} \bar{\eta}^{(1)} & \dots & \bar{\eta}^{(K)} \end{bmatrix}^\top \in \mathbb{R}^K$, and $\mathbf{N} = \begin{bmatrix} N^{(1)} & \dots & N^{(K)} \end{bmatrix}^\top \in \mathbb{Z}^K$ is the integer ambiguity vector that is to be determined.

2.2 Problem Proposition

Eqn. (2.13) can be rewritten as follows:

$$\mathbf{y} = \mathbf{G}\cdot\mathbf{x} + \mathbf{N} + \mathbf{v} \tag{2.14}$$

where $\mathbf{y} = \delta\Delta\boldsymbol{\phi}$ is the double differenced measurement, $\mathbf{G} = \lambda^{-1}\mathbf{H}$ is the observation matrix characterizing the satellite-user geometry and $\mathbf{v} = \bar{\boldsymbol{\eta}} \in \mathbb{R}^K$ is the vector of phase measurement errors. The covariance matrix of the measurement error is $\boldsymbol{\Sigma_{vv}} = cov(\bar{\boldsymbol{v}})$.

GPS integer ambiguity problem can be solved as a Maximum Likelihood (ML) estimation problem. That is, given GPS measurements, we would like to find the estimates of $\mathbf{N}$ and $\mathbf{x}$ that maximize the conditional probability $f(\mathbf{y}|\mathbf{N},\mathbf{x})$. This problem can be formulated as follows:

$$\begin{aligned}
\left(\hat{\mathbf{N}},\hat{\mathbf{x}}\right) &= \arg\max_{\mathbf{N}\in\mathbb{Z}^K,\mathbf{x}\in\mathbb{R}^n} f(\mathbf{y}|\mathbf{N},\mathbf{x}) \\
&= \arg\max_{\mathbf{N}\in\mathbb{Z}^K,\mathbf{x}\in\mathbb{R}^n} \ln f(\mathbf{y}|\mathbf{N},\mathbf{x}) \\
&= \arg\max_{\mathbf{N}\in\mathbb{Z}^K,\mathbf{x}\in\mathbb{R}^n} \ln\left(\frac{e^{-\frac{1}{2}(\mathbf{y}-\mathbf{G}\mathbf{x}-\mathbf{N})^T\boldsymbol{\Sigma}^{-1}(\mathbf{y}-\mathbf{G}\mathbf{x}-\mathbf{N})}}{(2\pi)^{K/2}\left|\boldsymbol{\Sigma_{vv}}\right|^{1/2}}\right) \\
&= \arg\min_{\mathbf{N}\in\mathbb{Z}^K,\mathbf{x}\in\mathbb{R}^n} (\mathbf{y}-\mathbf{G}\mathbf{x}-\mathbf{N})^T\boldsymbol{\Sigma}_{\boldsymbol{vv}}^{-1}(\mathbf{y}-\mathbf{G}\mathbf{x}-\mathbf{N}).
\end{aligned} \tag{2.15}$$

Therefore, the GPS integer ambiguity problem is also an Integer Weighted Least-Square

(IWLS) problem [33]. Our objective is to find $\mathbf{N} \in \mathbb{Z}^K$, $\mathbf{x} \in \mathbb{R}^K$ that minimize the cost function

$$\begin{aligned} c(\mathbf{x}, \mathbf{N}) &= \|\mathbf{y} - \mathbf{G} \cdot \mathbf{x} - \mathbf{N}\|^2_{\mathbf{\Sigma}_{vv}} \\ &= (\mathbf{y} - \mathbf{G}\mathbf{x} - \mathbf{N})^T \mathbf{\Sigma}_{\boldsymbol{vv}}^{-1} (\mathbf{y} - \mathbf{G}\mathbf{x} - \mathbf{N}). \end{aligned} \tag{2.16}$$

In practice, the determination of the integer vector N is usually separated into two steps: integer estimation and integer validation. In the remainder of this chapter, we will discuss integer estimation problem, in which we tend to find the best integer vector that minimize the cost function. The step of integer validation, which will be discussed in Chapter 5, we decide whether this estimate is acceptable or not.

2.3 Literature Review

The problem of GPS integer ambiguity estimation has drawn much interest both in theoretical study and practical implementation [26]. In the following, we review some of the leading algorithms.

2.3.1 LMS

One of the leading algorithms in integer ambiguity problem is LMS (Local Minima Search) [30], inspired by a very useful insight [20]: although Eqn. (2.14) contains $(K + n)$ unknown variables, there are only n degrees of freedom. Given any $\mathbf{x}$, all the integer ambiguities can be resolved; on the other hand, given any n integers, the states $\mathbf{x}$ can be computed accurately. These remarks show that not all combinations of integers are admissible and the challenge is to reformulate Eqn. (2.14) properly to find admissible integer

vectors efficiently.

The basic idea of LMS is to search only over the admissible combinations of integer candidates so that the searching space can be decreased. In LMS, the integer vector $\mathbf{N}$ is divided into two subvectors $\mathbf{N}_C$ and $\mathbf{N}_D$, where $\mathbf{N}_D$ contains n integers and $\mathbf{N}_C$ contains the remaining $(K-n)$ integers. The integers in $\mathbf{N}_D$ are searched exhaustively over some range of d integers and for each candidate of $\mathbf{N}_D$, the remaining integers are computed as real value estimates and are rounded to an optimally selected integer (described below) to get the estimate of $\mathbf{N}_C$. This yields d^n integer vectors in $\mathbb{Z}^K$. By evaluating the cost function for each integer vector candidate, LMS can select the best of the d^n integer vector candidates. The original LMS procedure of LMS is introduced in [30]. Alternative implementations are presented in [14, 29, 43].

LMS decreases the search dimension from K to n, which decreases the number of integer vector candidates from d^K to d^n. However, because the integer estimation error vector can be highly correlated, which renders that the level curves of the cost function are tilted and elongated hyper-ellipsoids, the rounding in the standard LMS approach may yield incorrect integer estimates and cause a significant cost increase.

2.3.2 LAMBDA

LAMBDA (Least-squares Ambiguity Decorrelation Adjustment) is designed to address the correlation of the integer estimate error vector. It is based on ideas from [17], and systematically developed the idea of decorrelation in a series of well cited papers [33, 35, 36]. In LAMBDA, an invertible, integer-to-integer transformation, denoted by Z, is derived such that the correlation matrix for the transformed integer vector is nearly diagonal.

In this circumstance, it has been proven that under certain conditions, the real-valued estimates from a least square solution can be rounded to achieve the optimal vector integer estimate [37]. However, computation of the decorrelation transformation Z involves an iterative process whose computational complexity grows exponentially with the integer vector dimension.

2.3.3 Lattice Theory and Integer Ambiguity Problem

In [19], GPS integer ambiguity problem (or integer parameter estimation problem in general) was interpreted as a "nearest lattice vector problem". The technique of LLL (Lenstra, Lenstra, and Lovász) algorithm [28], which is based on integer Gram-Schmidt orthogonalization, was brought into the field of integer parameter estimation for integer decorrelation. An algorithm was proposed use LLL algorithm for lattice base reduction and decorrelation so that the bases are "almost orthogonal" and the integer estimate can be rounded from float solutions.

The algorithm is suboptimal, but reduce the computation time from NP-hard [39] to polynomial time. In [42], it has been shown that the decorrelation technique in this algorithm equivalent to the concept of decorrelation proposed by Teunissen [34].

2.3.4 Others

In the history of research on GPS integer ambiguity problems, there has been a wide collection of literature discussing the problem from different point of views. Some of the widely used algorithms in the research history will be presented here.

Some of the early work focuses on linear combinations of measurements at different

frequencies [1], proper weighting of measurements from different satellites [9] and smoothing observations over time [25]. Based on smoothed measurements, the integers can be directly calculated from float estimation [1, 25], or the searching space can be reduced [6, 15].

Some other work, known as AFM (Ambiguity Function Method) [11] proposed an ambiguity function, the value of which was not affected by the whole-cycle changes so that the baseline can be accurately estimated without knowing the exact value of the integer ambiguity. This algorithm was later improved in [18].

In [17], GPS integer ambiguity estimation are formed as an integer programming problem. This method can be improved and leads to the LLL algorithm [28].

2.3.5 Summary

In early days, the research on integer ambiguity focuses on improving the computational efficiency of the searching process. Most of the algorithms proposed in early times are rarely used nowadays but of some historical interest.

In early 1990's, some significant progress was made in this area. With the improvement of modern computers, many algorithms proposed at that time computational sufficient enough for most practical applications. After that, trends of the research are switched onto the performance. LAMBDA [33, 35, 36] has been the leading algorithm in this area, and several variations are proposed [2, 22]. Some of the good reviews of different ambiguity estimation approaches can be found in [18, 21, 24, 26], and the references therein.

More recently, with the process of GPS modernization, people started to work on more challenging situations, like more reliable real-time result and long baseline applications. For these applications, multi-frequency measurements and the incorporation of other GNSS

sources (GALILIEO, GLONASS, COMPASS, etc.) are usually involved [23].

2.4 Improved Integer Ambiguity Resolution by Combining LMS and LAMBDA

In this section, we present a new integer ambiguity resolution method that combines the advantages of LMS and LAMBDA. The proposed method follows the idea of the LMS method to reduce the search space to get the float esitmate and employs the LAMBDA Z-transformation prior to rounding. In this manner, rounding achieves the optimal integer estimate derived from the float solution and the dimension of the Z transformation matrix is decreased from K to $(K-n)$ (e.g., from 7 to 4 in typical GPS applications).

Therefore, the proposed method has lower computation complexity compared to LAMBDA and higher success rate compared to LMS. The derivation of the method is presented as follow.

2.4.1 Generating Searching Candidates

Given Eqn. (2.14), for a given integer ambiguity $\mathbf{N}$, the weighted least square estimate of $\mathbf{x}$ would be:

$$\hat{\mathbf{x}} = \left(\mathbf{G}^T\boldsymbol{\Sigma}_{\boldsymbol{vv}}^{-1}\mathbf{G}\right)^{-1}\mathbf{G}^T\boldsymbol{\Sigma}_{\boldsymbol{vv}}^{-1}\left(\mathbf{y}-\mathbf{N}\right) \tag{2.17}$$

and the residual vector is

$$\begin{aligned}\hat{\boldsymbol{\varepsilon}} &= \mathbf{y} - \mathbf{G}\cdot\hat{\mathbf{x}} - \mathbf{N} \\ &= \left(\mathbf{I} - \mathbf{G}\left(\mathbf{G}^T\boldsymbol{\Sigma}_{\boldsymbol{vv}}^{-1}\mathbf{G}\right)^{-1}\mathbf{G}^T\boldsymbol{\Sigma}_{\boldsymbol{vv}}^{-1}\right)(\mathbf{y}-\mathbf{N}) \\ &= \mathbf{Q}_{\boldsymbol{\Sigma}}(\mathbf{y}-\mathbf{N}). \end{aligned} \tag{2.18}$$

where

$$\mathbf{Q}_{\boldsymbol{\Sigma}} = \mathbf{I} - \mathbf{P}_{\boldsymbol{\Sigma}}, \tag{2.19}$$

$$\mathbf{P}_{\boldsymbol{\Sigma}} = \mathbf{G}\left(\mathbf{G}^T\boldsymbol{\Sigma}_{\boldsymbol{vv}}^{-1}\mathbf{G}\right)^{-1}\mathbf{G}^T\boldsymbol{\Sigma}_{\boldsymbol{vv}}^{-1}. \tag{2.20}$$

Proposition 1 *Both $\boldsymbol{P}_{\boldsymbol{\Sigma}}$ and $\boldsymbol{Q}_{\boldsymbol{\Sigma}}$ are idempotent. Rank($\boldsymbol{P}$) = n, rank($\boldsymbol{Q}$) = (K − n).*

Proof. It is trivial to prove that

$$\begin{aligned}\mathbf{P}_{\boldsymbol{\Sigma}}\mathbf{P}_{\boldsymbol{\Sigma}} &= \mathbf{P}_{\boldsymbol{\Sigma}} \\ \mathbf{Q}_{\boldsymbol{\Sigma}}\mathbf{Q}_{\boldsymbol{\Sigma}} &= \mathbf{Q}_{\boldsymbol{\Sigma}}\end{aligned}$$

Thus, both $\mathbf{P}_{\boldsymbol{\Sigma}}$ and $\mathbf{Q}_{\boldsymbol{\Sigma}}$ are idempotent.

Because $\boldsymbol{\Sigma}_{\boldsymbol{vv}} > 0$ is a covariance matrix, $\boldsymbol{\Sigma}_{\boldsymbol{vv}}^{-1}$ is symmetric and positive definite. Thus, it can be factored as

$$\boldsymbol{\Sigma}_{\boldsymbol{vv}}^{-1} = \mathbf{W}^\top\mathbf{M}^\top\mathbf{M}\mathbf{W}, \tag{2.21}$$

and

$$\boldsymbol{\Sigma}_{\boldsymbol{vv}} = \mathbf{W}^\top\mathbf{M}^{-\top}\mathbf{M}^{-1}\mathbf{W}, \tag{2.22}$$

where $\mathbf{W} \in \mathbb{R}^{K\times K}$ is a unitary matrix (i.e., $\mathbf{W}\mathbf{W}^\top = \mathbf{W}^\top\mathbf{W} = \mathbf{I}$) and $\mathbf{M}^\top = \mathbf{M}$ is a diagonal matrix with positive elements on the diagonal. Substituting Eqn. (2.21) into

Eqn. (2.20), we have

$$\begin{aligned}
\mathbf{P}_{\mathbf{\Sigma}} &= \mathbf{G}(\mathbf{G}^\top \mathbf{\Sigma}_{vv}^{-1} \mathbf{G})^{-1} \mathbf{G}^\top \mathbf{\Sigma}_{vv}^{-1} \\
&= \mathbf{G}(\mathbf{G}^\top \mathbf{W}^\top \mathbf{M}^\top \mathbf{M}\mathbf{W}\mathbf{G})^{-1} \mathbf{G}^\top \mathbf{W}^\top \mathbf{M}^\top \mathbf{M}\mathbf{W} \\
&= \mathbf{G}(\mathbf{A}^\top \mathbf{A})^{-1} \mathbf{A}^\top \mathbf{M}\mathbf{W} \\
&= \mathbf{W}^\top \mathbf{M}^{-1} \mathbf{A}(\mathbf{A}^\top \mathbf{A})^{-1} \mathbf{A}^\top \mathbf{M}\mathbf{W} \\
&= \mathbf{W}^\top \mathbf{M}^{-1} \mathbf{P}\mathbf{M}\mathbf{W}, \qquad (2.23)
\end{aligned}$$

where $\mathbf{P} = \mathbf{A}(\mathbf{A}^\top \mathbf{A})^{-1} \mathbf{A}^\top$ and $\mathbf{A} = \mathbf{M}\mathbf{W}\mathbf{G}$. Eqn. (2.23) shows that $\mathbf{P}_{\mathbf{\Sigma}}$ is similar to $\mathbf{P}$ where $\mathbf{P}$ is a projection matrix onto the range of $\mathbf{A}$; therefore, $rank(\mathbf{P}) = rank(\mathbf{A})$. Because $\mathbf{M}$ and $\mathbf{W}$ are both nonsingular, $rank(\mathbf{A}) = rank(\mathbf{G}) = n$. Hence, $rank(\mathbf{P}_{\mathbf{\Sigma}}) = rank(\mathbf{P}) = n$.

Let $\mathbf{Q} = \mathbf{I} - \mathbf{P}$, then $\mathbf{Q}$ is a projection matrix onto the subspace orthogonal to the range space of $\mathbf{A}$, and has rank $(K - n)$. The following analysis shows that $\mathbf{Q}_{\mathbf{\Sigma}}$ is similar to $\mathbf{Q}$:

$$\begin{aligned}
\mathbf{Q}_{\mathbf{\Sigma}} &= \mathbf{I} - \mathbf{P}_{\mathbf{\Sigma}} \\
&= \mathbf{I} - \mathbf{W}^\top \mathbf{M}^{-1} \mathbf{P}\mathbf{M}\mathbf{W} \\
&= \mathbf{W}^\top \mathbf{M}^{-1} (\mathbf{I} - \mathbf{P})\mathbf{M}\mathbf{W} \\
&= \mathbf{W}^\top \mathbf{M}^{-1} \mathbf{Q}\mathbf{M}\mathbf{W}. \qquad (2.24)
\end{aligned}$$

Therefore, $\mathbf{Q}_{\mathbf{\Sigma}}$ also has rank $(K - n)$. ■

From Eqn. (2.16), the cost function evaluated from candidate $\mathbf{N}$ is

$$\begin{aligned} c(\mathbf{N}) &= \|\mathbf{y} - \mathbf{G}\mathbf{x} - \mathbf{N}\|^2_{\mathbf{\Sigma}_{vv}} \\ &= \|\mathbf{Q}_{\mathbf{\Sigma}}(\mathbf{y} - \mathbf{N})\|^2_{\mathbf{\Sigma}_{vv}} \\ &= (\mathbf{y} - \mathbf{N})^\top \mathbf{Q}_{\mathbf{\Sigma}}^\top \mathbf{\Sigma}_{vv}^{-1} \mathbf{Q}_{\mathbf{\Sigma}} (\mathbf{y} - \mathbf{N}) \\ &= (\mathbf{y} - \mathbf{N})^\top \mathbf{Q}_0 (\mathbf{y} - \mathbf{N}) \end{aligned} \tag{2.25}$$

where

$$\begin{aligned} \mathbf{Q}_0 &= \mathbf{Q}_{\mathbf{\Sigma}}^\top \mathbf{\Sigma}_{vv}^{-1} \mathbf{Q}_{\mathbf{\Sigma}} \\ &= (\mathbf{I} - \mathbf{P}_{\mathbf{\Sigma}})^\top \mathbf{\Sigma}_{vv}^{-1} (\mathbf{I} - \mathbf{P}_{\mathbf{\Sigma}}) \\ &= \mathbf{\Sigma}_{vv}^{-1} - \mathbf{\Sigma}_{vv}^{-1}\mathbf{P}_{\mathbf{\Sigma}} - \mathbf{P}_{\mathbf{\Sigma}}^\top \mathbf{\Sigma}_{vv}^{-1} + \mathbf{P}_{\mathbf{\Sigma}}^\top \mathbf{\Sigma}_{vv}^{-1} \mathbf{P}_{\mathbf{\Sigma}} \\ &= \mathbf{\Sigma}_{vv}^{-1} - 2\mathbf{\Sigma}_{vv}^{-1}\mathbf{G}(\mathbf{G}^\top \mathbf{\Sigma}_{vv}^{-1}\mathbf{G})^{-1}\mathbf{G}^\top \mathbf{\Sigma}_{vv}^{-1} \\ &\quad + \mathbf{\Sigma}_{vv}^{-1}\mathbf{G}(\mathbf{G}^\top \mathbf{\Sigma}_{vv}^{-1}\mathbf{G})^{-1}\mathbf{G}^\top \mathbf{\Sigma}_{vv}^{-1}\mathbf{G}(\mathbf{G}^\top \mathbf{\Sigma}_{vv}^{-1}\mathbf{G})^{-1}\mathbf{G}^\top \mathbf{\Sigma}_{vv}^{-1} \\ &= \mathbf{\Sigma}_{vv}^{-1} - \mathbf{\Sigma}_{vv}^{-1}\mathbf{G}(\mathbf{G}^\top \mathbf{\Sigma}_{vv}^{-1}\mathbf{G})^{-1}\mathbf{G}^\top \mathbf{\Sigma}_{vv}^{-1} \\ &= \mathbf{\Sigma}_{vv}^{-1} (\mathbf{I} - \mathbf{P}_{\mathbf{\Sigma}}) \\ &= \mathbf{\Sigma}_{vv}^{-1} \mathbf{Q}_{\mathbf{\Sigma}} \end{aligned} \tag{2.26}$$

Proposition 2 *Rank*$(\boldsymbol{Q}_0) = (K - n)$.

Proof. First, we should notice that by using Eqns. (2.22) and (2.24), $\mathbf{Q}_0$ can be written as:

$$\begin{aligned}
\mathbf{Q}_0 &= \mathbf{Q}_{\mathbf{\Sigma}}^{\top}\mathbf{\Sigma}_{\boldsymbol{vv}}^{-1}\mathbf{Q}_{\mathbf{\Sigma}} \\
&= (\mathbf{W}^{\top}\mathbf{M}^{-1}\mathbf{Q}\mathbf{M}\mathbf{W})^{\top} \\
&\quad (\mathbf{W}^{\top}\mathbf{M}^{\top}\mathbf{M}\mathbf{W})(\mathbf{W}^{\top}\mathbf{M}^{-1}\mathbf{Q}\mathbf{M}\mathbf{W}) \\
&= \mathbf{W}^{\top}\mathbf{M}^{\top}\mathbf{Q}\mathbf{M}^{-T}\mathbf{W}\mathbf{W}^{\top}\mathbf{M}^{\top}\mathbf{M}\mathbf{W}\mathbf{W}^{\top}\mathbf{M}^{-1}\mathbf{Q}\mathbf{M}\mathbf{W} \\
&= \mathbf{W}^{\top}\mathbf{M}^{\top}\mathbf{Q}\mathbf{M}\mathbf{W}. \qquad (2.27)
\end{aligned}$$

Following Eqn. (2.23), we stated that $\mathbf{Q}$ is a projection matrix with rank $(K-n)$. Because $\mathbf{M}$ and $\mathbf{W}$ are nonsingular, $\mathbf{Q}_0$ is similar to $\mathbf{Q}$; therefore, $rank(\mathbf{Q}_0) = (K-n)$. ■

Let the SVD (single value decomposition) of $\mathbf{Q}_0$ be

$$\mathbf{Q}_0 = \mathbf{U}\mathbf{S}^2\mathbf{U}^{\top},$$

where $\mathbf{U}$ is unitary and $\mathbf{S}$ is diagonal with $diag(\mathbf{S}) = [s_1, \ldots, s_{(K-n)}, 0, \ldots, 0]$ with all $s_i > 0$ for $i = 1, \ldots, (K-n)$.

Define $\mathbf{B} = \mathbf{S}\mathbf{U}^{\top}$ such that

$$\mathbf{Q}_0 = \mathbf{B}^{\top}\mathbf{B} \qquad (2.28)$$

where the last n rows of $\mathbf{B}$ are zero.

Given the above analysis, the cost function of Eqn. (2.25) can be rewritten as

$$\begin{aligned}
c(\mathbf{N}) &= (\mathbf{y}-\mathbf{N})^{\top}\mathbf{B}^{\top}\mathbf{B}(\mathbf{y}-\mathbf{N}) \\
&= \|\mathbf{B}(\mathbf{y}-\mathbf{N})\|^2. \qquad (2.29)
\end{aligned}$$

Because $\mathbf{B}$ does not have full rank, the null space of $\mathbf{B}$ is not empty. Therefore, there exists (non-unique) $\hat{\mathbf{N}} \in \mathbb{R}^m$ such that $(\mathbf{y} - \mathbf{N})$ is in the null space of $\mathbf{B}$:

$$\mathbf{B}\left(\mathbf{y} - \hat{\mathbf{N}}\right) = \mathbf{0}, \tag{2.30}$$

$$\mathbf{B}\mathbf{y} = \mathbf{B}\hat{\mathbf{N}}. \tag{2.31}$$

As the last n rows of $\mathbf{B}$ are all zeros, the matrix $\mathbf{B}$ can be represent as

$$\mathbf{B} = \begin{bmatrix} \mathbf{C} & \mathbf{D} \\ \mathbf{0} & \mathbf{0} \end{bmatrix},$$

where $\mathbf{C} \in \mathbb{R}^{(K-n)\times(K-n)}$ and $\mathbf{D} \in \mathbb{R}^{(K-n)\times n}$.

Decompose the vector $\hat{\mathbf{N}}$ into two subvectors $\hat{\mathbf{N}} = \begin{bmatrix} \hat{\mathbf{N}}_C^\top & \hat{\mathbf{N}}_D^\top \end{bmatrix}^\top$ with $\hat{\mathbf{N}}_C \in \mathbb{R}^{m-n}$ and $\hat{\mathbf{N}}_D \in \mathbb{R}^n$. Similarly, decompose $\mathbf{y}$ as $\mathbf{y} = \begin{bmatrix} \mathbf{y}_C^\top & \mathbf{y}_D^\top \end{bmatrix}^\top$ with $\mathbf{y}_C \in \mathbb{R}^{(m-n)}$ and $\mathbf{y}_D \in \mathbb{R}^n$. This decomposition allows Eqn. (2.31), to be manipulated as follows:

$$\begin{bmatrix} \mathbf{C} & \mathbf{D} \\ \mathbf{0} & \mathbf{0} \end{bmatrix} \begin{bmatrix} \mathbf{y}_C \\ \mathbf{y}_D \end{bmatrix} = \begin{bmatrix} \mathbf{C} & \mathbf{D} \\ \mathbf{0} & \mathbf{0} \end{bmatrix} \begin{bmatrix} \hat{\mathbf{N}}_C \\ \hat{\mathbf{N}}_D \end{bmatrix},$$

$$\begin{bmatrix} \mathbf{C} \\ \mathbf{0} \end{bmatrix} \hat{\mathbf{N}}_C = \begin{bmatrix} \mathbf{C} & \mathbf{D} \\ \mathbf{0} & \mathbf{0} \end{bmatrix} \begin{bmatrix} \mathbf{y}_C \\ \mathbf{y}_D \end{bmatrix} - \begin{bmatrix} \mathbf{D} \\ \mathbf{0} \end{bmatrix} \hat{\mathbf{N}}_D,$$

$$\mathbf{C}\hat{\mathbf{N}}_C = \mathbf{C}\mathbf{y}_C + \mathbf{D}\mathbf{y}_D + \mathbf{D}\hat{\mathbf{N}}_D.$$

Therefore, given a hypothesized vector $\mathbf{N}_D \in \mathbb{Z}^n$, the real-valued estimate of $\hat{\mathbf{N}}_C$ is given by:

$$\hat{\mathbf{N}}_C = \mathbf{y}_C + \mathbf{C}^{-1}\mathbf{D}(\mathbf{y}_D - \mathbf{N}_D) \tag{2.32}$$

The integer candidates $\hat{\mathbf{N}}_D$ can be searched exhaustively over some finite range of integers using n "for" loops as shown in Figure 2.1. This requires $(2d+1)^n$ iterations of Eqn. (2.32) and associated logic for keeping the best integer vector candidate.

$\mathbf{A} = \mathbf{C}^{-1}\mathbf{D}$
for $i = -d : d$
  for $j = -d : d$
    for $k = -d : d$
      $\mathbf{N}_D = [i, j, k, 0]^\top$
      $\hat{\mathbf{N}}_C = \mathbf{y}_C + \mathbf{A}\,(\mathbf{y}_D - \mathbf{N}_D)$
      ... use $\hat{\mathbf{N}}_C$ to compute $\mathbf{N}_C$ minimizing $J(\mathbf{N}_C)$
      $\mathbf{N}^\top = [\mathbf{N}_C, \mathbf{N}_D]^\top$, if $c(\mathbf{N}) <$ current minimum
        Save $\mathbf{N}$
        current minimum $= c(\mathbf{N})$
      $\vdots$

Figure 2.1: Triple 'for' loop to compute $\hat{\mathbf{N}}_C$.

For any hypothesized integer vector $\mathbf{N}_D$, Eqn. (2.32) calculates the unique $\hat{\mathbf{N}}_C \in \mathbb{R}^{(K-n)}$ such that $c(\hat{\mathbf{N}}) = 0$. The next step will be to use $\hat{\mathbf{N}}_C$ to find an integer $\mathbf{N}_C$ such that $c(\mathbf{N})$ is minimum.

2.4.2 Rounding $\hat{\mathbf{N}}_C$

Given $\hat{\mathbf{N}}_C$, in order to get the optimal integer estimate of $\mathbf{N}_C$, we would like to find an integer vector $\check{\mathbf{N}}_C$ which is close to $\hat{\mathbf{N}}_C$. As discussed in [36, 37], as the integer estimation error vector can be highly correlated, visualized by the level curves of the cost function being tilted and elongated ellipses, directly rounding $\hat{\mathbf{N}}_C$ to $\check{\mathbf{N}}_C$ may yield incorrect integer estimates and cause a significant cost increase.

Consider the cost function

$$\begin{aligned} J(\mathbf{N}_C) &= \|\mathbf{N}_C - \hat{\mathbf{N}}_C\|^2_{\boldsymbol{\Sigma}_{\hat{\mathbf{N}}_C}} \\ &= (\mathbf{N}_C - \hat{\mathbf{N}}_C)^\top \boldsymbol{\Sigma}^{-1}_{\hat{\mathbf{N}}_C} (\mathbf{N}_C - \hat{\mathbf{N}}_C), \end{aligned} \tag{2.33}$$

where the covariance of $\hat{\mathbf{N}}_C$

$$\mathbf{\Sigma}_{\hat{\mathbf{N}}_C} = \mathbf{\Sigma}_{CC} + \mathbf{C}^{-1}\mathbf{D}\Sigma_{DD}\mathbf{D}^{\top}\mathbf{C}^{-T}, \tag{2.34}$$

$$\Sigma_{CC} = cov(\mathbf{y}_C), \Sigma_{CC} = cov(\mathbf{y}_D).$$

The purpose of this section is to show that the cost functions $c(\mathbf{N})$ defined in Eqn. (2.25) and $J(\mathbf{N}_C)$ defined in Eqn. (2.33) are both minimized by the same integer estimate $\mathbf{N}_C$.

Proposition 3 *The cost functions $c(\boldsymbol{N})$ defined in Eqn. (2.25) and $J(\boldsymbol{N}_C)$ defined in Eqn. (2.33) are both minimized by the same integer estimate $\boldsymbol{N}_C$.*

Proof. Let

$$\mathbf{Q}_{\mathbf{\Sigma}} = \begin{bmatrix} \mathbf{Q}_{CC} & \mathbf{Q}_{CD} \\ \mathbf{Q}_{DC} & \mathbf{Q}_{DD} \end{bmatrix} \tag{2.35}$$

where $\mathbf{Q}_{CC} \in \mathbb{R}^{(K-n)\times(K-n)}$, $\mathbf{Q}_{DD} \in \mathbb{R}^{n\times n}$ and $\mathbf{Q}_{CD}, \mathbf{Q}_{DC}^{\top} \in \mathbb{R}^{(K-n)\times n}$.

Similarly, denote the covariance matrix as the covariance matrix $\mathbf{\Sigma}_{vv}$ as

$$\mathbf{\Sigma}_{vv} = \begin{bmatrix} \mathbf{\Sigma}_{CC} & \mathbf{\Sigma}_{CD} \\ \mathbf{\Sigma}_{DC} & \mathbf{\Sigma}_{DD} \end{bmatrix},$$

where $\mathbf{\Sigma}_{CC} \in \mathbb{R}^{(K-n)\times(K-n)}$, $\mathbf{\Sigma}_{DD} \in \mathbb{R}^{n\times n}$, $\mathbf{\Sigma}_{CD}, \mathbf{\Sigma}_{DC}^{\top} \in \mathbb{R}^{(K-n)\times n}$. Let the inverse of $\mathbf{\Sigma}_{vv}$ be

$$\mathbf{\Sigma}_{vv}^{-1} = \mathbf{\Upsilon} = \begin{bmatrix} \mathbf{\Upsilon}_{CC} & \mathbf{\Upsilon}_{CD} \\ \mathbf{\Upsilon}_{DC} & \mathbf{\Upsilon}_{DD} \end{bmatrix} \tag{2.36}$$

where $\mathbf{\Upsilon}_{CC} \in \mathbb{R}^{(K-n)\times(K-n)}$, $\mathbf{\Upsilon}_{DD} \in \mathbb{R}^{n\times n}$, $\mathbf{\Upsilon}_{CD}, \mathbf{\Upsilon}_{DC}^{\top} \in \mathbb{R}^{(K-n)\times n}$. We can also obtain

$$\mathbf{\Upsilon}_{CC} = (\mathbf{\Sigma}_{CC} - \mathbf{\Sigma}_{CD}\mathbf{\Sigma}_{DD}^{-1}\mathbf{\Sigma}_{DC})^{-1} \tag{2.37}$$

$$\mathbf{\Upsilon}_{CD} = -\mathbf{\Upsilon}_{CC}\mathbf{\Sigma}_{CD}\mathbf{\Sigma}_{DD}^{-1}. \tag{2.38}$$

Substitute Eqns. (2.36) and (2.35) into Eqn. (2.26), we have

$$\begin{aligned}
\mathbf{Q}_0 &= \boldsymbol{\Sigma}_{\boldsymbol{vv}}^{-1}\mathbf{Q}_{\boldsymbol{\Sigma}} \\
&= \begin{bmatrix} \boldsymbol{\Upsilon}_{CC} & \boldsymbol{\Upsilon}_{CD} \\ \boldsymbol{\Upsilon}_{DC} & \boldsymbol{\Upsilon}_{DD} \end{bmatrix} \begin{bmatrix} \mathbf{Q}_{CC} & \mathbf{Q}_{CD} \\ \mathbf{Q}_{DC} & \mathbf{Q}_{DD} \end{bmatrix} \\
&= \begin{bmatrix} \boldsymbol{\Upsilon}_{CC}\mathbf{Q}_{CC} + \boldsymbol{\Upsilon}_{CD}\mathbf{Q}_{DC} & \boldsymbol{\Upsilon}_{CC}\mathbf{Q}_{CD} + \boldsymbol{\Upsilon}_{CD}\mathbf{Q}_{DD} \\ \boldsymbol{\Upsilon}_{DC}\mathbf{Q}_{CC} + \boldsymbol{\Upsilon}_{DD}\mathbf{Q}_{DC} & \boldsymbol{\Upsilon}_{DC}\mathbf{Q}_{CD} + \boldsymbol{\Upsilon}_{DD}\mathbf{Q}_{DD} \end{bmatrix}. \qquad (2.39)
\end{aligned}$$

From Eqn. (2.29), for any $\mathbf{N} \in \mathbb{Z}^K$,

$$\begin{aligned}
c(\mathbf{N}) &= (\mathbf{y}-\mathbf{N})^\top \mathbf{B}^\top \mathbf{B}(\mathbf{y}-\mathbf{N}) \\
&= (\mathbf{y}-\hat{\mathbf{N}}-\mathbf{N}+\hat{\mathbf{N}})^\top \mathbf{B}^\top \mathbf{B}(\mathbf{y}-\hat{\mathbf{N}}-\mathbf{N}+\hat{\mathbf{N}}) \\
&= \|\mathbf{B}(\mathbf{y}-\hat{\mathbf{N}})\|^2 - 2(\mathbf{N}-\hat{\mathbf{N}})^\top \mathbf{B}^\top \mathbf{B}(\mathbf{y}-\hat{\mathbf{N}}) + \|\mathbf{B}(\mathbf{N}-\hat{\mathbf{N}})\|^2 \qquad (2.40)
\end{aligned}$$

where $\hat{\mathbf{N}}$ is the optimal real-valued estimate of $\mathbf{N}$, which satisfies $\mathbf{B}(\mathbf{y}-\hat{\mathbf{N}}) = 0$. Also, because the vector candidates $\mathbf{N}$ are generated as shown in Fig. 2.1, $\hat{\mathbf{N}}_D$ is an integer vector that satisfies $\hat{\mathbf{N}}_D = \mathbf{N}_D$. Hence, the cost function can be written as

$$\begin{aligned}
c(\mathbf{N}) &= \|\mathbf{B}(\mathbf{N}-\hat{\mathbf{N}})\|^2 \\
&= \left(\mathbf{N}-\hat{\mathbf{N}}\right)^\top \mathbf{B}^\top \mathbf{B} \left(\mathbf{N}-\hat{\mathbf{N}}\right) \\
&= \left(\mathbf{N}-\hat{\mathbf{N}}\right)^\top \mathbf{Q}_0 \left(\mathbf{N}-\hat{\mathbf{N}}\right) \\
&= \begin{bmatrix} \mathbf{N}_C - \hat{\mathbf{N}}_C \\ \mathbf{0} \end{bmatrix} \begin{bmatrix} \boldsymbol{\Upsilon}_{CC}\mathbf{Q}_{CC} + \boldsymbol{\Upsilon}_{CD}\mathbf{Q}_{DC} & \boldsymbol{\Upsilon}_{CC}\mathbf{Q}_{CD} + \boldsymbol{\Upsilon}_{CD}\mathbf{Q}_{DD} \\ \boldsymbol{\Upsilon}_{DC}\mathbf{Q}_{CC} + \boldsymbol{\Upsilon}_{DD}\mathbf{Q}_{DC} & \boldsymbol{\Upsilon}_{DC}\mathbf{Q}_{CD} + \boldsymbol{\Upsilon}_{DD}\mathbf{Q}_{DD} \end{bmatrix} \begin{bmatrix} \mathbf{N}_C - \hat{\mathbf{N}}_C \\ \mathbf{0} \end{bmatrix} \\
&= \left(\mathbf{N}_C - \hat{\mathbf{N}}_C\right)^\top (\boldsymbol{\Upsilon}_{CC}\mathbf{Q}_{CC} + \boldsymbol{\Upsilon}_{CD}\mathbf{Q}_{DC}) \left(\mathbf{N}_C - \hat{\mathbf{N}}_C\right). \qquad (2.41)
\end{aligned}$$

Comparison of Eqns. (2.33) and (2.41) shows that if we can prove $\boldsymbol{\Sigma}_{\hat{\mathbf{N}}_C}^{-1} = (\boldsymbol{\Upsilon}_{CC}\mathbf{Q}_{CC} + \boldsymbol{\Upsilon}_{CD}\mathbf{Q}_{DC})$, then these two cost functions are equivalent.

From Eqn. (2.31), we know that

$$\mathbf{B}\hat{\mathbf{N}} = \mathbf{B}\mathbf{y},$$

multiplying on the left by $\mathbf{B}^\top$ yields

$$\mathbf{B}^\top\mathbf{B}\mathbf{N} = \mathbf{B}^\top\mathbf{B}\mathbf{y},$$

which provides the following constraint on the covariance

$$\begin{aligned}
\mathbf{B}^\top\mathbf{B}\boldsymbol{\Sigma}_{NN}\mathbf{B}^\top\mathbf{B} &= \mathbf{B}^\top\mathbf{B}\boldsymbol{\Sigma}_{\boldsymbol{vv}}\mathbf{B}^\top\mathbf{B} \\
\mathbf{Q}_0\boldsymbol{\Sigma}_{NN}\mathbf{Q}_0^\top &= \mathbf{Q}_0\boldsymbol{\Sigma}_{\boldsymbol{vv}}\mathbf{Q}_0^\top \\
\boldsymbol{\Sigma}_{\boldsymbol{vv}}^{-1}\mathbf{Q}_{\boldsymbol{\Sigma}}\boldsymbol{\Sigma}_{NN}\mathbf{Q}_{\boldsymbol{\Sigma}}^\top\boldsymbol{\Sigma}_{\boldsymbol{vv}}^{-T} &= \boldsymbol{\Sigma}_{\boldsymbol{vv}}^{-1}\mathbf{Q}_{\boldsymbol{\Sigma}}\boldsymbol{\Sigma}_{\boldsymbol{vv}}\mathbf{Q}_{\boldsymbol{\Sigma}}^\top\boldsymbol{\Sigma}_{\boldsymbol{vv}}^{-T}
\end{aligned} \tag{2.42}$$

where

$$\boldsymbol{\Sigma}_{NN} = \begin{bmatrix} \boldsymbol{\Sigma}_{\hat{\mathbf{N}}_C} & \mathbf{0} \\ \mathbf{0} & \mathbf{0} \end{bmatrix}$$

as there is no uncertainty in $\mathbf{N}_D$.

Because $\boldsymbol{\Sigma}_{\boldsymbol{vv}}$ is nonsingular, Eqn. (2.42) reduces to

$$\begin{aligned}
\mathbf{Q}_{\boldsymbol{\Sigma}}\boldsymbol{\Sigma}_{NN}\mathbf{Q}_{\boldsymbol{\Sigma}}^\top &= \mathbf{Q}_{\boldsymbol{\Sigma}}\boldsymbol{\Sigma}_{\boldsymbol{vv}}\mathbf{Q}_{\boldsymbol{\Sigma}}^\top \\
&= \mathbf{Q}_{\boldsymbol{\Sigma}}\boldsymbol{\Sigma}_{\boldsymbol{vv}},
\end{aligned} \tag{2.43}$$

as

$$\begin{aligned}
\mathbf{Q}_{\boldsymbol{\Sigma}}\boldsymbol{\Sigma}_{\boldsymbol{vv}}\mathbf{Q}_{\boldsymbol{\Sigma}}^\top &= \left(\mathbf{W}^\top\mathbf{M}^{-1}\mathbf{Q}\mathbf{M}\mathbf{W}\right)\left(\mathbf{W}^\top\mathbf{M}^{-1}\mathbf{M}^{-T}\mathbf{W}\right)\left(\mathbf{W}^\top\mathbf{M}^\top\mathbf{Q}^\top\mathbf{M}^{-T}\mathbf{W}\right) \\
&= \mathbf{W}^\top\mathbf{M}^\top\mathbf{Q}\mathbf{Q}^\top\mathbf{M}^{-T}\mathbf{W} \\
&= \left(\mathbf{W}^\top\mathbf{M}^{-1}\mathbf{Q}\mathbf{M}\mathbf{W}\right)\left(\mathbf{W}^\top\mathbf{M}^{-1}\mathbf{M}^{-T}\mathbf{W}\right) \\
&= \mathbf{Q}_{\boldsymbol{\Sigma}}\boldsymbol{\Sigma}_{\boldsymbol{vv}},
\end{aligned}$$

according to Eqns. (2.24) and (2.22).

Therefore,

$$\mathbf{Q}_{\mathbf{\Sigma}}\left(\mathbf{\Sigma}_{NN}\mathbf{Q}_{\mathbf{\Sigma}}^{\top}-\mathbf{\Sigma}_{\boldsymbol{vv}}\right)=0. \tag{2.44}$$

From Sylvesters rank inequality: "If A is a $m-by-n$ matrix and B is $n-by-k$, then $rank(A)+rank(B)-n\leq rank(AB)$."

As $\mathbf{Q}_{\mathbf{\Sigma}}\in\mathbb{R}^{K\times K}$, $\left(\mathbf{\Sigma}_{NN}\mathbf{Q}_{\mathbf{\Sigma}}^{\top}-\mathbf{\Sigma}_{\boldsymbol{vv}}\right)\in\mathbb{R}^{K\times K}$ and $rank(\mathbf{Q}_{\mathbf{\Sigma}})=(K-n)$. Therefore, $rank\left(\mathbf{\Sigma}_{NN}\mathbf{Q}_{\mathbf{\Sigma}}^{\top}-\mathbf{\Sigma}_{\boldsymbol{vv}}\right)\leq n$.

Referring to Eqn. (2.35),

$$\left(\mathbf{\Sigma}_{NN}\mathbf{Q}_{\mathbf{\Sigma}}^{\top}-\mathbf{\Sigma}_{\boldsymbol{vv}}\right)=\begin{bmatrix}\mathbf{\Sigma}_{\hat{\mathbf{N}}_C}\mathbf{Q}_{CC}^{\top}-\mathbf{\Sigma}_{CC} & \mathbf{\Sigma}_{\hat{\mathbf{N}}_C}\mathbf{Q}_{DC}^{\top}-\mathbf{\Sigma}_{CD}\\ -\mathbf{\Sigma}_{DC} & -\mathbf{\Sigma}_{DD}\end{bmatrix}.$$

As the block $-\mathbf{\Sigma}_{DD_j}$ has rank n, to make $rank\left(\mathbf{\Sigma}_{NN}\mathbf{Q}_{\mathbf{\Sigma}}^{\top}-\mathbf{\Sigma}_{\boldsymbol{vv}}\right)\leq n$, the first $(K-n)$ columns are the linear combination of the later n ones. As

$$-\mathbf{\Sigma}_{DC} = -\mathbf{\Sigma}_{DD}\mathbf{\Sigma}_{DD}^{-1}\mathbf{\Sigma}_{DC},$$

we have

$$\begin{aligned}\left(\mathbf{\Sigma}_{\hat{\mathbf{N}}_C}\mathbf{Q}_{CC}^{\top}-\mathbf{\Sigma}_{CC}\right) &= \left(\mathbf{\Sigma}_{\hat{\mathbf{N}}_C}\mathbf{Q}_{DC}^{\top}-\mathbf{\Sigma}_{CD}\right)\mathbf{\Sigma}_{DD}^{-1}\mathbf{\Sigma}_{DC}\\ \mathbf{\Sigma}_{\hat{\mathbf{N}}_C}\mathbf{Q}_{CC}^{\top}-\mathbf{\Sigma}_{CC} &= \mathbf{\Sigma}_{\hat{\mathbf{N}}_C}\mathbf{Q}_{DC}^{\top}\mathbf{\Sigma}_{DD}^{-1}\mathbf{\Sigma}_{DC}-\mathbf{\Sigma}_{CD}\mathbf{\Sigma}_{DD}^{-1}\mathbf{\Sigma}_{DC}\\ \mathbf{\Sigma}_{\hat{\mathbf{N}}_C}\left(\mathbf{Q}_{CC}^{\top}-\mathbf{Q}_{DC}^{\top}\mathbf{\Sigma}_{DD}^{-1}\mathbf{\Sigma}_{DC}\right) &= \mathbf{\Sigma}_{CC}-\mathbf{\Sigma}_{CD}\mathbf{\Sigma}_{DD}^{-1}\mathbf{\Sigma}_{DC}\\ &= \mathbf{\Upsilon}_{CC}^{-1}.\end{aligned}$$

Therefore,

$$\mathbf{\Sigma}_{\hat{\mathbf{N}}_C}^{-1} = \left(\mathbf{Q}_{CC}^{\top}-\mathbf{Q}_{DC}^{\top}\mathbf{\Sigma}_{DD}^{-1}\mathbf{\Sigma}_{DC}\right)\mathbf{\Upsilon}_{CC}$$

As $\mathbf{\Sigma}_{\hat{\mathbf{N}}_C}$ is symmetric,

$$\begin{aligned}
\mathbf{\Sigma}_{\hat{\mathbf{N}}_C}^{-1} &= \mathbf{\Sigma}_{\hat{\mathbf{N}}_C}^{-T} \\
&= \mathbf{\Upsilon}_{CC}\left(\mathbf{Q}_{CC} - \mathbf{\Sigma}_{CD}\mathbf{\Sigma}_{DD}^{-1}\mathbf{Q}_{DC}\right) \\
&= \mathbf{\Upsilon}_{CC}\mathbf{Q}_{CC} - \mathbf{\Upsilon}_{CC}\mathbf{\Sigma}_{CD}\mathbf{\Sigma}_{DD}^{-1}\mathbf{Q}_{DC} \qquad (2.45)
\end{aligned}$$

by substituting Eqn. (2.38) into Eqn. (2.45), we have

$$\mathbf{\Sigma}_{\hat{\mathbf{N}}_C}^{-1} = \mathbf{\Upsilon}_{CC}\mathbf{Q}_{CC} - \mathbf{\Upsilon}_{CD}\mathbf{Q}_{DC}. \qquad (2.46)$$

Hence we finished the proof by comparing Eqns. (2.33) and (2.41). ■

To find the integer vector that minimizes Eqn. (2.33), we follow the idea of LAMBDA to employ a Z-transform $\mathbf{Z}$ which decorrelates $\mathbf{\Sigma}_{\hat{\mathbf{N}}_C}$. Here, the $\mathbf{Z}$ transform should have the following properties:

- $\mathbf{Z}$ is an integer-to-integer transformation, thus every element of $\mathbf{Z}$ and $\mathbf{Z}^{-1}$ is an integer. In other words, $\mathbf{Z}$ is a unimodular matrix with determinate being 1.
- To decorrelate $\mathbf{\Sigma}_{\hat{\mathbf{N}}_C}$, we would like find $\mathbf{Z}$ that $\left(\mathbf{Z}\mathbf{\Sigma}_{NC}\mathbf{Z}^T\right)^{-1}$ to be nearly diagonal.

The procedure to find the Z-transformation was described in detail in [12].

Let $\hat{\mathbf{M}}_C = \mathbf{Z}\hat{\mathbf{N}}_C$, then the cost function written in terms of $\mathbf{M}_C$ is

$$J(\mathbf{M}_C) = (\mathbf{M}_C - \hat{\mathbf{M}}_C)^\top \mathbf{\Sigma}_{\hat{M}_C}^{-1}(\mathbf{M}_C - \hat{\mathbf{M}}_C), \qquad (2.47)$$

where $\mathbf{\Sigma}_{\hat{M}_C} = \boldsymbol{Z}\mathbf{\Sigma}_{\hat{N}_C}\boldsymbol{Z}^\top$. Because $\mathbf{\Sigma}_{\hat{M}_C}^{-1}$ is nearly diagonal, $J(\mathbf{M}_C)$ can be minimized by rounding $\hat{\mathbf{M}}_C$ to the nearest integer; therefore, the integer-valued estimate of $\mathbf{N}_C$ can be

computed as:

$$\hat{\mathbf{M}}_C = \boldsymbol{Z}\hat{\mathbf{N}}_C \tag{2.48}$$

$$\check{\mathbf{M}}_C = [\hat{\mathbf{M}}_C]_{roundoff} \tag{2.49}$$

$$\check{\mathbf{N}}_C = \boldsymbol{Z}^{-1}\check{\mathbf{M}}_C. \tag{2.50}$$

At this point we have an integer vector candidate $\left[\check{\mathbf{N}}_C^\top \mathbf{N}_D^\top\right]^\top$. One such candidate will be generated for each iteration of the 'for' loop in Fig. 2.1. We can compare each integer vector candidate using Eqn. (2.25). Selecting the candidate vector with the lowest value (subject to validity tests) as the best. In this manner, by rounding off the float estimate $\hat{\mathbf{N}}_C$ in a decorrelated domain, i.e. $\mathbf{M}_C$, we have a better chance to achieve optimal integer estimate $\check{\mathbf{N}}_C$ and therefore have higher success rate than the original LMS. Moreover, comparing to the original LAMBDA, the decorrelation is computed for the subvector $\mathbf{N}_C$ rather than the whole vector $\mathbf{N}$, therefore, the Z transformation dimension is reduced from $\mathbb{R}^{K\times K}$ to $\mathbb{R}^{(K-n)\times(K-n)}$ (e.g., from $\mathbb{R}^{7\times 7}$ to $\mathbb{R}^{4\times 4}$ in typical GPS applications). Therefore, the proposed method has less computational complexity compared to LAMBDA.

The decorrelation of $\hat{N}_C$ is one of the key steps in the proposed method. An example of the level curves of the correlation matrix in terms of correlated integer vector $\mathbf{N}_C$ and decorrelated integer vector $\mathbf{M}_C$ are show in Fig. 2.2 and Fig. 2.3. Here, we follow the algorithm described in [12] to find the Z-transform.

The level curves for the vector $\mathbf{N}_C$ form hyper-ellipsoids. In both figures, we plot each section of the hyper-ellipsoid and $\mathbf{N}_C$. In this case, $K = 9$, $n = 4$ and $\mathbf{N}_C \in \mathbb{Z}^5$. In Fig. 2.2, the 'x' denotes the float estimate of $\hat{\mathbf{N}}_C$, the '*'denotes the nearest integer vector to the float estimate, and the 'o' denotes the integer vector with lowest cost. The ellipses denote

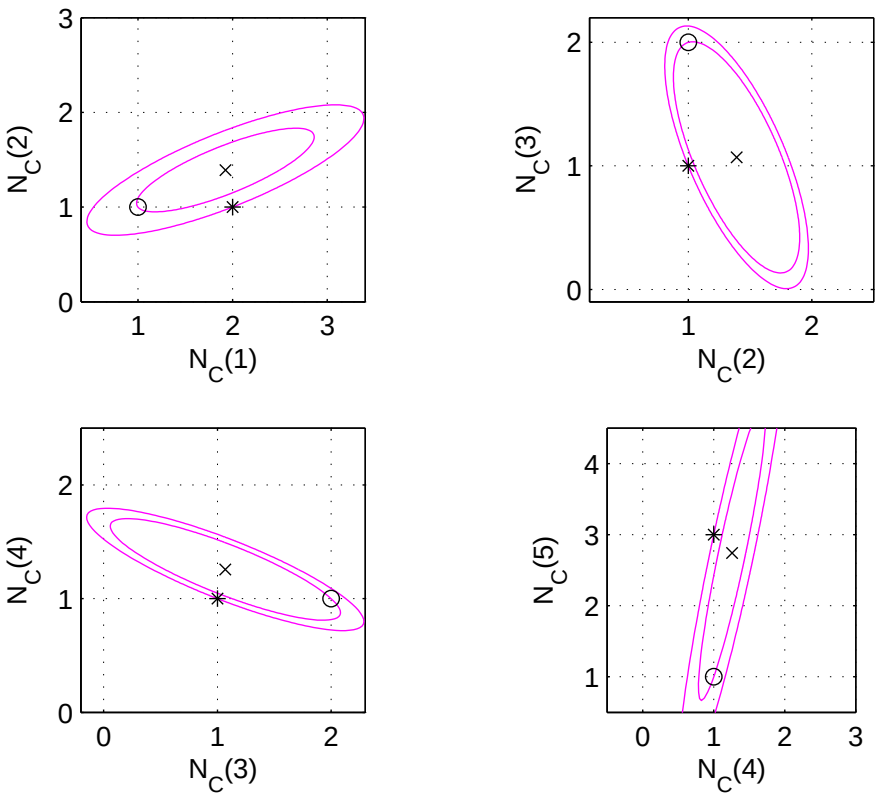

Figure 2.2: Sections of the level curves of the cost function for $\mathbf{N}_C$ (see Eqn. (2.33))

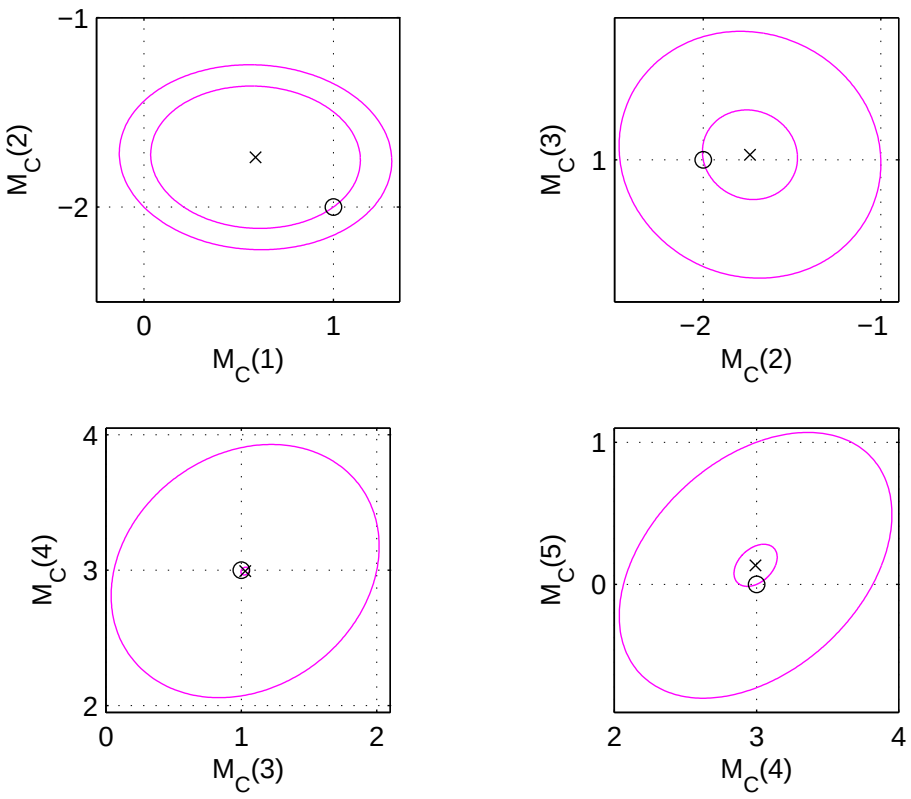

Figure 2.3: Sections of the level curves of the cost function for $\mathbf{M}_C$ (see Eqn. (2.47))

the section of the level curves of the cost function $J(\mathbf{N}_C) = \|\mathbf{N}_C - \hat{\mathbf{N}}_C\|^2_{\Sigma_N}$, the larger the ellipse is, the larger $J(\mathbf{N}_C)$ is. The float estimate $\hat{\mathbf{N}}_C \approx [1.92 \;\; 1.39 \;\; 1.07 \;\; 1.26 \;\; 2.74]^T$ and its nearest integer vector is $\bar{\mathbf{N}}_C = [2 \;\; 1 \;\; 1 \;\; 1 \;\; 3]^T$. As the level curves $J(\mathbf{N}_C)$ are elongated, tilted hyper-ellipsoids, $\check{\mathbf{N}}_C$ is not the optimal estimate as the vector $\check{\mathbf{N}}_C = [1 \;\; 1 \;\; 2 \;\; 1 \;\; 1]^T$ has smaller cost $J(N_C)$.

In Fig. 2.3, the transformed float and integer estimates are plotted. After applying the Z-transformation

$$Z = \begin{bmatrix} 1 & 0 & 0 & 2 & 0 \\ -1 & 0 & -1 & 1 & 0 \\ 0 & -2 & 1 & 0 & 1 \\ 1 & 0 & 1 & 0 & 0 \\ 0 & 1 & 0 & -1 & 0 \end{bmatrix},$$

the float and integer estimate in $\mathbf{M}$-domain will be:

$$\begin{aligned} \hat{\mathbf{M}}_C &= \begin{bmatrix} 0.59 & -1.74 & 1.028 & 3.00 & 0.13 \end{bmatrix}^T \\ \check{\mathbf{M}}_C &= \begin{bmatrix} 1 & -2 & 1 & 3 & 0 \end{bmatrix}^T \\ \check{\mathbf{N}}_C &= Z^{-1}\check{\mathbf{M}}_C = \begin{bmatrix} 1 & 1 & 2 & 1 & 1 \end{bmatrix} \end{aligned}$$

The covariance matrix for the transformed integer vector $\mathbf{\Sigma}_{MC}$ is nearly diagonal, the level curves of $J(\mathbf{M}_C) = \|\mathbf{M}_C - \hat{\mathbf{M}}_C\|^2_{\mathbf{\Sigma}_{MC}}$ which pass the closest and second closest integer vectors to $\hat{\mathbf{M}}_C$ are plotted. As the shape of the level curve sections are round ellipses, rounding off $\hat{\mathbf{M}}_C$ to $\check{\mathbf{M}}_C$ does give the least $J(\mathbf{M}_C)$ increase, and $\mathbf{N}_C$ can be determined.

2.5 Integer Ambiguity Estimation Strategies

To implement GPS integer ambiguity estimation algorithm, various strategies are possible. In deciding an estimation strategy, we would like to have minimum volume to search and maximum number of measurements. In this section, we will first discuss the linear combination of GPS dual frequency measurements, based on which we can discuss two most popular integer estimation strategies: bootstrapping and batch.

2.5.1 Linear Combinations of Dual Frequency Measurements

Currently GPS signals are broadcasted in two frequencies: the primary frequencies L1 at $f_1 = 1575.42MHz$ and the L2 at $f_2 = 1227.6MHz$. Here we consider the differential code and phase measurements at both frequencies. We rewrite the differential code and phase measurements described in eqns. (2.7) and (2.8) in L1 and L2 as:

$$\Delta\rho_{L1}^{(i)} = R^{(i)} + c\delta\bar{t}_r + \bar{\epsilon}_{L1}^{(i)}, \tag{2.51}$$

$$\lambda_1\Delta\phi_{L1}^{(i)} = R^{(i)} + c\delta\bar{t}_r + \lambda N_{L1}^{(i)} + \bar{\eta}_{L1}^{(i)} \tag{2.52}$$

$$\Delta\rho_{L2}^{(i)} = R^{(i)} + c\delta\bar{t}_r + \bar{\epsilon}_{L2}^{(i)}, \tag{2.53}$$

$$\lambda_2\Delta\phi_{L2}^{(i)} = R^{(i)} + c\delta\bar{t}_r + \lambda N_{L2}^{(i)} + \bar{\eta}_{L2}^{(i)} \tag{2.54}$$

Where $\lambda_1 = \dfrac{c}{f_1} \approx 19.0cm$ and $\lambda_2 = \dfrac{c}{f_2} \approx 24.4cm$. As discussed in Chapter 2, $\bar{\epsilon}^{(i)} \sim \mathcal{N}\left(0, \sigma_{\rho_i}^2\right)$ and $\bar{\eta}^{(i)} \sim \mathcal{N}\left(0, \sigma_{\Phi_i}^2\right)$. In typical GPS applications, σ_{ρ_i} is at the meter level and σ_{Φ_i} is at the centimeter level and all the noise terms are uncorrelated with each other.

Various other quantities can be computed as linear combinations of the phase measurements. Of particular interest are those that maintain the integer nature of the offset due to

the integer ambiguities. Linear combinations from L1 and L2 can be represent in forms of

$$\begin{aligned}
\Delta\rho^{(i)}_{\alpha,\beta} &= \lambda_{\alpha,\beta}\left(\alpha\frac{\Delta\rho^{(i)}_{L1}}{\lambda_1}+\beta\frac{\Delta\rho^{(i)}_{L2}}{\lambda_2}\right) \\
&= \lambda_{\alpha,\beta}\left(\frac{\alpha}{\lambda_1}+\frac{\beta}{\lambda_2}\right)\left(R^{(i)}+c\delta\bar{t}_r\right)+\lambda_{\alpha,\beta}\left(\alpha\frac{\bar{\epsilon}^{(i)}_{L1}}{\lambda_1}+\beta\frac{\bar{\epsilon}^{(i)}_{L2}}{\lambda_2}\right) \qquad (2.55)\\
\lambda_{\alpha,\beta}\Delta\phi^{(i)}_{\alpha,\beta} &= \lambda_{\alpha,\beta}\left(\alpha\Delta\phi^{(i)}_{L1}+\beta\Delta\phi^{(i)}_{L2}\right) \\
&= \lambda_{\alpha,\beta}\left(\frac{\alpha}{\lambda_1}+\frac{\beta}{\lambda_2}\right)\left(R^{(i)}+c\delta\bar{t}_r\right)+\lambda_{\alpha,\beta}N^{(i)}_{\alpha,\beta}+\lambda_{\alpha,\beta}\left(\alpha\frac{\bar{\eta}^{(i)}_{L1}}{\lambda_1}+\beta\frac{\bar{\eta}^{(i)}_{L2}}{\lambda_2}\right) \qquad (2.56)
\end{aligned}$$

To preserve the unit scale factor for $R^{(i)}$, the wavelength $\lambda_{\alpha,\beta}$ is defined as

$$\lambda_{\alpha,\beta}=\frac{\lambda_1\lambda_2}{\alpha\lambda_1+\beta\lambda_2}=\frac{c}{\alpha f_1+\beta f_2}, \qquad (2.57)$$

where c is the speed of light. The integer ambiguity for the linear combination measurement is defined as $N^{(i)}_{\alpha,\beta}=\alpha N^{(i)}_{l1}+\beta N^{(i)}_{L2}$.

The standard deviation of the measurement noise is:

$$\begin{aligned}
\sigma^2_{\rho^{(i)}_{\alpha,\beta}} &= \lambda^2_{\alpha,\beta}\left(\alpha^2\frac{\sigma^2_{\rho_i}}{\lambda^2_1}+\beta\frac{\sigma^2_{\rho_i}}{\lambda^2_2}\right) \\
&= \frac{\alpha^2\lambda^2_2+\beta^2\lambda^2_1}{(\alpha\lambda_2+\beta\lambda_1)^2}\,\sigma^2_{\rho_i}, \qquad (2.58)
\end{aligned}$$

By the same token, the covariance of the linear combination phase measurement noise is:

$$\sigma^2_{\phi^{(i)}_{\alpha,\beta}} = \frac{\alpha^2\lambda^2_2+\beta^2\lambda^2_1}{(\alpha\lambda_2+\beta\lambda_1)^2}\,\sigma^2_{\phi_i}. \qquad (2.59)$$

Some commonly chosen value for α and β are:

- $\alpha=1,\beta=1$. This is referred to as narrow lane measurement. Narrow lane code and

phase measurement which can be computed as:

$$\begin{aligned}\Delta\rho_{NR}^{(i)} &= \lambda_n\left(\frac{\Delta\rho_{L1}^{(i)}}{\lambda_1}+\frac{\Delta\rho_{L2}^{(i)}}{\lambda_2}\right)\\ &= R^{(i)}+c\delta\bar{t}_r+\bar{\epsilon}_{NR}^{(i)}, \qquad (2.60)\\ \lambda_n\Delta\phi_{NR}^{(i)} &= \lambda_n\left(\Delta\phi_{L1}^{(i)}+\Delta\phi_{L2}^{(i)}\right)\\ &= R^{(i)}+c\delta\bar{t}_r+\lambda N_{NR}^{(i)}+\bar{\eta}_{NR}^{(i)} \qquad (2.61)\end{aligned}$$

where $\lambda_n = \dfrac{\lambda_1\lambda_2}{\lambda_1+\lambda_2} \approx 0.107m$ and $N_{NR}^{(i)} = N_{L1}^{(i)} + N_{L2}^{(i)}$. The measurement noise for narrow lane code and measurement are $\bar{\epsilon}_{NR}^{(i)} = \lambda_n\left(\dfrac{\bar{\epsilon}_{L1}^{(i)}}{\lambda_1}+\dfrac{\bar{\epsilon}_{L2}^{(i)}}{\lambda_2}\right)$ and $\bar{\eta}_{NR}^{(i)} = \lambda_n\left(\dfrac{\bar{\eta}_{L1}^{(i)}}{\lambda_1}+\dfrac{\bar{\eta}_{L2}^{(i)}}{\lambda_2}\right)$, separately. Narrow lane measurement has short wavelength, but the standard deviation of the measurement noise is decreased to about 0.707 of L1 or L2 measurements.

- $\alpha = 1, \beta = -1$. This is referred to as wide lane measurement. Narrow lane code and phase measurement which can be computed as:

$$\begin{aligned}\Delta\rho_{WD}^{(i)} &= \lambda_w\left(\frac{\Delta\rho_{L1}^{(i)}}{\lambda_1}-\frac{\Delta\rho_{L2}^{(i)}}{\lambda_2}\right)\\ &= R^{(i)}+c\delta\bar{t}_r+\bar{\epsilon}_{WD}^{(i)}, \qquad (2.62)\\ \lambda_w\Delta\phi_{WD}^{(i)} &= \lambda_w\left(\Delta\phi_{L1}^{(i)}-\Delta\phi_{L2}^{(i)}\right)\\ &= R^{(i)}+c\delta\bar{t}_r+\lambda N_{WD}^{(i)}+\bar{\eta}_{WD}^{(i)} \qquad (2.63)\end{aligned}$$

where $\lambda_w = \dfrac{\lambda_1\lambda_2}{\lambda_1-\lambda_2} \approx 0.862m$ and $N_{WD}^{(i)} = N_{L1}^{(i)} - N_{L2}^{(i)}$. The measurement noise for wide lane code and measurement are $\bar{\epsilon}_{WD}^{(i)} = \lambda_w\left(\dfrac{\bar{\epsilon}_{L1}^{(i)}}{\lambda_1}-\dfrac{\bar{\epsilon}_{L2}^{(i)}}{\lambda_2}\right)$ and $\bar{\eta}_{WD}^{(i)} = \lambda_w\left(\dfrac{\bar{\eta}_{L1}^{(i)}}{\lambda_1}-\dfrac{\bar{\eta}_{L2}^{(i)}}{\lambda_2}\right)$, separately. Wide lane measurements feature in long wavelength, but the measurement noises are also been amplified about 5.7 times.

2.5.2 Bootstrapping

In this approach, the narrow lane pseudorange measurements are used to initialize the estimate of widelane integers $N_{WD}^{(i)}$. With the wide lane integers, the wide lane phase range can then be used to initialize the estimation of L1 integers $N_{L1}^{(i)}$. At this point the L2 and narrow integers can be directly computed.

Differentiating the narrow lane code measurement and wide lane phase measurement yields a float number estimate of the wide lane integer

$$\begin{aligned} \bar{N}_{WD}^{(i)} &= \frac{\Delta\rho_{NR}^{(i)} - \lambda_w \Delta\phi_{WD}^{(i)}}{\lambda_w} \\ &= N_{WD}^{(i)} + \frac{\bar{\epsilon}_{NR}^{(i)} - \bar{\eta}_{WD}^{(i)}}{\lambda_w}. \end{aligned} \tag{2.64}$$

This initial float estimate of wide lane integer estimate $\bar{N}_{WD}^{(i)} \sim \mathcal{N}\left(N_{WD}^{(i)}, \sigma^2_{\bar{N}_{WD}^{(i)}}\right)$, where $\sigma_{\bar{N}_{WD}^{(i)}} \approx 0.837\ cycle^2$. If we search ± 1 integers around the $\bar{N}_{WD}^{(i)}$, the probability that $N_{WD}^{(i)}$ being included in the searching space is only 72.9%. If we increase the searching space to be ± 2 around $\bar{N}_{WD}^{(i)}$, the probability increases to 97.2%, which gives us 5 candidates to search per satellite.

To search the the L1 integer $N_{L1}^{(i)}$, following the same methodology, we initialize the float estimate $\bar{N}_{L1}^{(i)} = \dfrac{\hat{R}_{WD}^{(i)} - \lambda_1 \Delta\phi_{L1}^{(i)}}{\lambda_1}$, it can be computed that the mean and covariance of $\bar{N}_{L1}^{(i)}$ are

$$\begin{aligned} \mu_{\bar{N}_{L1}^{(i)}} &= N_{L1}^{(i)}\ cycle \\ \sigma^2_{\bar{N}_{L1}^{(i)}} &= [\frac{1}{\lambda_1}, -\frac{1}{\lambda_1}] \begin{bmatrix} (0.11m)^2 & 0 \\ 0 & (0.02m)^2 \end{bmatrix} \begin{bmatrix} \frac{1}{\lambda_1} \\ -\frac{1}{\lambda_1} \end{bmatrix} = (0.588\ cycle)^2 \end{aligned}$$

If we search ± 1 integers around the $\bar{N}_{L1}^{(i)}$, the probability that $N_{L1}^{(i)}$ being included in the searching space is 91.1%. This gives us 3 candidates to search per satellite.

Therefore, if we apply the integer estimate algorithm with bootstrapping, the usual number of candidates to search is: $5^4 + 3^4 = 706$. With K satellites in view, there will be K measurements for each searching process.

2.5.3 Batch

In this approach, the various measurements are stacked as a column measurement and the integer vector is jointly solved in a batch process. For typical L1/L2 receivers, the narrow lane pseudorange measurements are used to initialize both the L1 and L2 integers.

The initialize the float estimate of L1 and L2 integers are:

$$\begin{aligned} \bar{N}_{L1}^{(i)} &= \frac{\Delta\rho_{NR}^{(i)} - \lambda_1 \Delta\phi_{L1}^{(i)}}{\lambda_1} \\ \bar{N}_{L2}^{(i)} &= \frac{\Delta\rho_{NR}^{(i)} - \lambda_2 \Delta\phi_{L2}^{(i)}}{\lambda_1} \end{aligned}$$

, then the mean and covariance of $\bar{N}_{L1}^{(i)}$ are

$$\begin{aligned} \mu_{\bar{N}_{L1}^{(i)}} &= N_{L1}^{(i)}\ cycle \\ \sigma^2_{\bar{N}_{L1}^{(i)}} &= [\frac{1}{\lambda_1}, -\frac{1}{\lambda_1}] \begin{bmatrix} (0.71m)^2 & 0 \\ 0 & (0.02m)^2 \end{bmatrix} \begin{bmatrix} \frac{1}{\lambda_1} \\ -\frac{1}{\lambda_1} \end{bmatrix} = (3.74\ cycle)^2 \\ \mu_{\bar{N}_{L1}^{(i)}} &= N_{L1}^{(i)}\ cycle \\ \sigma^2_{\bar{N}_{L1}^{(i)}} &= [\frac{1}{\lambda_2}, -\frac{1}{\lambda_2}] \begin{bmatrix} (0.71m)^2 & 0 \\ 0 & (0.02m)^2 \end{bmatrix} \begin{bmatrix} \frac{1}{\lambda_2} \\ -\frac{1}{\lambda_2} \end{bmatrix} = (2.91\ cycle)^2 \end{aligned}$$

If we search ± 6 integers around the $\left[\bar{N}_{L1}^{(i)}\ \bar{N}_{L1}^{(i)}\right]^\top$, the probabilities that the correct L1 and L2 integers being included in the searching space are 89.0% and 96.1%. This gives us 13 candidates to search per satellite.

Therefore, if we apply the integer estimate algorithm with batch strategy, the usual number of candidates to search is: $13^4 = 28561$. However, with K satellites in view, there will be $2K$ measurements the searching process, which will increase the chance to get the correct integer estimate.

2.6 Test Results

Tests for the proposed method have been performed both in MATLAB simulations and on GPS hardware.

2.6.1 Simulation Results

In the MATLAB simulations, the test is epoch-by-epoch with a set of double difference GPS carrier phase measurements. For each noise level, 1000 measurement epochs with randomly picked satellite elevation and azimuth angles were generated. We use the LMS algorithm, LAMBDA algorithm and the proposed algorithm to estimate the integer ambiguity and compare with the true one, and the success rates are calculated thereby. The success rate of each method is plot versus different noise level in Fig. 2.4.

From the figure, we can see that with 8 double difference GPS measurement, the proposed method has similar performance to the LAMBDA algorithm, which has a higher success rate than LMS.

The computation time is also compared. The test is carried out using MATLAB in a Laptop with Genuine Intel CPU with frequency $1.60GHz$ and $1GB$ of RAM, and the computation for Z-transform follows the algorithm presented by Jonge *et al.* [12]. For each number of measurements K, 1000 sets of data are generated and the average computation

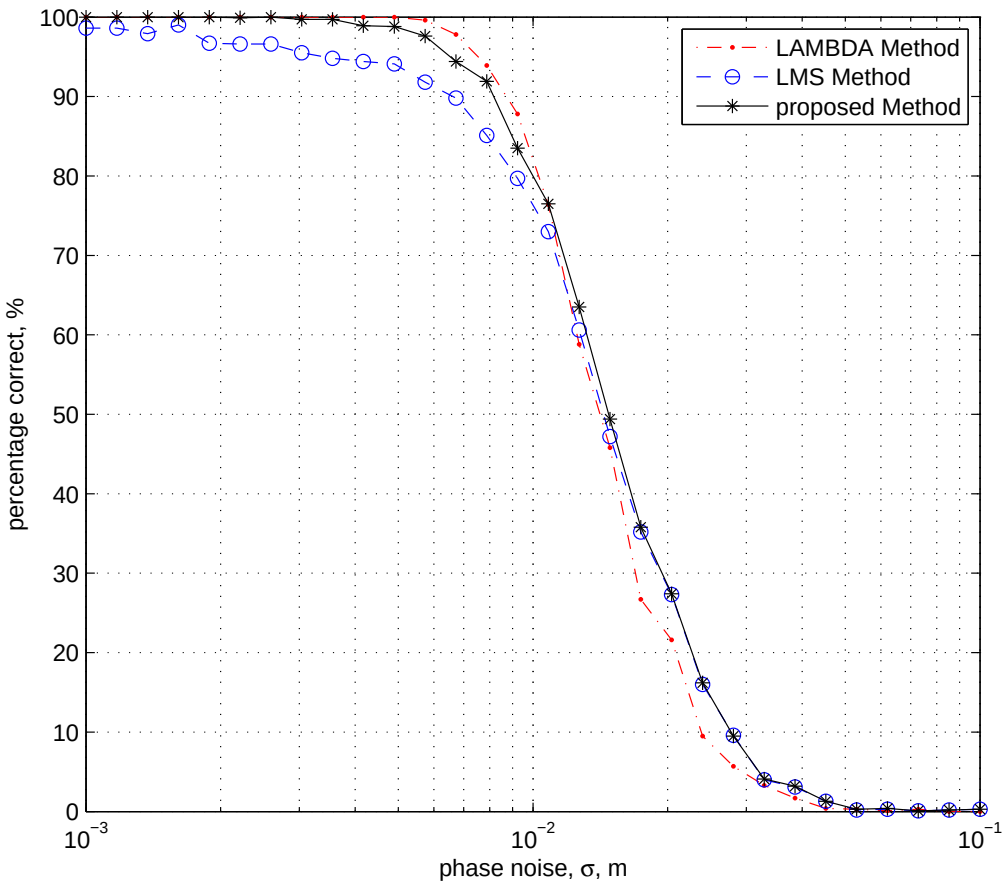

Figure 2.4: Rate of correct integer resolution vs. phase measurement noise

for each method are listed in Table 2.1.

2.6.2 Test Results with Real-world Data

Using real-world data, two sets of tests were performed over baselines of $6m$ and $5km$. Each test used each epoch of data separately. The data from each epoch included dual-frequency, double-differenced data from eight satellites. For the $6m$ baseline, the test included 6002 data epochs. Using LMS the success rate was 87.1% while for the proposed

Table 2.1: Computation time of LMS, LAMBDA and the proposed method, in ms

K	LMS	LAMBDA	Proposed Method
6	1.95	5.17	3.03
7	1.96	6.81	3.26
8	1.97	9.73	3.56
9	2.03	13.6	3.93
10	2.06	18.1	4.27
11	2.08	24.5	4.76

Table 2.2: Rate of correct integer resolution of LMS and proposed method, from real-world data

Baseline	Num of Epoches	LMS	Proposed Method
6m	6002	87.1%	90.6%
5Km	3005	66.1%	68.0%

algorithm the success rate was 90.6%. For the $5km$ baseline, 3005 data epochs was included in the test data and the success rates were 66.1% for LMS and 68.0% for the proposed algorithm, respectively. These results confirmed that the proposed method has a better success rate than the LMS method and less computational complexity than the LAMBDA method.

Two tests with real-world data with dual-frequency signal from 8 satellites were performed over baselines of $6m$ and $5km$. Each test used each epoch of data separately using bootstrapping strategy. We compare the success rate of LMS and the proposed method and show them in Table 2.2.

2.7 Chapter Summary

In this Chapter, we briefly introduced the model of GPS code and phase measurements, and led to the proposal of the GPS integer ambiguity problem, which is the key challenge

to high-precision GPS positioning. After a brief review of existing algorithms, we proposed a new integer ambiguity estimation algorithm by combing two of the leading algorithms, LMS and LAMBDA. The applicability and effectiveness of the the proposed algorithm were shown by both simulations and real-world data.

Chapter 3

GPS Integer Ambiguity Resolution with Auxiliary Measurements

In many navigation applications, external sensors are available which can provide auxiliary measurements to improve integer ambiguity resolution achieved by only using GPS, especially in GPS challenging conditions (e.g., few satellites available, high measurement noise due to multipath). For example, in land vehicle control and guidance, the altitude of the roadway as a function of arclength might be available. In [8], a fast and efficient technique was proposed to solve GPS integer ambiguity with altitude aiding. The disadvantage of this method is that the accurate altitude information is only available in limited trajectories.

3.1 Introduction

Integrated GPS/INS (Inertial Navigation System) is a popular tool for localization [13, 14] and has been extensively studied over the last couple of decades. Localization accuracies of a few centimeters can be achieved using carrier phase processing given rapid and accurate on-the-fly integer ambiguity resolution. One of the main advantages of GPS/INS integration over a stand-alone GPS system is the capability of the former to maintain the accuracy of the position estimate during short GPS denied periods. This INS state estimate can be used to facilitate GPS integer ambiguity resolution which is the topic of this chapter. This would be helpful especially in GPS challenging areas (e.g. urban canyons, tunnels, thick canopy etc.) where the GPS receiver may not be able to track a sufficient number of satellites to resolve the integer ambiguities.

Incorporating INS measurements in GPS integer ambiguity resolution has been studied in [31], in which the INS data were used to reduce integer searching space. However, in [31], the closed form of the searching space was not derived, and the weighting factor between GPS and INS measurements are based on experiences, both of which reduce the computation efficiency and estimation performance of the algorithm.

In this chapter, we extend the approach in Chapter 2 with auxiliary position estimate measurements from INS. We will introduce a fast and efficient method for GPS integer ambiguity resolution as well as its theoretical derivation. Two sets of simulations will be carried out to show the effectiveness of the proposed approach.

3.2 Measurement Model

3.2.1 GPS Residual Measurements

The GPS phase residual measurement is as defined in Eqn. (2.14).

3.2.2 INS Measurements

In most navigation systems, GPS cooperates with other sensors to offer continuous positioning information. A typical such application is GPS/INS systems [13, 14].

In GPS/INS systems, INS will keep propagating the navigation states and the covariance matrix of the estimate error during GPS outage. Assuming that at some time, the position estimate from INS is $\delta\hat{\mathbf{p}}$ with covariance $\mathbf{\Sigma_p}$. This information from the INS can be represent as

$$\delta\hat{\mathbf{p}} = \mathbf{J}\ \mathbf{x} + \mathbf{n}, \tag{3.1}$$

where $\mathbf{J} \in \mathbb{R}^{p\times n}$, and $\mathbf{n} \in \mathbb{R}^p$ with $cov(\mathbf{n}) = \mathbf{\Sigma_p}$, $\mathbf{x}$ is as defined in Eqn. (2.13). In typical GPS/INS systems, $p = 3$ and $\mathbf{J} = \begin{bmatrix} \mathbf{I} & \mathbf{0} \end{bmatrix}$, as the INS state keeps track of the 3 dimensional position but not the receiver clock bias. This prior knowledge of $\delta\hat{\mathbf{p}}$ from the INS can facilitate GPS integer ambiguity resolution.

3.3 Problem Statement

INS aided GPS integer ambiguity problem can be modeled as a Bayesian problem, which is, given the prior of GPS measurements $\mathbf{y} = \mathbf{G}\mathbf{x} + \mathbf{N} + \boldsymbol{v}$ as in Eqn. (2.14) and INS

measurements of $\mathbf{J}\ \mathbf{x} \sim \mathcal{N}\left(\delta\hat{\mathbf{p}}, \boldsymbol{\Sigma}_{\boldsymbol{p}}\right)$, we would like to find the estimate of $\mathbf{N}$ and $\mathbf{x}$ that

$$\left(\hat{\mathbf{N}}, \hat{\mathbf{x}}\right) = \arg \max_{\mathbf{N}\in\mathbb{Z}^m, \mathbf{x}\in\mathbb{R}^n} f\left(\mathbf{N}, \mathbf{x}|\mathbf{y}\right).$$

According to Bayesian Rule,

$$\left(\hat{\mathbf{N}}, \hat{\mathbf{x}}\right) = \arg \max_{\mathbf{N}\in\mathbb{Z}^m, \mathbf{x}\in\mathbb{R}^n} \frac{f\left(\mathbf{y}|\mathbf{N}, \mathbf{x}\right) f\left(\mathbf{N}|\mathbf{x}\right) f\left(\mathbf{x}\right)}{f\left(\mathbf{y}\right)}$$

As there is no uncertainty in $\mathbf{N}$ given $\mathbf{x}$ and $f\left(\mathbf{y}\right)$ is independent of $\mathbf{x}$ and $\mathbf{N}$,

$$\begin{aligned}\left(\hat{\mathbf{N}}, \hat{\mathbf{x}}\right) &= \arg \max_{\mathbf{N}\in\mathbb{Z}^m, \mathbf{x}\in\mathbb{R}^n} f\left(\mathbf{y}|\mathbf{N}, \mathbf{x}\right) f\left(\mathbf{x}\right) \\ &= \arg \max_{\mathbf{N}\in\mathbb{Z}^m, \mathbf{x}\in\mathbb{R}^n} \ln\left(f\left(\mathbf{y}|\mathbf{N}, \mathbf{x}\right) f\left(\mathbf{x}\right)\right). \end{aligned} \tag{3.2}$$

As

$$f\left(\mathbf{y}|\mathbf{N}, \mathbf{x}\right) = \frac{e^{-\frac{1}{2}(\mathbf{y}-\mathbf{G}\mathbf{x}-\mathbf{N})^T \Sigma_{vv}^{-1}(\mathbf{y}-\mathbf{G}\mathbf{x}-\mathbf{N})}}{\left(2\pi\right)^{K/2} \left|\bar{\boldsymbol{\Sigma}}_{vv}\right|^{1/2}}$$

and

$$f\left(\mathbf{x}\right) = f\left(\mathbf{J}\ \mathbf{x}\right) = \frac{e^{-\frac{1}{2}(\mathbf{J}\mathbf{x}-\delta\hat{\mathbf{p}})^T \boldsymbol{\Sigma}_{\boldsymbol{p}}^{-1}(\mathbf{J}\mathbf{x}-\delta\hat{\mathbf{p}})}}{\left(2\pi\right)^{p/2} \left|\boldsymbol{\Sigma}_{\boldsymbol{p}}\right|^{1/2}},$$

we have

$$\begin{aligned}\left(\hat{\mathbf{N}}, \hat{\mathbf{x}}\right) &= \arg \max_{\mathbf{N}\in\mathbb{Z}^m, \mathbf{x}\in\mathbb{R}^n} \ln\left(\frac{e^{-\frac{1}{2}(\mathbf{y}-\mathbf{G}\mathbf{x}-\mathbf{N})^T \Sigma_{vv}^{-1}(\mathbf{y}-\mathbf{G}\mathbf{x}-\mathbf{N})}}{\left(2\pi\right)^{K/2} \left|\bar{\boldsymbol{\Sigma}}_{vv}\right|^{1/2}} \cdot \frac{e^{-\frac{1}{2}(\mathbf{J}\mathbf{x}-\delta\hat{\mathbf{p}})^T \boldsymbol{\Sigma}_{\boldsymbol{p}}^{-1}(\mathbf{J}\mathbf{x}-\delta\hat{\mathbf{p}})}}{\left(2\pi\right)^{p/2} \left|\boldsymbol{\Sigma}_{\boldsymbol{p}}\right|^{1/2}}\right) \\ &= \arg \max_{\mathbf{N}\in\mathbb{Z}^m, \mathbf{x}\in\mathbb{R}^n} \Big(\left(\mathbf{y}-\mathbf{G}\mathbf{x}-\mathbf{N}\right)^T \Sigma_{vv}^{-1} \left(\mathbf{y}-\mathbf{G}\mathbf{x}-\mathbf{N}\right) \\ &\qquad + \left(\mathbf{J}\mathbf{x}-\delta\hat{\mathbf{p}}\right)^T \boldsymbol{\Sigma}_{\boldsymbol{p}}^{-1} \left(\mathbf{J}\mathbf{x}-\delta\hat{\mathbf{p}}\right)\Big) \end{aligned} \tag{3.3}$$

We reformulate the measurements by stacking the INS prior with GPS only measurements as

$$\bar{\mathbf{y}} = \bar{\mathbf{G}}\mathbf{x} + \mathbf{L}\mathbf{N} + \bar{\mathbf{n}} \tag{3.4}$$

where the new measurement vector $\bar{\mathbf{y}}^\top = \begin{bmatrix} \mathbf{y}^\top & \delta\hat{\mathbf{p}}^\top \end{bmatrix} \in \mathbb{R}^{K+p}$, the new measurement noise vector $\bar{\mathbf{n}}^\top = \begin{bmatrix} \mathbf{v}^\top & \mathbf{n}^\top \end{bmatrix} \in \mathbb{R}^{K+p}$, and $\bar{\mathbf{G}}^\top = \begin{bmatrix} \mathbf{G}^\top & \mathbf{J}^\top \end{bmatrix} \in \mathbb{R}^{(K+p)\times n}$, $\mathbf{L}^\top = \begin{bmatrix} \mathbf{I} & \mathbf{0} \end{bmatrix} \in \mathbb{R}^{(K+p)\times K}$. For the simplicity of notation, let $m = K + p$.

As INS state uncertainty $\mathbf{n}$ is not correlated with GPS measurement noise $\mathbf{v}$, the covariance matrix of the whole measurement noise vector is

$$\bar{\mathbf{\Sigma}} = cov\left(\begin{bmatrix} \mathbf{v} \\ \mathbf{n} \end{bmatrix}\right) = \begin{bmatrix} \bar{\mathbf{\Sigma}}_{vv} & \mathbf{0} \\ \mathbf{0} & \mathbf{\Sigma}_{\boldsymbol{p}} \end{bmatrix}. \tag{3.5}$$

Our objective is to find $\mathbf{N} \in \mathbb{Z}^K$, $\mathbf{x} \in \mathbb{R}^n$ that minimize the cost function

$$\begin{aligned} c(\mathbf{x}, \mathbf{N}) &= (\mathbf{y} - \mathbf{G}\mathbf{x} - \mathbf{L}\mathbf{N})^T \mathbf{\Sigma}_{\boldsymbol{vv}}^{-1} (\mathbf{y} - \mathbf{G}\mathbf{x} - \mathbf{L}\mathbf{N}) + (\mathbf{J}\mathbf{x} - \delta\hat{\mathbf{p}})^T \mathbf{\Sigma}_{\boldsymbol{p}}^{-1} (\mathbf{J}\mathbf{x} - \delta\hat{\mathbf{p}}) \\ &= \left(\bar{\mathbf{y}} - \bar{\mathbf{G}} \cdot \mathbf{x} - \mathbf{L}\mathbf{N}\right)^\top \bar{\mathbf{\Sigma}}^{-1} \left(\bar{\mathbf{y}} - \bar{\mathbf{G}} \cdot \mathbf{x} - \mathbf{L}\mathbf{N}\right) \\ &= \|\bar{\mathbf{y}} - \bar{\mathbf{G}} \cdot \mathbf{x} - \mathbf{L}\mathbf{N}\|^2_{\bar{\mathbf{\Sigma}}}. \end{aligned} \tag{3.6}$$

3.4 Integer Ambiguity Resolution

3.4.1 Generating Searching Candidates

Implementing method described in Chapter 2 on Eqn. (3.4) yields the following derivation. For a given integer ambiguity $\mathbf{N}$, the weighted least square estimate of $\mathbf{x}$ would be:

$$\hat{\mathbf{x}} = \left(\bar{\mathbf{G}}^T \bar{\mathbf{\Sigma}}^{-1} \bar{\mathbf{G}}\right)^{-1} \bar{\mathbf{G}}^T \bar{\mathbf{\Sigma}}^{-1} (\bar{\mathbf{y}} - \mathbf{L}\mathbf{N}) \tag{3.7}$$

and the residual vector is

$$\begin{aligned} \hat{\boldsymbol{\varepsilon}} &= \bar{\mathbf{y}} - \bar{\mathbf{G}}\hat{\mathbf{x}} - \mathbf{L}\mathbf{N} \\ &= \left(\mathbf{I} - \bar{\mathbf{G}} \left(\bar{\mathbf{G}}^T \bar{\mathbf{G}}\right)^{-1} \bar{\mathbf{\Sigma}}^{-1} \bar{\mathbf{G}}^T \bar{\mathbf{\Sigma}}^{-1}\right) (\bar{\mathbf{y}} - \mathbf{L}\mathbf{N}) \\ &= \bar{\mathbf{Q}}_{\boldsymbol{\Sigma}} (\bar{\mathbf{y}} - \mathbf{L}\mathbf{N}). \end{aligned} \tag{3.8}$$

where

$$\bar{\mathbf{P}}_{\mathbf{\Sigma}} = \bar{\mathbf{G}}\left(\bar{\mathbf{G}}^T\bar{\mathbf{\Sigma}}^{-1}\bar{\mathbf{G}}\right)^{-1}\bar{\mathbf{G}}^T\bar{\mathbf{\Sigma}}^{-1}, \tag{3.9}$$

$$\bar{\mathbf{Q}}_{\mathbf{\Sigma}} = \mathbf{I} - \bar{\mathbf{P}}_{\mathbf{\Sigma}}. \tag{3.10}$$

Note that both $\bar{\mathbf{P}}_{\mathbf{\Sigma}}$ and $\bar{\mathbf{Q}}_{\mathbf{\Sigma}}$ are idempotent and that $Rank(\bar{\mathbf{P}}) = n$ and $Rank(\bar{\mathbf{Q}}) = (m-n)$. This can be proved by the same token presented in Chapter 2. The detailed proof is presented in [4].

From Eqn. (3.6), the cost function evaluated from candidate $\mathbf{N}$ is

$$\begin{aligned} c(\mathbf{N}) &= \|\bar{\mathbf{y}} - \bar{\mathbf{G}}\cdot\mathbf{x} - \mathbf{LN}\|^2_{\bar{\mathbf{\Sigma}}} \\ &= \|\bar{\mathbf{Q}}_{\mathbf{\Sigma}}(\bar{\mathbf{y}} - \mathbf{LN})\|^2_{\bar{\mathbf{\Sigma}}} \\ &= (\bar{\mathbf{y}} - \mathbf{LN})^\top\bar{\mathbf{Q}}_{\mathbf{\Sigma}}^\top\bar{\mathbf{\Sigma}}^{-1}\bar{\mathbf{Q}}_{\mathbf{\Sigma}}(\bar{\mathbf{y}} - \mathbf{LN}) \\ &= (\bar{\mathbf{y}} - \mathbf{LN})^\top\bar{\mathbf{Q}}_0(\bar{\mathbf{y}} - \mathbf{LN}) \end{aligned} \tag{3.11}$$

where

$$\bar{\mathbf{Q}}_0 = \bar{\mathbf{Q}}_{\mathbf{\Sigma}}^\top\bar{\mathbf{\Sigma}}^{-1}\bar{\mathbf{Q}}_{\mathbf{\Sigma}} \tag{3.12}$$

Then $\bar{\mathbf{Q}}_0$ also has the rank $(m-n)$.

Let the SVD (single value decomposition) of $\bar{\mathbf{Q}}_0$ be

$$\bar{\mathbf{Q}}_0 = \bar{\mathbf{U}}\bar{\mathbf{S}}^2\bar{\mathbf{U}}^\top,$$

where $\bar{\mathbf{U}}$ is unitary and $\bar{\mathbf{S}}$ is diagonal with $diag(\bar{\mathbf{S}}) = [\bar{s}_1, \ldots, \bar{s}_{m-n}, 0, \ldots, 0]$ with all $\bar{s}_i > 0$ for $i = 1, \ldots, m-n$.

Define $\bar{\mathbf{B}} = \bar{\mathbf{S}}\bar{\mathbf{U}}^\top$ such that

$$\bar{\mathbf{Q}}_0 \;=\; \bar{\mathbf{B}}^\top \bar{\mathbf{B}} \tag{3.13}$$

where the last n rows of $\mathbf{B}$ are zero.

As the last n rows of $\bar{\mathbf{B}}$ are zero, matrix $\bar{\mathbf{B}}$ can be represent as

$$\bar{\mathbf{B}} = \begin{bmatrix} \bar{\mathbf{A}} \\ \\ \mathbf{0} \end{bmatrix} = \begin{bmatrix} \bar{\mathbf{C}} & \bar{\mathbf{D}} & \bar{\mathbf{E}} \\ \\ \mathbf{0} & \mathbf{0} & \mathbf{0} \end{bmatrix},$$

where $\bar{\mathbf{A}} \in \mathbb{R}^{(m-n)\times m}$, $\bar{\mathbf{C}} \in \mathbb{R}^{(m-n)\times(K-n)}$, $\bar{\mathbf{D}} \in \mathbb{R}^{(m-n)\times n}$ and $\bar{\mathbf{E}} \in \mathbb{R}^{(m-n)\times p}$.

Given the above analysis, the cost function of Eqn. (3.11) can be rewritten as

$$\begin{aligned} c(\mathbf{N}) &= (\bar{\mathbf{y}} - \mathbf{L}\mathbf{N})^\top \bar{\mathbf{B}}^\top \bar{\mathbf{B}} (\bar{\mathbf{y}} - \mathbf{L}\mathbf{N}) \\ &= \|\bar{\mathbf{B}}\,(\bar{\mathbf{y}} - \mathbf{L}\mathbf{N})\,\|^2. \end{aligned} \tag{3.14}$$

Because $\bar{\mathbf{B}}$ does not have full rank, the null space of $\mathbf{B}$ is not empty. Therefore, there exists (non-unique) $\hat{\mathbf{N}} \in \mathbb{R}^m$ such that $(\bar{\mathbf{y}} - \mathbf{L}\hat{\mathbf{N}})$ is in the null space of $\bar{\mathbf{B}}$:

$$\bar{\mathbf{B}}(\bar{\mathbf{y}} - \mathbf{L}\hat{\mathbf{N}}) = \mathbf{0}. \tag{3.15}$$

Let the last n elements of $\hat{\mathbf{N}}$ to be integers. We denote this subvector as $\hat{\mathbf{N}}_D$. Our goal is to find $\hat{\mathbf{N}}$ such that

$$\bar{\mathbf{B}}\bar{\mathbf{y}} = \bar{\mathbf{B}}\mathbf{L}\hat{\mathbf{N}} \tag{3.16}$$

$$
\begin{aligned}
\begin{bmatrix} \bar{\mathbf{A}} \\ \mathbf{0} \end{bmatrix} \bar{\mathbf{y}} &= \begin{bmatrix} \bar{\mathbf{A}} \\ \mathbf{0} \end{bmatrix} \begin{bmatrix} \mathbf{I} \\ \mathbf{0} \end{bmatrix} \hat{\mathbf{N}} \\
\begin{bmatrix} \bar{\mathbf{A}} \\ \mathbf{0} \end{bmatrix} \bar{\mathbf{y}} &= \begin{bmatrix} \bar{\mathbf{C}} & \bar{\mathbf{D}} & \bar{\mathbf{E}} \\ \mathbf{0} & \mathbf{0} & \mathbf{0} \end{bmatrix} \begin{bmatrix} \mathbf{I} \\ \mathbf{0} \end{bmatrix} \begin{bmatrix} \hat{\mathbf{N}}_C \\ \hat{\mathbf{N}}_D \end{bmatrix} \\
\begin{bmatrix} \bar{\mathbf{A}} \\ \mathbf{0} \end{bmatrix} \bar{\mathbf{y}} &= \begin{bmatrix} \bar{\mathbf{C}} & \bar{\mathbf{D}} \\ \mathbf{0} & \mathbf{0} \end{bmatrix} \begin{bmatrix} \hat{\mathbf{N}}_C \\ \hat{\mathbf{N}}_D \end{bmatrix} \\
\begin{bmatrix} \bar{\mathbf{A}} \\ \mathbf{0} \end{bmatrix} \bar{\mathbf{y}} &= \begin{bmatrix} \bar{\mathbf{C}}\hat{\mathbf{N}}_C + \bar{\mathbf{D}}\hat{\mathbf{N}}_D \\ \mathbf{0} \end{bmatrix} \\
\bar{\mathbf{A}}\bar{\mathbf{y}} &= \bar{\mathbf{C}}\hat{\mathbf{N}}_C + \bar{\mathbf{D}}\hat{\mathbf{N}}_D,
\end{aligned}
$$

Therefore, if we decompose $\mathbf{y}$ as $\mathbf{y} = \begin{bmatrix} \mathbf{y}_C^\top & \mathbf{y}_D^\top \end{bmatrix}^\top$ with $\mathbf{y}_C \in \mathbb{R}^{(K-n)}$ and $\mathbf{y}_D \in \mathbb{R}^n$ and given a hypothesized vector $\hat{\mathbf{N}}_D \in \mathbb{Z}^n$, then the real-value estimate of $\hat{\mathbf{N}}_C$ is:

$$
\begin{aligned}
\hat{\mathbf{N}}_C &= \left(\bar{\mathbf{C}}^\top \bar{\mathbf{C}}\right)^{-1} \bar{\mathbf{C}}^\top \left(\bar{\mathbf{A}}\bar{\mathbf{y}} - \bar{\mathbf{D}}\hat{\mathbf{N}}_D\right) \\
&= \mathbf{y}_C + \left(\bar{\mathbf{C}}^\top \bar{\mathbf{C}}\right)^{-1} \bar{\mathbf{C}}^\top \left(\bar{\mathbf{E}}\delta\hat{\mathbf{p}} + \bar{\mathbf{D}}\left(\mathbf{y}_D - \hat{\mathbf{N}}_D\right)\right), \qquad (3.17)
\end{aligned}
$$

In Eqn. (3.17), other than the information from GPS measurements, the information from INS states is also involved in calculation, represented as the term $\bar{\mathbf{E}}\hat{\mathbf{x}}_{a0}$.

From Eqn. (3.17), the integer candidates $\hat{\mathbf{N}}_D$ can be searched exhaustively over some finite range of integers as described in Fig. 3.1.

3.4.2 Rounding $\hat{\mathbf{N}}_C$

Having $\hat{\mathbf{N}}_C$, to get the optimal integer estimate of $\mathbf{N}_C$, we would like to find an integer vector $\check{\mathbf{N}}_C$ which is close to $\hat{\mathbf{N}}_C$. As discussed in Chapter 2, we would like to find $\check{\mathbf{N}}_C$ to

```
for i = −d : d
    for j = −d : d
        for k = −d : d
            N_D = [i, j, k, 0]^⊤
            N̂_C = y_C + (C̄^⊤ C̄)^{−1} C̄^⊤ (Ē x̂_{a0} + D̄ (y_D − N̂_D))
            ... use N̂_C to compute Ň_C minimizing J(N_C)
            N^⊤ = [ Ň_C   N_D ]^⊤
            if c(N) < current minimum
                Save N
                current minimum = c(N)
            ⋮
```

Figure 3.1: Triple 'for' loop to compute $\hat{\mathbf{N}}_C$ and $\mathbf{N}$ for the case where $n = 4$.

minimize the cost function

$$\begin{aligned} J(\mathbf{N}_C) &= \|\mathbf{N}_C - \hat{\mathbf{N}}_C\|^2_{\boldsymbol{\Sigma}_{\hat{\mathbf{N}}_C}} \\ &= (\mathbf{N}_C - \hat{\mathbf{N}}_C)^\top \boldsymbol{\Sigma}^{-1}_{\hat{\mathbf{N}}_C} (\mathbf{N}_C - \hat{\mathbf{N}}_C), \end{aligned} \tag{3.18}$$

where the covariance of $\hat{\mathbf{N}}_C$

$$\begin{aligned} \boldsymbol{\Sigma}_{\hat{\mathbf{N}}_C} &= \boldsymbol{\Sigma}_{CC} + \left(\bar{\mathbf{C}}^\top \bar{\mathbf{C}}\right)^{-1} \bar{\mathbf{C}} \\ &\qquad \left(\bar{\mathbf{E}} \bar{\mathbf{P}} \bar{\mathbf{E}}^\top + \bar{\mathbf{D}} \boldsymbol{\Sigma}_{DD} \bar{\mathbf{D}}^\top\right) \bar{\mathbf{C}}^\top \left(\bar{\mathbf{C}}^\top \bar{\mathbf{C}}\right)^{-\top}, \\ \boldsymbol{\Sigma}_{CC} &= cov(\mathbf{y}_C), \\ \boldsymbol{\Sigma}_{DD} &= cov(\mathbf{y}_D), \end{aligned} \tag{3.19}$$

from Eqn. (3.17).

By the same token as in Chapter 2, we can prove that the cost function $c(\mathbf{N})$ defined in Eqn. (3.11) will be minimized by the same integer estimate that minimize $J(\mathbf{N}_C)$ defined in Eqn. (3.18) [4].

To find the integer vector that minimizes Eqn. (3.18), we follow the idea of LAMBDA to find a matrix $\boldsymbol{Z} \in \mathbb{Z}^{(m-n)\times(m-n)}$, such that $\boldsymbol{Z}^{-1} \in \mathbb{Z}^{(m-n)\times(m-n)}$, and $(\boldsymbol{Z}\boldsymbol{\Sigma}_{\hat{N}_C}\boldsymbol{Z}^\top)^{-1}$ is nearly diagonal. The procedure is the same as we discussed in Chapter 2.

The integer-valued estimate of $\mathbf{N}_C$ can be computed as:

$$\hat{\mathbf{M}}_C = \boldsymbol{Z}\hat{\mathbf{N}}_C \tag{3.20}$$

$$\check{\mathbf{M}}_C = [\hat{\mathbf{M}}_C]_{roundoff} \tag{3.21}$$

$$\check{\mathbf{N}}_C = \boldsymbol{Z}^{-1}\check{\mathbf{M}}_C. \tag{3.22}$$

At this point we have an integer vector candidate $\left[\check{\mathbf{N}}_C^\top \mathbf{N}_D^\top\right]^\top$. One such candidate will be generated for each iteration of the 'for' loop in Fig. 3.1. We can compare each integer vector candidate using Eqn. (3.11). The candidate vector with the lowest value (subject to validity tests) is chosen as the best. By rounding off the float estimate $\hat{\mathbf{N}}_C$ in the decorrelated domain of $\hat{\mathbf{M}}_C$, we have a better chance to achieve optimal integer estimate $\check{\mathbf{N}}_C$.

3.5 Test Results

Two sets of tests for the proposed method have been performed both via MATLAB simulations.

3.5.1 Tests Over Different Noise Levels

In this set of MATLAB simulations, the tests are epoch-by-epoch with a set of single difference GPS L1 ($\lambda \approx 0.19m$) carrier phase measurements with $K = 8$ at different noise levels. For each noise level, 1000 measurement epochs with randomly picked satellite eleva-

tion and azimuth angles were generated. We compared the success rate of getting all the integers correctly with GPS only and with INS aiding with different noise levels. The success rates of GPS only resolution and GPS aided by INS with different level of covariances are plotted versus different noise levels in Fig. 3.2.

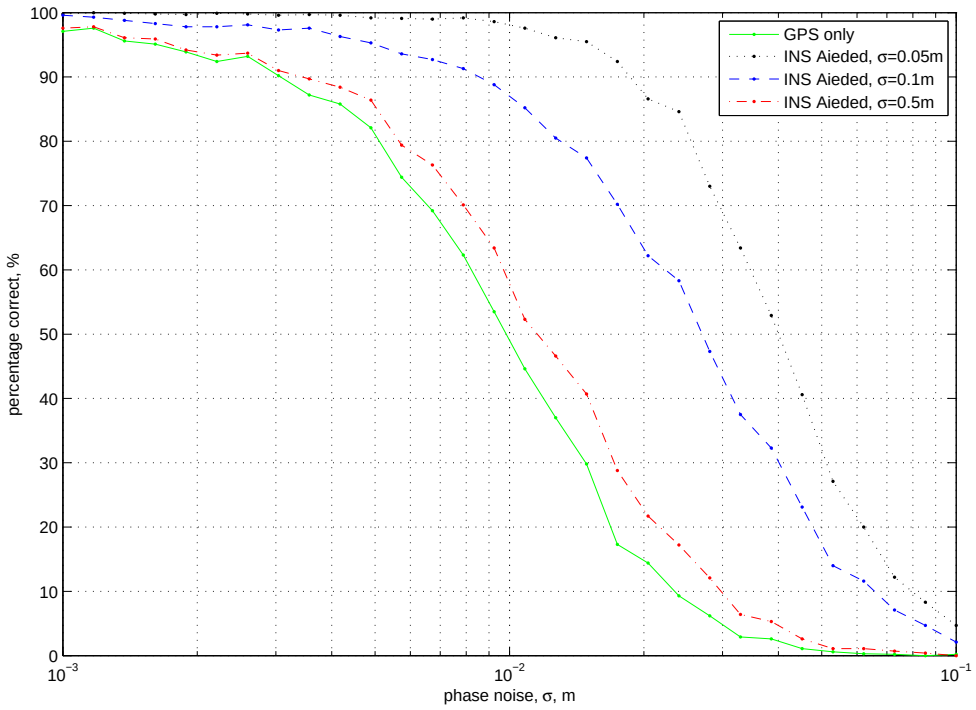

Figure 3.2: Rate of correct integer resolution vs. phase measurement noise

From the figure, we can see that the success rate with INS aiding is significantly improved. Even when the standard deviation of INS position estimate is as big as $0.5m$ (which is more than 2.5 times the wavelength), the success rate is still better than the GPS only resolution.

3.5.2 Tests Over Different Number of Satellites

The second set of tests is performed to show the performance of proposed approach over different number of satellites. For each number of satellites, 1000 measurement epochs with randomly picked satellite elevation and azimuth angles were generated with standard deviation of each phase measurement be $0.01m$ and standard deviation of INS position estimate be $0.1m$. We compared the success rate of getting all the integers correctly in single epoch. The success rate of each method is plotted versus the number of available satellites in Fig. 3.3.

From the figure, we can see that INS aiding improved the chance to get correct GPS integers, especially when the number of satellites is low. For example, with 5 satellites in view, it's unlikely to get a correct integer ambiguity with GPS only method while the success rate has been improved to 67% with INS aiding.

3.6 Chapter Summary

In this Chapter, we considered GPS integer ambiguity estimation problem with auxiliary information from inertial sensors. We formed the measurement model so that the problem can be solved by similar methodology proposed in Chapter 2. Simulation results indicated that by incorporating the measurement from INS, we have better chances to get the correct integer estimate, especially in GPS challenging areas where the number of satellites are limited or has bigger measurement noise.

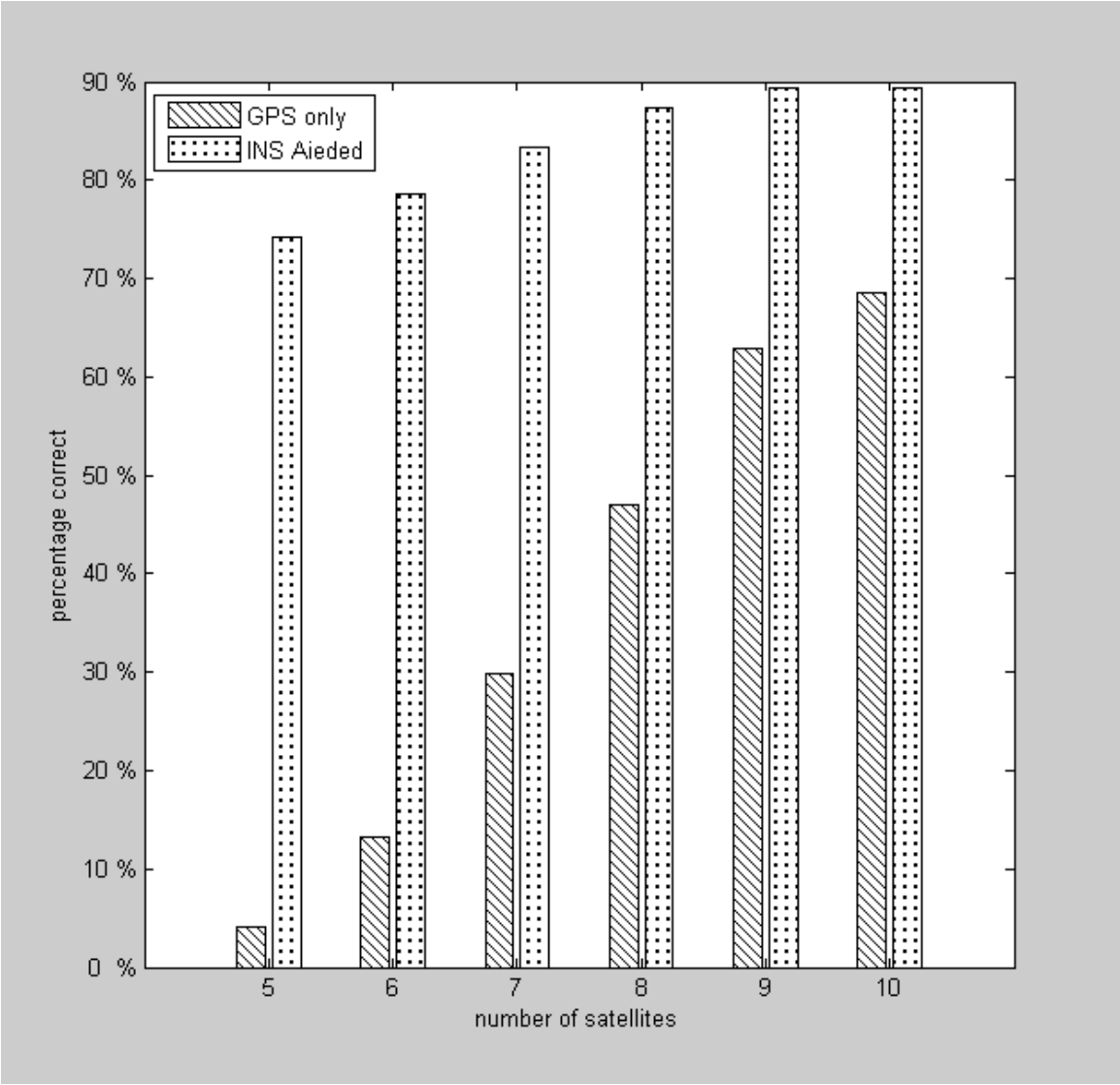

Figure 3.3: Rate of correct integer resolution vs. number of available satellites

Chapter 4

Integer Ambiguity Resolution with Multiple Epoches

4.1 Introduction

In GPS challenging areas (e.g. urban canyons, tunnels, thick canopy etc.) the GPS receiver may not be able to track a sufficient number of satellites to resolve the integer ambiguities within one epoch. In this chapter, we would like to find the optimal solution by combining the measurements from several epoches.

For example, if there are few satellites in view, it will be difficult to solve the integer ambiguity with single epoch data. As we discussed in Chapter 2, under the assumption that we have K ($K > n$) satellites in view each second, the single epoch GPS ambiguity problem has n ($n = 4$ for single DGPS scenario) degrees of freedom. Taking into the account that combining each additional epoch adds another n degrees of freedom but also adds K extra measurements, we can conclude that combining GPS measurements from multiple epoches

will help with GPS integer ambiguity resolution.

In this chapter, we extend the approach presented in Chapter 2 to work with integer ambiguity resolution problem with measurements from multiple epoches. We first present its theoretical derivation and then introduce a fast and efficient method for GPS integer ambiguity resolution. Two sets of simulations will be carried out to show the effectiveness of the proposed approach.

4.2 Literature Review

In early study of GPS integer ambiguity resolution, many algorithms were based on multiple epoches measurements [26]. Early papers utilize multiple epoches measurements mainly for two purposes. First, the measurements are smoothed over long time period to get more precise initial estimate, e.g., [25]. Second, the cost function is smoothed over time, e.g. [27].

However, these algorithms require more than 6 satellites per epoch to achieve satisfying performance, and the computational efficiencies are not guaranteed.

4.3 Measurement Model over Multi Epoches

The GPS phase residual measurements in single epoch is as defined in Eqn. (2.12). For solving the problem for multi epoch scenario, in this Chapter, we rewrite the GPS measurement at time t_j as:

$$\mathbf{y}_j = \mathbf{G}_j\mathbf{x}_j + \mathbf{N}_j + \mathbf{v}_j \tag{4.1}$$

where $\mathbf{y}_j = \delta\boldsymbol{\phi} \in \mathbb{R}^K$ represents the DGPS phase measurements at time t_j, $\mathbf{x}_j \in \mathbb{R}^n$ and $\mathbf{N}_j \in \mathbb{Z}^K$ are the parameters to be estimated, and $n = 4$. $\mathbf{G}_j = \lambda^{-1}\mathbf{H}_j \in \mathbb{R}^{K\times n}$ is the observation matrix characterizing the satellite-user geometry, the noise term $\mathbf{v}_j = \boldsymbol{\eta}_j/\lambda \in \mathbb{R}^K$ and $\mathbf{v}_j \sim \mathcal{N}\left(\mathbf{0}, \boldsymbol{\Sigma}_{vv_j}\right)$.

Assuming that from time t_1 to time t_M, the receiver maintains lock to the satellites, i.e., $\mathbf{N} = \mathbf{N}_1 = \cdots = \mathbf{N}_M$, then the measurements from t_1 to t_M can be grouped as:

$$\acute{\mathbf{y}} = \acute{\mathbf{G}}\mathbf{X} + \mathbf{V}\mathbf{N} + \acute{\mathbf{v}} \tag{4.2}$$

where the measurement $\acute{\mathbf{y}}^\top = \begin{bmatrix} \mathbf{y}_1^\top & \cdots & \mathbf{y}_M^\top \end{bmatrix} \in \mathbb{R}^{MK}$; the grouped state vector $\mathbf{X}^\top = \begin{bmatrix} \mathbf{x}_1^\top & \cdots & \mathbf{x}_M^\top \end{bmatrix} \in \mathbb{R}^{MK}$; the measurement noise $\acute{\mathbf{v}}^\top = \begin{bmatrix} \mathbf{v}_1^\top & \cdots & \mathbf{v}_M^\top \end{bmatrix} \in \mathbb{R}^{MK}$ with $cov(\mathbf{v}_j) = \boldsymbol{\Sigma}_{vv_j}$,

$$\begin{aligned} \acute{\mathbf{G}} &= \begin{bmatrix} \mathbf{G}_1 & & \mathbf{0} \\ & \ddots & \\ \mathbf{0} & & \mathbf{G}_M \end{bmatrix}, \\ \mathbf{V}^\top &= \begin{bmatrix} \mathbf{I} & \cdots & \mathbf{I} \end{bmatrix}, \end{aligned}$$

where $\mathbf{I}$ represents K-by-K identity matrix, and $\acute{\mathbf{G}} \in \mathbb{R}^{MK\times Mn}$ and $\mathbf{V} \in \mathbb{R}^{MK\times K}$.

Assuming that the GPS carrier phase measurement noise is uncorrelated over time, the covariance matrix of the noise vector $\acute{\mathbf{v}}$ is

$$\acute{\boldsymbol{\Sigma}} = \begin{bmatrix} \boldsymbol{\Sigma}_{vv_1} & & \mathbf{0} \\ & \ddots & \\ \mathbf{0} & & \boldsymbol{\Sigma}_{vv_M} \end{bmatrix}.$$

4.4 Problem Statement

GPS integer ambiguity problem over multiple epoches can be solved as a Maximum Likelihood (ML) estimation problem: given the GPS measurements, we would like to find the estimate of $\mathbf{N}$ and $\mathbf{X}$ that maximize the conditional probability $f\left(\acute{\mathbf{y}}|\mathbf{N},\mathbf{X}\right)$.

$$\begin{aligned}
\left(\hat{\mathbf{N}},\hat{\mathbf{X}}\right) &= \arg\max_{\mathbf{N}\in\mathbb{Z}^K,\mathbf{X}\in\mathbb{R}^n} f\left(\acute{\mathbf{y}}|\mathbf{N},\mathbf{X}\right) \\
&= \arg\max_{\mathbf{N}\in\mathbb{Z}^K,\mathbf{X}\in\mathbb{R}^n} \ln f\left(\acute{\mathbf{y}}|\mathbf{N},\mathbf{X}\right) \\
&= \arg\max_{\mathbf{N}\in\mathbb{Z}^K,\mathbf{X}\in\mathbb{R}^n} \ln\left(\frac{e^{-\frac{1}{2}\left(\acute{\mathbf{y}}-\acute{\mathbf{G}}\mathbf{X}-\mathbf{V}\mathbf{N}\right)^T\mathbf{\Sigma}^{-1}\left(\acute{\mathbf{y}}-\acute{\mathbf{G}}\mathbf{X}-\mathbf{V}\mathbf{N}\right)}}{\left(2\pi\right)^{MK/2}\left|\acute{\mathbf{\Sigma}}\right|^{1/2}}\right) \\
&= \arg\min_{\mathbf{N}\in\mathbb{Z}^K,\mathbf{X}\in\mathbb{R}^n} \left(\acute{\mathbf{y}}-\acute{\mathbf{G}}\mathbf{X}-\mathbf{V}\mathbf{N}\right)^T\acute{\mathbf{\Sigma}}^{-1}\left(\acute{\mathbf{y}}-\acute{\mathbf{G}}\mathbf{X}-\mathbf{V}\mathbf{N}\right). \qquad (4.3)
\end{aligned}$$

Our objective is to find $\mathbf{N}\in\mathbb{Z}^K$, $\mathbf{X}\in\mathbb{R}^{Mn}$ that minimize the cost function

$$c\left(\mathbf{X},\mathbf{N}\right) = \left(\acute{\mathbf{y}}-\acute{\mathbf{G}}\mathbf{X}-\mathbf{N}\right)^T\mathbf{\Sigma}^{-1}\left(\acute{\mathbf{y}}-\acute{\mathbf{G}}\mathbf{X}-\mathbf{N}\right). \qquad (4.4)$$

By forming the problem as Eqn. (4.2), we would solve the GPS integer ambiguity using measurements over the interval from $t_1,\ \cdots,\ t_M$. In practice, we will first attempt to solve the integer ambiguity problem at $t=t_1$, if we succeed, then we have a real time solution. If we fail, then at $t=t_2$, we attempt to solve the problem using $\mathbf{y}_1$ and $\mathbf{y}_2$, etc. If the problem is solved at time $t>t_1$, the answer is attained in near real time, etc.

4.5 Integer Ambiguity Resolution

4.5.1 Generating Searching Candidates

Implementing method described in Chapter 2 on Eqn. (3.4) yields the following derivation. For a given integer ambiguity $\mathbf{N}$, the weighted least square estimate of $\mathbf{x}$ would be:

$$\hat{\mathbf{x}} = \left(\acute{\mathbf{G}}^T \acute{\mathbf{\Sigma}}^{-1} \acute{\mathbf{G}}\right)^{-1} \acute{\mathbf{G}}^T \acute{\mathbf{\Sigma}}^{-1} (\acute{\mathbf{y}} - \mathbf{VN}) \tag{4.5}$$

and the residual vector is

$$\begin{aligned} \hat{\boldsymbol{\varepsilon}} &= \acute{\mathbf{y}} - \acute{\mathbf{G}}\hat{\mathbf{x}} - \mathbf{VN} \\ &= \left(\mathbf{I} - \acute{\mathbf{G}} \left(\acute{\mathbf{G}}^T \acute{\mathbf{G}}\right)^{-1} \acute{\mathbf{\Sigma}}^{-1} \acute{\mathbf{G}}^T \acute{\mathbf{\Sigma}}^{-1}\right) (\acute{\mathbf{y}} - \mathbf{VN}) \\ &= \acute{\mathbf{Q}}_{\mathbf{\Sigma}} (\acute{\mathbf{y}} - \mathbf{VN}) . \end{aligned} \tag{4.6}$$

where

$$\acute{\mathbf{P}}_{\mathbf{\Sigma}} = \acute{\mathbf{G}} \left(\acute{\mathbf{G}}^T \acute{\mathbf{\Sigma}}^{-1} \acute{\mathbf{G}}\right)^{-1} \acute{\mathbf{G}}^T \acute{\mathbf{\Sigma}}^{-1}, \tag{4.7}$$

$$\acute{\mathbf{Q}}_{\mathbf{\Sigma}} = \mathbf{I} - \acute{\mathbf{P}}_{\mathbf{\Sigma}}. \tag{4.8}$$

Note that both $\acute{\mathbf{P}}_{\mathbf{\Sigma}}$ and $\acute{\mathbf{Q}}_{\mathbf{\Sigma}}$ are idempotent and that $Rank(\acute{\mathbf{P}}) = Mn$ and $Rank(\acute{\mathbf{Q}}) = M(K-n)$. This can be proved by the same token as presented in Chapter 2. The detailed proof is presented in [5].

From Eqn. (3.6), the cost function evaluated from candidate $\mathbf{N}$ is

$$\begin{aligned} c(\mathbf{N}) &= \|\acute{\mathbf{y}} - \acute{\mathbf{G}} \cdot \mathbf{x} - \mathbf{VN}\|^2_{\acute{\mathbf{\Sigma}}} \\ &= \|\acute{\mathbf{Q}}_{\mathbf{\Sigma}}(\acute{\mathbf{y}} - \mathbf{VN})\|^2_{\acute{\mathbf{\Sigma}}} \\ &= (\acute{\mathbf{y}} - \mathbf{VN})^\top \acute{\mathbf{Q}}_{\mathbf{\Sigma}}^\top \acute{\mathbf{\Sigma}}^{-1} \acute{\mathbf{Q}}_{\mathbf{\Sigma}} (\acute{\mathbf{y}} - \mathbf{VN}) \\ &= (\acute{\mathbf{y}} - \mathbf{VN})^\top \acute{\mathbf{Q}}_0 (\acute{\mathbf{y}} - \mathbf{VN}) \end{aligned} \tag{4.9}$$

where

$$\acute{\mathbf{Q}}_0 \;=\; \acute{\mathbf{Q}}_{\mathbf{\Sigma}}^{\top}\acute{\mathbf{\Sigma}}^{-1}\acute{\mathbf{Q}}_{\mathbf{\Sigma}}.$$

Then $\acute{\mathbf{Q}}_0$ is symmetric and also has the rank $M(K-n)$.

Let the SVD (single value decomposition) of $\acute{\mathbf{Q}}_0$ be

$$\acute{\mathbf{Q}}_0 = \acute{\mathbf{U}}\acute{\mathbf{S}}^2\acute{\mathbf{U}}^{\top},$$

where $\acute{\mathbf{U}}$ is unitary and $\acute{\mathbf{S}}$ is diagonal with $diag(\acute{\mathbf{S}}) = [\acute{s}_1, \ldots, \acute{s}_M K - n, 0, \ldots, 0]$ with all $\acute{s}_i > 0$ for $i = 1, \ldots, M(K-n)$.

Define $\acute{\mathbf{B}} = \acute{\mathbf{S}}\acute{\mathbf{U}}^{\top}$ such that

$$\acute{\mathbf{Q}}_0 \;=\; \acute{\mathbf{B}}^{\top}\acute{\mathbf{B}} \tag{4.10}$$

where the last Mn rows of $\mathbf{B}$ are zero.

Given the above analysis, the cost function of Eqn. (4.9) can be rewritten as

$$\begin{aligned} c(\mathbf{N}) \;&=\; (\acute{\mathbf{y}} - \mathbf{V}\mathbf{N})^{\top}\acute{\mathbf{B}}^{\top}\acute{\mathbf{B}}(\acute{\mathbf{y}} - \mathbf{V}\mathbf{N}) \\ &=\; \|\acute{\mathbf{B}}\,(\acute{\mathbf{y}} - \mathbf{V}\mathbf{N})\,\|^2. \end{aligned} \tag{4.11}$$

Because $\acute{\mathbf{B}}$ does not have full rank, the null space of $\mathbf{B}$ is not empty. Therefore, there exists (non-unique) $\hat{\mathbf{N}} \in \mathbb{R}^m$ such that $(\acute{\mathbf{y}} - \mathbf{V}\hat{\mathbf{N}})$ is in the null space of $\acute{\mathbf{B}}$:

$$\begin{aligned} \acute{\mathbf{B}}(\acute{\mathbf{y}} - \mathbf{V}\hat{\mathbf{N}}) \;&=\; \mathbf{0}, \\ \acute{\mathbf{B}}\acute{\mathbf{y}} \;&=\; \acute{\mathbf{B}}\mathbf{V}\hat{\mathbf{N}} \end{aligned} \tag{4.12}$$

The matrix $\acute{\mathbf{B}}$ can be represent as

$$\acute{\mathbf{B}} = \begin{bmatrix} \acute{\mathbf{A}} \\ \\ \mathbf{0} \end{bmatrix},$$

where $\acute{\mathbf{A}} \in \mathbb{R}^{M(K-n)\times MK}$.

Our goal is to find an integer vector $\hat{\mathbf{N}}$ such that

$$\begin{aligned} \begin{bmatrix} \acute{\mathbf{A}} \\ \mathbf{0} \end{bmatrix} \acute{\mathbf{y}} &= \begin{bmatrix} \acute{\mathbf{A}} \\ \mathbf{0} \end{bmatrix} \mathbf{V}\hat{\mathbf{N}} \\ \acute{\mathbf{A}}\acute{\mathbf{y}} &= \acute{\mathbf{A}}\mathbf{V}\hat{\mathbf{N}} \end{aligned} \tag{4.13}$$

Noting that $\acute{\mathbf{A}}\mathbf{V} \in \mathbb{R}^{M(K-n)\times K}$, we may let $\acute{\mathbf{A}}\mathbf{V} = \begin{bmatrix} \acute{\mathbf{C}} & \acute{\mathbf{D}} \end{bmatrix}$, where $\acute{\mathbf{C}} \in \mathbb{R}^{M(K-n)\times(K-n)}$ and $\acute{\mathbf{D}} \in \mathbb{R}^{M(K-n)\times n}$.

Let the last n elements of $\hat{\mathbf{N}}$ be integers. We denote this subvector as $\hat{\mathbf{N}}_D$ and the first $K-n$ elements of $\hat{\mathbf{N}}$ as $\hat{\mathbf{N}}_C$. Then Eqn. (4.13) can be rewritten as

$$\acute{\mathbf{A}}\acute{\mathbf{y}} = \begin{bmatrix} \acute{\mathbf{C}} & \acute{\mathbf{D}} \end{bmatrix} \begin{bmatrix} \hat{\mathbf{N}}_C \\ \hat{\mathbf{N}}_D \end{bmatrix}.$$

Therefore, if we decompose $\mathbf{y}$ as $\mathbf{y} = \begin{bmatrix} \mathbf{y}_C^\top & \mathbf{y}_D^\top \end{bmatrix}^\top$ with $\mathbf{y}_C \in \mathbb{R}^{(K-n)}$ and $\mathbf{y}_D \in \mathbb{R}^n$ and given a hypothesized vector $\hat{\mathbf{N}}_D \in \mathbb{Z}^n$, then the real-value estimate of $\hat{\mathbf{N}}_C$ is:

$$\hat{\mathbf{N}}_C = \left(\acute{\mathbf{C}}^\top \acute{\mathbf{C}}\right)^{-1} \acute{\mathbf{C}}^\top \left(\acute{\mathbf{A}}\acute{\mathbf{y}} - \acute{\mathbf{D}}\hat{\mathbf{N}}_D\right). \tag{4.14}$$

The integer candidates $\mathbf{N}_D$ can be searched exhaustively over some finite range of integers using n 'for' loops as shown in Fig. 4.1. For each integer vector $\mathbf{N}_D$, Eqn. (4.14) provides a float estimate $\hat{\mathbf{N}}_C$.

$$\begin{aligned} c(\mathbf{N}) &= (\acute{\mathbf{y}} - \mathbf{V}\mathbf{N})^\top \acute{\mathbf{B}}^\top \acute{\mathbf{B}}(\acute{\mathbf{y}} - \mathbf{V}\mathbf{N}) \\ &= \|\acute{\mathbf{B}}\,(\acute{\mathbf{y}} - \mathbf{V}\mathbf{N})\,\|^2. \end{aligned} \tag{4.15}$$

for $i = -d : d$
  for $j = -d : d$
    for $k = -d : d$
      $\mathbf{N}_D = [i, j, k, 0]^\top$
      $\hat{\mathbf{N}}_C = \left(\acute{\mathbf{C}}^\top \acute{\mathbf{C}}\right)^{-1} \acute{\mathbf{C}}^\top \left(\acute{\mathbf{A}}\acute{\mathbf{y}} - \acute{\mathbf{D}}\hat{\mathbf{N}}_D\right)$
      ... use $\hat{\mathbf{N}}_C$ to compute $\check{\mathbf{N}}_C$ minimizing $J(\mathbf{N}_C)$
      $\mathbf{N}^\top = \begin{bmatrix} \check{\mathbf{N}}_C & \mathbf{N}_D \end{bmatrix}^\top$
      if $c(\mathbf{N}) <$ current minimum
        Save $\mathbf{N}$
        current minimum $= c(\mathbf{N})$
      $\vdots$

Figure 4.1: Triple 'for' loop to compute $\hat{\mathbf{N}}_C$ and $\mathbf{N}$ for the case where $n = 4$.

Because $\acute{\mathbf{B}}$ does not have full rank, the null space of $\acute{\mathbf{B}}$ is not empty. Therefore, there exists (non-unique) $\hat{\mathbf{N}} \in \mathbb{R}^K$ such that $(\acute{\mathbf{y}} - \mathbf{V}\hat{\mathbf{N}})$ is in the null space of $\acute{\mathbf{B}}$:

$$\acute{\mathbf{B}}(\acute{\mathbf{y}} - \mathbf{V}\hat{\mathbf{N}}) = \mathbf{0}. \tag{4.16}$$

Let the last n elements of $\hat{\mathbf{N}}$ to be integers. We denote this subvector as $\hat{\mathbf{N}}_D$. Our goal is to find $\hat{\mathbf{N}}$ such that

$$\acute{\mathbf{B}}\acute{\mathbf{y}} = \acute{\mathbf{B}}\mathbf{V}\hat{\mathbf{N}} \tag{4.17}$$

$$
\begin{aligned}
\begin{bmatrix} \acute{\mathbf{A}} \\ \mathbf{0} \end{bmatrix} \acute{\mathbf{y}} &= \begin{bmatrix} \acute{\mathbf{A}} \\ \mathbf{0} \end{bmatrix} \begin{bmatrix} \mathbf{I} \\ \mathbf{0} \end{bmatrix} \hat{\mathbf{N}} \\
\begin{bmatrix} \acute{\mathbf{A}} \\ \mathbf{0} \end{bmatrix} \acute{\mathbf{y}} &= \begin{bmatrix} \acute{\mathbf{C}} & \acute{\mathbf{D}} & \acute{\mathbf{E}} \\ \mathbf{0} & \mathbf{0} & \mathbf{0} \end{bmatrix} \begin{bmatrix} \mathbf{I} \\ \mathbf{0} \end{bmatrix} \begin{bmatrix} \hat{\mathbf{N}}_C \\ \hat{\mathbf{N}}_D \end{bmatrix} \\
\begin{bmatrix} \acute{\mathbf{A}} \\ \mathbf{0} \end{bmatrix} \acute{\mathbf{y}} &= \begin{bmatrix} \acute{\mathbf{C}} & \acute{\mathbf{D}} \\ \mathbf{0} & \mathbf{0} \end{bmatrix} \begin{bmatrix} \hat{\mathbf{N}}_C \\ \hat{\mathbf{N}}_D \end{bmatrix} \\
\begin{bmatrix} \acute{\mathbf{A}} \\ \mathbf{0} \end{bmatrix} \acute{\mathbf{y}} &= \begin{bmatrix} \acute{\mathbf{C}}\hat{\mathbf{N}}_C + \acute{\mathbf{D}}\hat{\mathbf{N}}_D \\ \mathbf{0} \end{bmatrix} \\
\acute{\mathbf{A}}\acute{\mathbf{y}} &= \acute{\mathbf{C}}\hat{\mathbf{N}}_C + \acute{\mathbf{D}}\hat{\mathbf{N}}_D.
\end{aligned}
$$

Therefore, if we decompose $\mathbf{y}$ as $\mathbf{y} = \begin{bmatrix} \mathbf{y}_C^\top & \mathbf{y}_D^\top \end{bmatrix}^\top$ with $\mathbf{y}_C \in \mathbb{R}^{(K-n)}$ and $\mathbf{y}_D \in \mathbb{R}^n$ and given a hypothesized vector $\hat{\mathbf{N}}_D \in \mathbb{Z}^n$, then the real-value estimate of $\hat{\mathbf{N}}_C$ is:

$$
\hat{\mathbf{N}}_C = \left(\acute{\mathbf{C}}^\top \acute{\mathbf{C}}\right)^{-1} \acute{\mathbf{C}}^\top \left(\acute{\mathbf{A}}\acute{\mathbf{y}} - \acute{\mathbf{D}}\hat{\mathbf{N}}_D\right). \tag{4.18}
$$

In Eqn. (4.18), other than the information from GPS measurements, the information from INS states is also involved in calculation, represented by the term $\acute{\mathbf{E}}\hat{\mathbf{x}}_{a0}$.

From Eqn. (3.17), the integer candidates $\hat{\mathbf{N}}_D$ can be searched exhaustively over some finite range of integers as described in Fig. 4.1.

4.5.2 Rounding $\hat{\mathbf{N}}_C$

Given $\hat{\mathbf{N}}_C$, in order to get the optimal integer estimate of $\mathbf{N}_C$, we would like to find an integer vector $\check{\mathbf{N}}_C$ which is close to $\hat{\mathbf{N}}_C$. As discussed in Chapter 2, we would like to find

$\check{\mathbf{N}}_C$ to minimize the cost function

$$\begin{aligned} J(\mathbf{N}_C) &= \|\mathbf{N}_C - \hat{\mathbf{N}}_C\|^2_{\mathbf{\Sigma}_{\hat{\mathbf{N}}_C}} \\ &= (\mathbf{N}_C - \hat{\mathbf{N}}_C)^\top \mathbf{\Sigma}^{-1}_{\hat{\mathbf{N}}_C} (\mathbf{N}_C - \hat{\mathbf{N}}_C), \end{aligned} \tag{4.19}$$

where

$$\mathbf{\Sigma}_{\hat{\mathbf{N}}_C} = \mathbf{C}^{-1}\mathbf{A}\mathbf{\Sigma}\mathbf{A}^\top\mathbf{C}^{-\top} \tag{4.20}$$

which is derived from Eqn. (3.17).

By the same token as in Chapter 2, we can prove that the cost function $c(\mathbf{N})$ defined in Eqn. (4.9) will be minimized by the same integer estimate that minimize $J(\mathbf{N}_C)$ as defined in Eqn. (4.19). The details are discussed in [5].

To find the integer vector that minimizes Eqn. (4.19), we follow the idea of LAMBDA to find a matrix $\boldsymbol{Z} \in \mathbb{Z}^{(m-n)\times(m-n)}$, such that $\boldsymbol{Z}^{-1} \in \mathbb{Z}^{(m-n)\times(m-n)}$, and $(\boldsymbol{Z}\mathbf{\Sigma}_{\hat{N}_C}\boldsymbol{Z}^\top)^{-1}$ is nearly diagonal. The procedure is the same as we discussed in Chapter 2.

The integer-valued estimate of $\mathbf{N}_C$ can be computed as:

$$\hat{\mathbf{M}}_C = \boldsymbol{Z}\hat{\mathbf{N}}_C \tag{4.21}$$

$$\check{\mathbf{M}}_C = [\hat{\mathbf{M}}_C]_{roundoff} \tag{4.22}$$

$$\check{\mathbf{N}}_C = \boldsymbol{Z}^{-1}\check{\mathbf{M}}_C. \tag{4.23}$$

At this point we have an integer vector candidate $\left[\check{\mathbf{N}}_C^\top \; \mathbf{N}_D^\top\right]^\top$. One such candidate will be generated for each iteration of the 'for' loop in Fig. 4.1. We can compare each integer vector candidate using Eqn. (4.9). Selecting the candidate vector with the lowest value (subject to validity tests) as the best. By rounding off the float estimate $\hat{\mathbf{N}}_C$ in the decorrelated domain of $\hat{\mathbf{M}}_C$, we have a better chance to achieve optimal integer estimate $\check{\mathbf{N}}_C$.

4.6 Test Results

Two sets of tests have been carried out to evaluate the effectiveness of the proposed method both via MATLAB simulations.

4.6.1 Tests Over Different Noise Levels

In this set of MATLAB simulations, the tests are epoch-by-epoch with a set of 6 single difference GPS L1 ($\lambda \approx 0.19m$) carrier phase measurements at different noise levels. For each noise level, 1000 measurement epochs with randomly picked satellite elevation and azimuth angles were generated. We compared the success rate of getting all the integers correctly with different number of GPS epoches. The success rates of GPS integer ambiguity resolution by using different number of epoches with different level of covariance are plotted versus different noise level in Fig. 4.2.

From Fig. 4.2, we see that by combing measurements from multiple epoches, we achieve a higher success rate of estimating the correct integer vector at each covariance level.

4.6.2 Tests Over Different Number of Satellites

The second set of tests is performed to analyze the performance of the proposed approach as a function of the number of satellites. For each number of satellites, 1000 measurement epochs with randomly picked satellite elevation and azimuth angles were generated with the standard deviation of each phase measurement equal to $0.01m$. We compared the success rates of getting all the integers correctly in one, two and three epoches. The success rate of each scenario is plotted in Fig. 4.3.

From Fig. 4.3, we can see that by combing measurements from multiple epoches, we

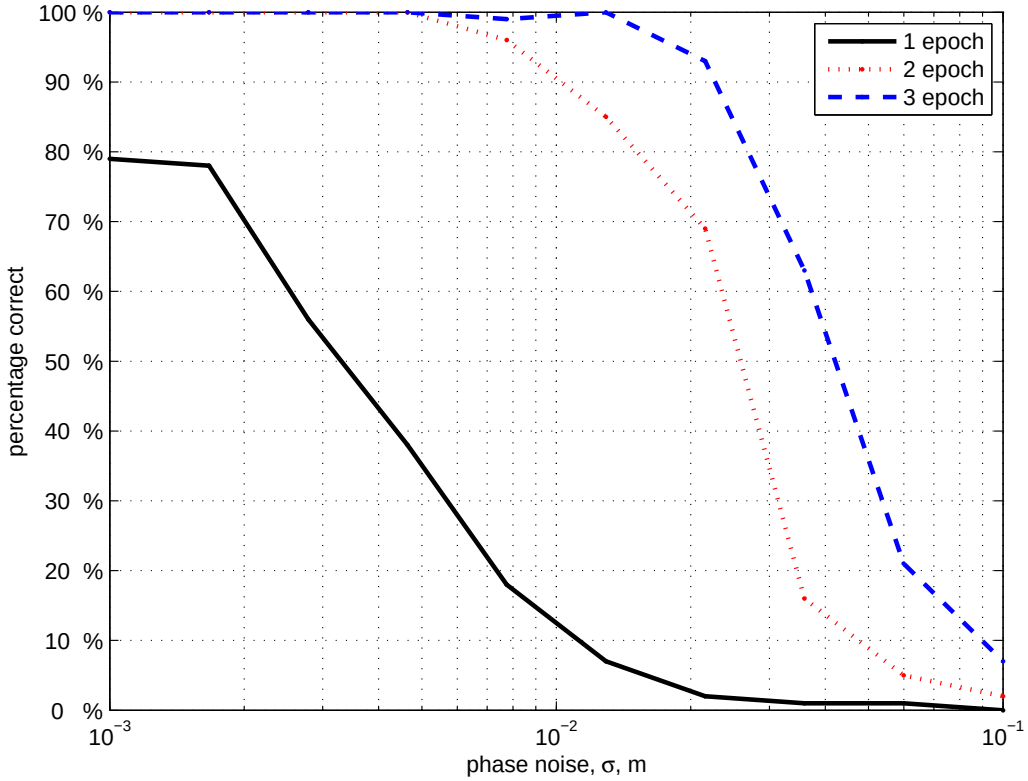

Figure 4.2: Rate of correct integer resolution vs. phase measurement noise

achieve a substantially higher rate of getting the right integer vector, especially when there are few satellites. We can see that with as few as 5 satellites, we have a 90% chance of getting the right integer within 3 epoches if we combine the measurements over epoches. With 6 or more satellites, we will get the right integer within 2 epoches with probability of higher than 95%.

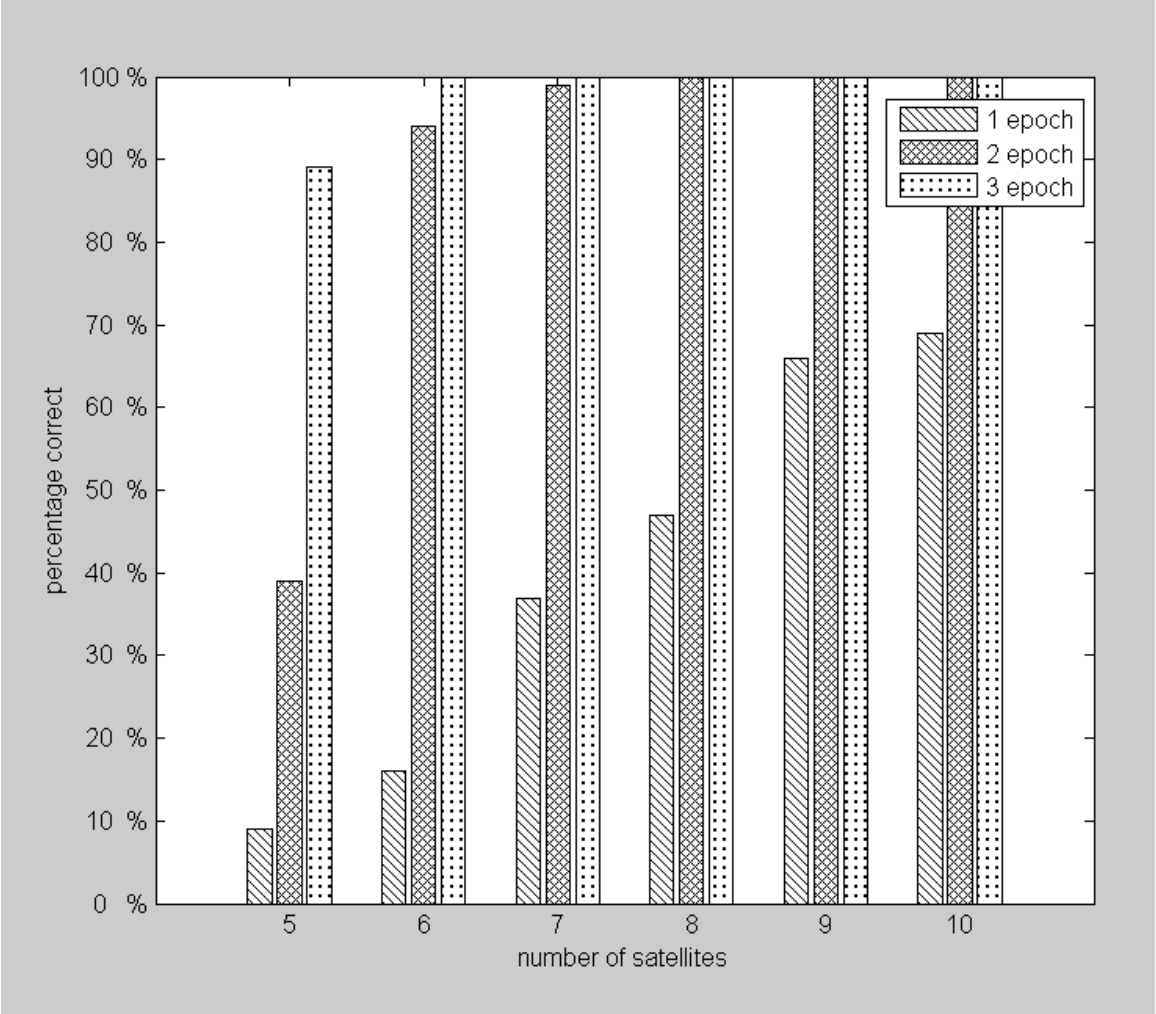

Figure 4.3: Rate of correct integer resolution vs. number of satellites

4.7 Chapter Summary

In this chapter, we extended the approach presented in Chapter 2 to work with integer ambiguity resolution problem with measurements from multiple epoches. Simulation results indicate that by incorporating with the measurements from multiple epoches, we have better chances to get the correct integer estimate, especially in GPS challenging areas where the number of satellites are limited, or has bigger measurement noise.

Chapter 5

Integer Ambiguity Validation

5.1 Introduction

Once the integer ambiguity is estimated, it is important to decide whether the estimate is acceptable or not. If the wrong integer estimates were accepted, they would corrupt the navigation state estimate. Therefore, integer ambiguity validation is critical. Integer validation methods can be divided into two categories. We can either validate the integers for all the satellites as a whole vector or validate each estimated integer individually.

To validate the integers for all satellites, the advantage is that more information can be achieved from more satellites to help with the decision. However, for DGPS systems where the degree of freedom $n = 4$, we need at least 5 satellites to have redundant information to perform the evaluation. The other disadvantage of methods in this category is that the whole integer vector may be rejected even only a few integers are wrong.

The estimated integers from each satellite can also be validated separately. The advantage of this kind of methods is that the whole integer vector will not be rejected when

few of the integers are wrong. This will be especially beneficial when there is some satellite at low elevation and thus has big measurement noise and/or multipath. However, for each integer estimate, the information can be used to perform evaluation is limited.

In this Chapter, we will discuss these two categories of methods separately.

5.2 Verify Each Integer Estimate Separately

The differential GPS measurement model is described in Eqns. (2.7) and (2.8). In this chapter, we assume that integer estimates of $N^{(i)}$ is available (through other approaches) and is denoted as $\hat{N}^{(i)}$. This section concerns about the detection of non-zero values for the integer errors

$$\delta N^{(i)} \quad = \quad \hat{N}^{(i)} - N^{(i)}. \tag{5.1}$$

5.2.1 Literature Review

To validate a single integer estimate, the most feasible information is from the measurements from different frequencies. Typical approaches include:

- Comparing certain linear combinations of phase ranges on multiple frequencies with linear combinations of code ranges on multiple frequencies [16].
- Comparing linear combinations of carrier phase ranges at different frequencies [7].

In this section, we will analytically discuss these two methods.

5.2.2 Comparing Phase Measurements with Code Measurements

Considering the characteristic of wide lane and narrow lane measurements, one of the techniques can be used for detecting wrong integer estimate is to compare wide lane phase measurement with narrow lane code measurement, as defined in Eqns. (2.63) and (2.60).

Differentiating these two measurements yields a float number estimate of the wide lane integer

$$\begin{aligned} \bar{N}_{WD}^{(i)} &= \frac{\Delta\rho_{NR}^{(i)} - \lambda_w \Delta\phi_{WD}^{(i)}}{\lambda_w} \\ &= N_{WD}^{(i)} + \frac{\bar{\epsilon}_{NR}^{(i)} - \bar{\eta}_{WD}^{(i)}}{\lambda_w}, \end{aligned} \tag{5.2}$$

For the residue between a given an integer estimate $\hat{N}_{WD}^{(i)}$ and $\bar{N}_{WD}^{(i)}$ is

$$\begin{aligned} \tilde{N}_{WD}^{(i)} &= \hat{N}_{WD}^{(i)} - \bar{N}_{WD}^{(i)} \\ &= N_{WD}^{(i)} + \delta N_{WD}^{(i)} - \left(N_{WD}^{(i)} + \frac{\bar{\epsilon}_{NR}^{(i)} - \bar{\eta}_{WD}^{(i)}}{\lambda_w} \right) \\ &= \delta N_{WD}^{(i)} - \frac{\bar{\epsilon}_{NR}^{(i)} - \bar{\eta}_{WD}^{(i)}}{\lambda_w} \end{aligned} \tag{5.3}$$

Assuming that $\sigma_{\rho_i} = 1m$ and $\sigma_{\phi_i} = 0.02m$, the standard deviation in narrow code measurement noise $\bar{\epsilon}_{NR}^{(i)}$ and wide lane phase measurement noise $\bar{\eta}_{WD}^{(i)}$ will be approximately $0.71m$ and $0.11m$, respectively. This implies that the mean and covariance of the residual will be

$$\mu_{\tilde{N}_{WD}^{(i)}} = \delta N_{WD}^{(i)}\ cycle \tag{5.4}$$

$$\sigma^2_{\tilde{N}_{WD}^{(i)}} = [\frac{1}{\lambda_w}, -\frac{1}{\lambda_w}] \begin{bmatrix} (0.71m)^2 & 0 \\ 0 & (0.11m)^2 \end{bmatrix} \begin{bmatrix} \frac{1}{\lambda_w} \\ -\frac{1}{\lambda_w} \end{bmatrix} = 0.701\ cycle^2, \tag{5.5}$$

under the assumption that the phase measurement noise at L1 and L2 are both $0.02m$.

Therefore, the residual $\tilde{N}_{WD}^{(i)}$ can be used as an indicator for wrong wide lane integer estimate, which can be further used to detect integer error in either L1 or L2. Moreover, considering the time correlation of GPS signals, a sudden change of $\tilde{N}_{WD}^{(i)}$ with amplitude bigger than 1 usually indicates cycle slips (an integer change not reported by the receiver).

A set of data are presented in Figs. 5.1 and 5.2 to show the value of $\tilde{N}_{WD}^{(i)}$. In Fig. 5.1, no cycle slip happens during the presented interval, $\tilde{N}_{WD}^{(i)}$ remains around 0 and changes smoothly. In Fig. 5.2, the residue was noisier from time $0 - 66s$ while the receiver was still able to track the signal with same integer ambiguity, and when cycle slip happened at $66s$, a clear jump in $\tilde{N}_{WD}^{(i)}$ was observed.

5.2.3 Comparing Phase Measurements at Different Frequencies

Comparing phase measurements at different frequencies is the criteria used in [7, 8], in which the residual between L1 and L2 phase range, the residual between L1 and wide lane phase range and the residual between L1 and narrow lane phase range are used to determine the correctness of the integers. In this section, we will give analytic analysis and extend the discussion to this criteria.

Given the L1 and L2 phase measurement in Eqn. (2.51) and (2.53), and let the integer estimate for L1 and L2 be $\hat{N}_{L1}^{(i)} = N_{L1}^{(i)} + \delta N_{L1}^{(i)}$ and $\hat{N}_{L2}^{(i)} = N_{L2}^{(i)} + \delta N_{L2}^{(i)}$, the predicted ranges

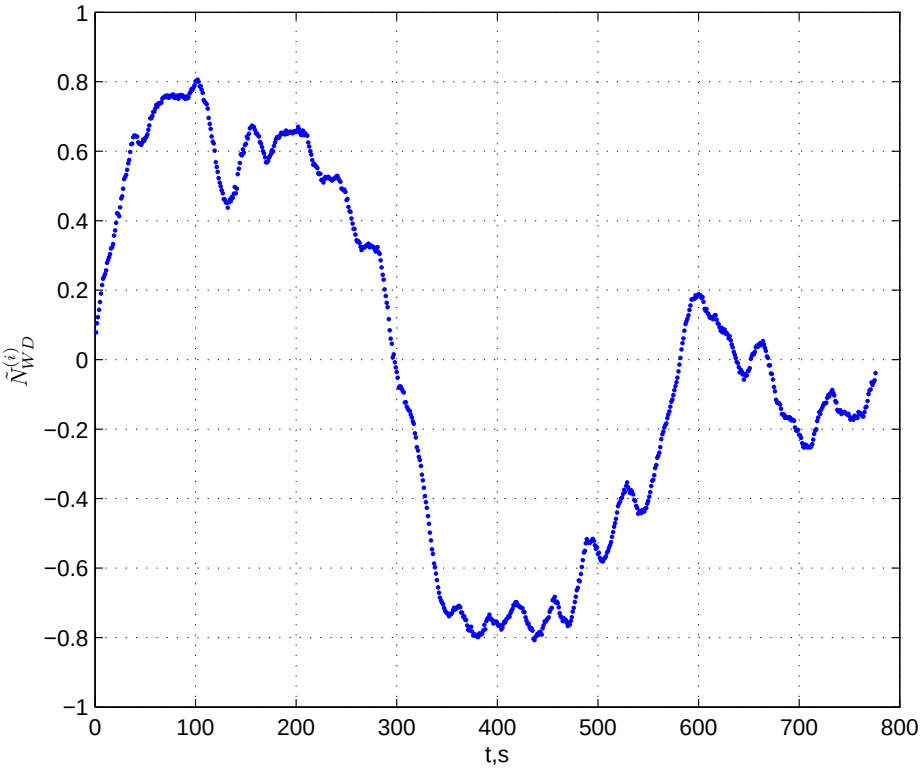

Figure 5.1: $\tilde{N}_{WD}^{(i)}$ over time, no cycle slip happened.

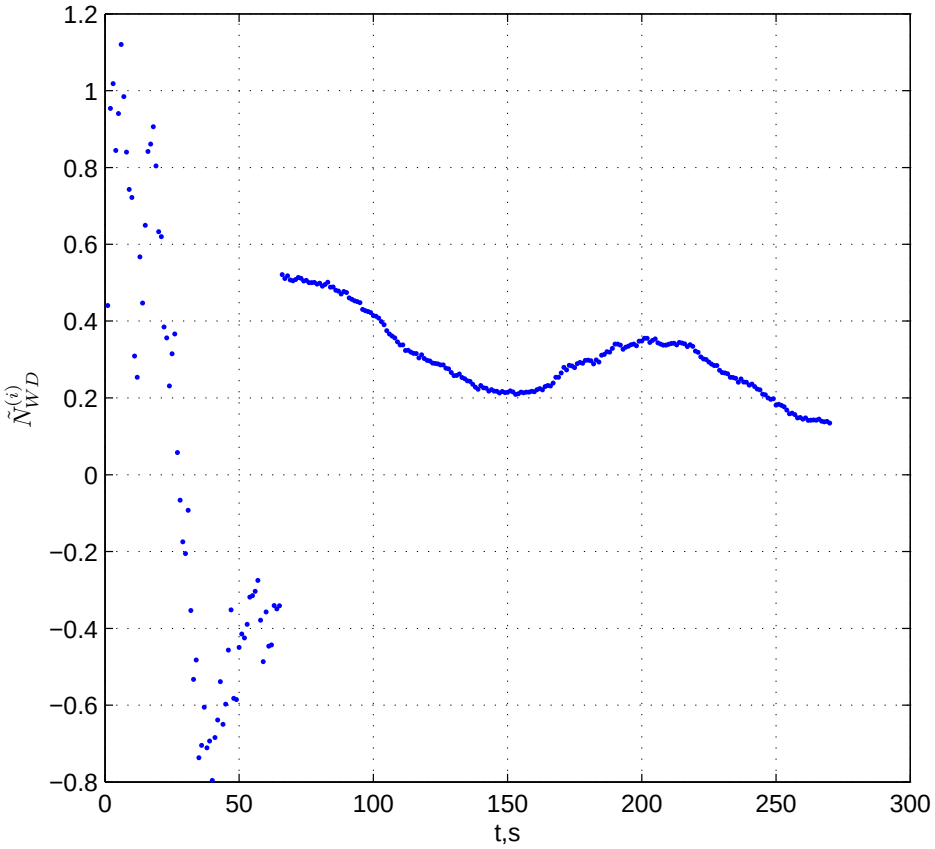

Figure 5.2: $\tilde{N}_{WD}^{(i)}$ over time, cycle slip happened at time $66s$.

can be calculated as follows:

$$\begin{aligned}
\hat{R}_{L1}^{(i)} &= \lambda_1 \Delta\phi_{L1}^{(i)} - \lambda_1 \hat{N}_{L1}^{(i)} \\
&= R^{(i)} + c\delta\bar{t}_r - \lambda_1 \delta N_{L1}^{(i)} + \bar{\eta}_{L1}^{(i)} \qquad (5.6) \\
\hat{R}_{L2}^{(i)} &= \lambda_2 \Delta\phi_{L2}^{(i)} - \lambda_2 \hat{N}_{L2}^{(i)} \\
&= R^{(i)} + c\delta\bar{t}_r + \lambda_2 \delta N_{L2}^{(i)} + \bar{\eta}_{L2}^{(i)}. \qquad (5.7)
\end{aligned}$$

Additional predicted ranges can be computed from wide lane and narrow lane phase measurements and integer estimates:

$$\begin{aligned}
\hat{R}_{WD}^{(i)} &= \lambda_1 \Delta\phi_{WD}^{(i)} - \lambda_w \hat{N}_{WD}^{(i)} \\
&= R^{(i)} + c\delta\bar{t}_r - \lambda_w \delta N_{WD}^{(i)} + \bar{\eta}_{WD}^{(i)} \\
&= R^{(i)} + c\delta\bar{t}_r - \lambda_w \left(\delta N_{L1}^{(i)} - \delta N_{L2}^{(i)}\right) + \left(\bar{\eta}_{L1}^{(i)} - \bar{\eta}_{L2}^{(i)}\right) \qquad (5.8) \\
\hat{R}_{NR}^{(i)} &= \lambda_1 \Delta\phi_{NR}^{(i)} - \lambda_n \hat{N}_{NR}^{(i)} \\
&= R^{(i)} + c\delta\bar{t}_r - \lambda_w \delta N_{NR}^{(i)} + \bar{\eta}_{NR}^{(i)} \\
&= R^{(i)} + c\delta\bar{t}_r - \lambda_n \left(\delta N_{L1}^{(i)} + \delta N_{L2}^{(i)}\right) + \left(\bar{\eta}_{L1}^{(i)} + \bar{\eta}_{L2}^{(i)}\right) \qquad (5.9)
\end{aligned}$$

Based on the above four range variables, six residual variables can be computed as:

$$\begin{aligned}
r_{12} &= \hat{R}_{L1}^{(i)} - \hat{R}_{L2}^{(i)}, \qquad (5.10) \\
r_{1w} &= \hat{R}_{L1}^{(i)} - \hat{R}_{WD}^{(i)}, \qquad (5.11) \\
r_{1n} &= \hat{R}_{L1}^{(i)} - \hat{R}_{NR}^{(i)}, \qquad (5.12) \\
r_{2w} &= \hat{R}_{L2}^{(i)} - \hat{R}_{WD}^{(i)}, \qquad (5.13) \\
r_{2n} &= \hat{R}_{L2}^{(i)} - \hat{R}_{NR}^{(i)}, \qquad (5.14) \\
r_{nw} &= \hat{R}_{NR}^{(i)} - \hat{R}_{WD}^{(i)}, \qquad (5.15)
\end{aligned}$$

where each is expressed in meters. The model of each residual error is

$$
\begin{aligned}
r_{12} &= \bar{\eta}_{L1}^{(i)} - \bar{\eta}_{L2}^{(i)} + \lambda_1 \delta N_1 - \lambda_2 \delta N_2, \\
r_{1w} &= \left(1 - \frac{\lambda_w}{\lambda_1}\right) \bar{\eta}_{L1}^{(i)} + \frac{\lambda_w}{\lambda_2} \bar{\eta}_{L2}^{(i)} + (\lambda_1 - \lambda_w)\delta N_1 + \lambda_w \delta N_2, \\
r_{1n} &= \left(1 - \frac{\lambda_n}{\lambda_1}\right) \bar{\eta}_{L1}^{(i)} - \frac{\lambda_n}{\lambda_2} \bar{\eta}_{L2}^{(i)} + (\lambda_1 - \lambda_n)\delta N_1 - \lambda_n \delta N_2, \\
r_{2w} &= -\frac{\lambda_w}{\lambda_1} \bar{\eta}_{L1}^{(i)} + \left(1 + \frac{\lambda_w}{\lambda_2}\right) \bar{\eta}_{L2}^{(i)} - \lambda_w \delta N_1 + (\lambda_2 + \lambda_w)\delta N_2, \\
r_{2n} &= -\frac{\lambda_n}{\lambda_1} \bar{\eta}_{L1}^{(i)} + \left(1 - \frac{\lambda_n}{\lambda_2}\right) \bar{\eta}_{L2}^{(i)} - \lambda_n \delta N_1 + (\lambda_2 - \lambda_n)\delta N_2, \\
r_{nw} &= \left(\frac{\lambda_n}{\lambda_1} - \frac{\lambda_w}{\lambda_1}\right) \bar{\eta}_{L1}^{(i)} + \left(\frac{\lambda_n}{\lambda_2} + \frac{\lambda_w}{\lambda_2}\right) \bar{\eta}_{L2}^{(i)} \\
&\quad + (\lambda_n - \lambda_w)\delta N_1 + (\lambda_n + \lambda_w)\delta N_2.
\end{aligned}
$$

These equations are more conveniently written in the vector form:

$$r = G\eta + H\delta N \tag{5.16}$$

where $r = [r_{12}, r_{1w}, r_{1n}, r_{2w}, r_{2n}, r_{nw}]^\top$, $\eta = [\bar{\eta}_{L1}^{(i)}, \bar{\eta}_{L2}^{(i)}]^\top$, $\delta N = [\delta N_1, \delta N_2]^\top$,

$$G = \begin{bmatrix} 1 & -1 \\ \left(\frac{\lambda_1 - \lambda_w}{\lambda_1}\right) & \frac{\lambda_w}{\lambda_2} \\ \left(\frac{\lambda_1 - \lambda_n}{\lambda_1}\right) & -\frac{\lambda_n}{\lambda_2} \\ -\frac{\lambda_w}{\lambda_1} & \left(\frac{\lambda_2 + \lambda_w}{\lambda_2}\right) \\ -\frac{\lambda_n}{\lambda_1} & \left(\frac{\lambda_2 - \lambda_n}{\lambda_2}\right) \\ \left(\frac{\lambda_n - \lambda_w}{\lambda_1}\right) & \left(\frac{\lambda_n + \lambda_w}{\lambda_2}\right) \end{bmatrix} \text{ and}$$

$$H = \begin{bmatrix} \lambda_1 & -\lambda_2 \\ (\lambda_1 - \lambda_w) & \lambda_w \\ (\lambda_1 - \lambda_n) & -\lambda_n \\ -\lambda_w & (\lambda_2 + \lambda_w) \\ -\lambda_n & (\lambda_2 - \lambda_n) \\ (\lambda_n - \lambda_w) & (\lambda_n + \lambda_w) \end{bmatrix}.$$

Let

$$\hat{g} = \begin{bmatrix} 1.000 \\ \frac{-\lambda_1}{\lambda_2 - \lambda_1} \\ \frac{\lambda_1}{\lambda_2 + \lambda_1} \\ \frac{-\lambda_2}{\lambda_2 - \lambda_1} \\ \frac{-\lambda_2}{\lambda_2 + \lambda_1} \\ \frac{2\lambda_1\lambda_2}{\lambda_2^2 - \lambda_1^2} \end{bmatrix} = \begin{bmatrix} 1.000 \\ -3.529 \\ 0.438 \\ -4.529 \\ -0.562 \\ -3.967 \end{bmatrix},$$

then it is trivial to show that

$$\begin{aligned} G &= [\hat{g}, -\hat{g}]\,, \\ H &= [\lambda_1 \hat{g}, -\lambda_2 \hat{g}]\,. \end{aligned}$$

We now want to consider each row of Eqn. (5.16). For this purpose, we define the k-th item of r and the k-th row of g as r_k and g_k, separately. Then each residual, as computed by Eqns. (5.10)–(5.15) could be used to test the validity of the integer candidates $\hat{N}_1$ and $\hat{N}_2$. The residual test could have the form:

$$\left.\begin{aligned} |r_k| \leq \tau_k &\rightarrow \left(\hat{N}_1 \text{ and } \hat{N}_2\right) \text{ are correct,} \\ |r_k| > \tau_k &\rightarrow \left(\hat{N}_1 \text{ or } \hat{N}_2\right) \text{ is incorrect.} \end{aligned}\right\} \tag{5.17}$$

The only parameter in this test is τ_k, which is selected by the designer to balance the risk of false alarms versus that of missed detections. Given the structure of G and H, this section further analyzes the above residual tests.

The k-th residual is equal to

$$\begin{aligned} r_k &= [g_k, -g_k]\eta + [g_k\lambda_1, -g_k\lambda_2]\delta N^{(i)} \\ &= g_i k \left([1, -1]\eta + [\lambda_1, -\lambda_2]\delta N^{(i)}\right) \\ q_k = \frac{r_k}{g_k} &= \left([1, -1]\eta + [\lambda_1, -\lambda_2]\delta N^{(i)}\right). \end{aligned}$$

From this analysis, we see that each residual is in fact the same random variable. For a given value of $\delta N^{(i)}$, the random variable q_i has mean

$$\mu_q = [\lambda_1, -\lambda_2]\delta N^{(i)}$$

with unit of meters and variance

$$\sigma_q^2 = [1, -1] \begin{bmatrix} \sigma_{\phi_i}^2 & 0 \\ 0 & \sigma_{\phi_i}^2 \end{bmatrix} \begin{bmatrix} 1 \\ -1 \end{bmatrix} = (0.028m)^2.$$

assuming that the standard deviation of phase measurement noise at L1 and L2 are both $0.02m$. The mean value of each q_i are shown in Table. 5.2.3.

Note that the magnitude of μ_q is determined in part by the relative directions between $h = [\lambda_1, -\lambda_2] \in \Re^2$ and $\hat{n} \in I^2$. Let z denote a vector in $\Re^2$. The equation $hz = 0$ defines a hyperplane (or line) in $\Re^2$. The normal to the plane is h and the distance from a point z to the hyperplane $d = hz$. Therefore, a test such as

$$\left.\begin{aligned} |q_i| \leq \bar{q} &\rightarrow \left(\hat{N}_1 \text{ and } \hat{N}_2\right) \text{ are correct,} \\ |q_i| > \bar{q} &\rightarrow \left(\hat{N}_1 \text{ or } \hat{N}_2\right) \text{ is incorrect.} \end{aligned}\right\} \tag{5.18}$$

will correctly detect incorrect integers that are at least a distance $\bar{q}$ from the hyperplane, but there is still a (potentially infinite) set of integer error vectors that will pass the threshold test. Figure 5.3 shows the grid of integers (n_1, n_2) by asterisks. The figure also shows the hyperplane $hz = 0$ as a blue line. The region between the two green lines contains the set of integer vectors that would pass the detection test of Eqn. (5.18) when the threshold is selected as $\bar{q} = 0.015m$.

It is clear from the above analysis that the first and third quadrants contain the troublesome vectors and that the points that will be problematic in these two quadrants will be related by a reflection through the origin. For the points in the first quadrant of Fig. 5.3, expected value of q is given in the Table 5.2.3.

From Fig. 5.3, we can see that the incorrect integer vector $\delta N = [4,\ 3]$, $\delta N = [-4,\ -3]$, $\delta N = [5,\ 4]$, $\delta N = [-5,\ -4]$ still have chances to incorrectly pass the detection with

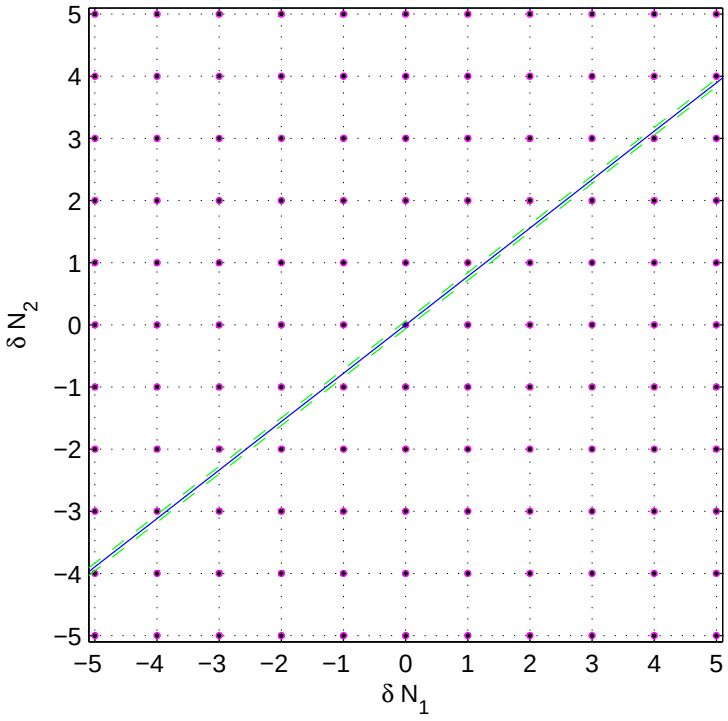

Figure 5.3: Depiction of the hyperplane $h\hat{n} = 0$, the set of integer vectors and the 95% ellipsoid. The region between two green dash lines would pass the error detection test for $\bar{q} = 0.015$.

5	-1.22	-1.03	0.84	-0.65	-0.46	-0.27
4	-0.98	-0.79	-0.60	-0.41	-0.22	-0.02
3	-0.73	-0.54	-0.35	-0.16	0.03	0.22
2	-0.49	-0.30	-0.11	0.08	0.28	0.46
1	-0.24	-0.06	0.14	0.33	0.52	0.71
0	0.00	0.19	0.38	0.57	0.76	0.95
	0	1	2	3	4	5

Table 5.1: Expected value of q at integer vectors in the first quadrant. The variable n_1 counts across the bottom of the table. The variable n_2 counts up along the first column of the table.

$\bar{q} = 0.015$. Assuming that any these incorrect integer estimate and the ones that are further to the origin than to these points could be detected by comparing phase range with code range, as discussed in Section 5.2.2, then the rate of miss detection will be less than 5% and the rate of false alarm is also smaller than 5%.

This test has also been implemented in our real-time GPS/INS system. Real-world data for q with correct integer estimates are shown in Fig. 5.4. In 969 epoches, for all the wrong integer estimate, the absolute value of q are greater than 0.02 (ranges between 0.02 to 0.255). These value are not plotted in Fig. 5.4 to improve its readability.

5.3 GPS Modernization and its Effect on GPS Ambiguity Validation

5.3.1 GPS Modernization

The GPS system has been fully functional since July 17, 1995. However, additional advances in technology and new demands on the existing system led to the effort to modernize the GPS system.

The major components of GPS modernization includes: increased signal power at the

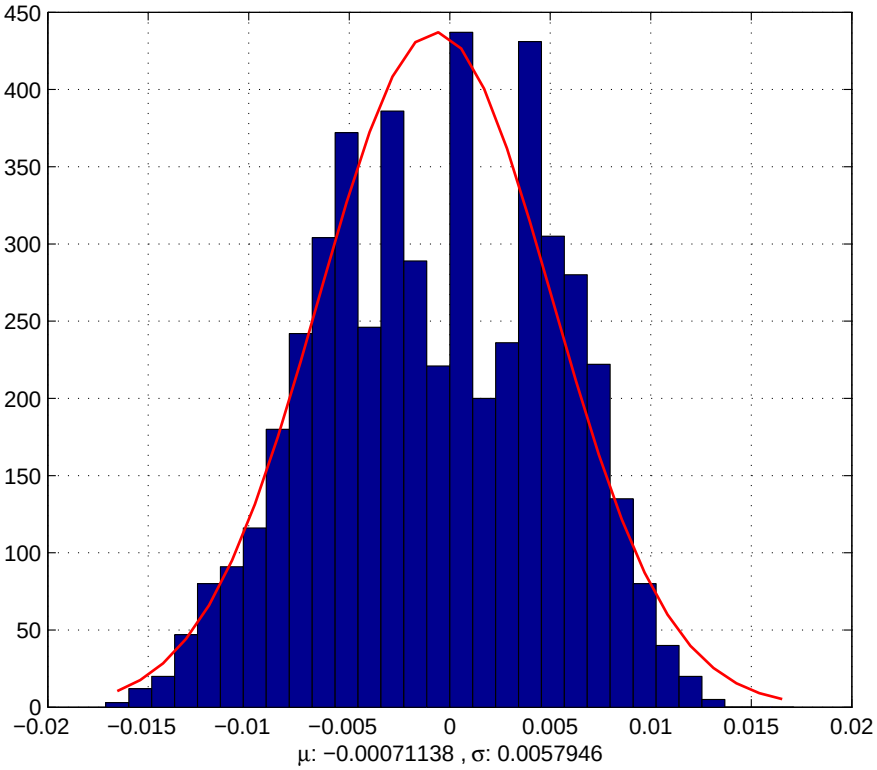

Figure 5.4: Histogram of q of correct integer estimate, data from 8 satellites in 969 epoches.

Earth's surface and a set of new Navigation Signals, including Civilian L2 (L2C), New Civilian L1 (L1C), the new "Safety of life" signal at L5, and the new Military code (M-code).

Of all the modernization progress, the one that has biggest effect on integer ambiguity resolution is the broadcasting of L5 signal. Users can incorporate the new "Safety of Life" signal broadcast on the L5 (1176.45 MHz) with the traditional L1 and L2 measurements, which will enable us with more linear combination of measurements at different frequencies. In this chapter, we will focus on the beneficial of incorporation of L5 to the resolution of integer ambiguity problem.

5.3.2 Linear Combination of GPS Code and Phase Measurements from Three Frequencies

In this section, we consider the linear combination from all the 3 frequencies.

We rewrite the differential code and phase measurements described in Eqns. (2.7) and (2.8) in L5 as:

$$\Delta\rho_{L5}^{(i)} = R^{(i)} + c\delta\bar{t}_r + \bar{\epsilon}_{L5}^{(i)}, \tag{5.19}$$

$$\lambda_1\Delta\phi_{L5}^{(i)} = R^{(i)} + c\delta\bar{t}_r + \lambda N_{L1}^{(i)} + \bar{\eta}_{L5}^{(i)}, \tag{5.20}$$

where $\lambda_5 = \dfrac{c}{f_5} \approx 25.5cm.$

By doing linear combination of measurements in L5 with measurements in L1 and L2 (as defined in Eqns. (2.51) - (2.54)), new measurements are available as:

$$\Delta\rho_{\alpha,\beta,\gamma}^{(i)} = \lambda_{\alpha,\beta,\gamma}\left(\alpha\frac{\Delta\rho_{L1}^{(i)}}{\lambda_1} + \beta\frac{\Delta\rho_{L2}^{(i)}}{\lambda_2} + \gamma\frac{\Delta\rho_{L3}^{(i)}}{\lambda_5}\right), \tag{5.21}$$

$$\lambda_{\alpha,\beta,\gamma}\Delta\phi_{\alpha,\beta,\gamma}^{(i)} = \lambda_{\alpha,\beta,\gamma}\left(\alpha\Delta\phi_{L1}^{(i)} + \beta\Delta\phi_{L2}^{(i)} + \gamma\Delta\phi_{L5}^{(i)}\right). \tag{5.22}$$

The measurements can be modeled as:

$$\begin{aligned}
\Delta\rho^{(i)}_{\alpha,\beta,\gamma} &= \lambda_{\alpha,\beta,\gamma}\left(\frac{\alpha}{\lambda_1}+\frac{\beta}{\lambda_2}+\frac{\gamma}{\lambda_5}\right)\left(R^{(i)}+c\delta t_r\right) \\
&\quad +\lambda_{\alpha,\beta}\left(\alpha\frac{\epsilon^{(i)}_1}{\lambda_1}+\beta\frac{\epsilon^{(i)}_2}{\lambda_2}+\gamma\frac{\epsilon^{(i)}_5}{\lambda_5}\right) \qquad (5.23)\\
\lambda_{\alpha,\beta,\gamma}\Delta\phi^{(i)}_{\alpha,\beta,\gamma} &= \lambda_{\alpha,\beta,\gamma}\left(\frac{\alpha}{\lambda_1}+\frac{\beta}{\lambda_2}+\frac{\gamma}{\lambda_5}\right)\left(R^{(i)}+c\delta t_r\right)+\lambda_{\alpha,\beta,\gamma}\left(\alpha N^{(i)}_{L1}+\beta N^{(i)}_{L2}+\gamma N^{(i)}_{L5}\right) \\
&\quad +\lambda_{\alpha,\beta,\gamma}\left(\alpha\frac{\eta^{(i)}_1}{\lambda_1}+\beta\frac{\eta^{(i)}_2}{\lambda_2}+\gamma\frac{\eta^{(i)}_5}{\lambda_5}\right) \qquad (5.24)
\end{aligned}$$

To preserve the unit scale factor for $R^{(i)}$, the wavelength $\lambda_{\alpha,\beta,\gamma}$ is defined as

$$\lambda_{\alpha,\beta,\gamma}=\frac{\lambda_1\lambda_2\lambda_5}{\alpha\lambda_2\lambda_5+\beta\lambda_1\lambda_5+\gamma\lambda_1\lambda_2}=\frac{c}{\alpha f_1+\beta f_2+\gamma f_5} \qquad (5.25)$$

and the covariance deviation of the receiver noise for code and phase measurements are

$$\begin{aligned}
\sigma^2_{\rho^{(i)}_{\alpha,\beta,\gamma}} &= \lambda^2_{\alpha,\beta,\gamma}\left(\frac{\alpha^2\cdot\sigma^2_\rho}{\lambda^2_1}+\frac{\beta^2\cdot\sigma^2_\rho}{\lambda^2_2}+\frac{\gamma^2\cdot\sigma^2_\rho}{\lambda^2_5}\right) \\
&= \frac{\alpha^2\lambda^2_2\lambda^2_5+\beta^2\lambda^2_1\lambda^2_5+\gamma^2\lambda^2_1\lambda^2_2}{(\alpha\lambda_2\lambda_5+\beta\lambda_1\lambda_5+\gamma\lambda_1\lambda_2)^2}\cdot\sigma^2_\rho, \qquad (5.26)\\
\sigma^2_{\Phi^{(i)}_{\alpha,\beta,\gamma}} &= \frac{\alpha^2\lambda^2_2\lambda^2_5+\beta^2\lambda^2_1\lambda^2_5+\gamma^2\lambda^2_1\lambda^2_2}{(\alpha\lambda_2\lambda_5+\beta\lambda_1\lambda_5+\gamma\lambda_1\lambda_2)^2}\cdot\sigma^2_{\Phi^{(i)}}. \qquad (5.27)
\end{aligned}$$

Assuming that the code and phase measurement standard deviation of L5 are the same as L1 and L2 measurements (at $1m$ and $0.02m$, separately), then the wavelength, standard deviation of code and phase measurement noise are listed in Table 5.3.2.

5.3.3 Comparing Code and Phase Measurements From Triple Frequency Measurements

From Table 5.3.2, we can see that by incorporating the measurement in L5, better indicators can be obtained by comparing code and phase measurement. For example, $\Delta\rho^{(i)}_{1,1,1}$

Table 5.2: Wavelength and noise standard deviation of measurements from linear combination of measurements from different frequencies

f_1	f_2	f_5	λ	σ_ρ	σ_ϕ
1	1		0.107 m	0.713 m	0.014 m
1	-1		0.862 m	5.742 m	0.115 m
1		1	0.109 m	0.715 m	0.014 m
1		-1	0.751 m	4.928 m	0.099 m
	1	1	0.125 m	0.707 m	0.141 m
	1	-1	5.861 m	33.24 m	0.665 m
1	1	1	0.075 m	0.583 m	0.016 m
-1	1	1	0.362 m	2.797 m	0.056 m
1	-1	1	0.197 m	1.521 m	0.030 m
1	1	-1	0.184 m	1.425 m	0.029 m

has the noise standard deviation of only $0.583m$, and $\Delta\phi^{(i)}_{0,1,-1}$ has the wavelength of $5.861m$.

Comparing this two ranges we can have the float estimate of the integer $N^{(i)}_{0,1,-1}$ be

$$\begin{aligned}
\bar{N^i}_{0,1,-1} &= \frac{\Delta\rho^{(i)}_{1,1,1} - \Delta\phi^{(i)}_{0,1,-1}}{\lambda_{0,1,-1}} \\
&= N^{(i)}_{0,1,-1} - \left(N^{(i)}_{0,1,-1} + \frac{\bar{\epsilon}^{(i)}_{1,1,1} - \bar{\eta}^{(i)}_{0,1,-1}}{\lambda_{0,1,-1}} \right) \\
&= N^{(i)}_{0,1,-1} - \frac{\bar{\epsilon}^{(i)}_{1,1,1} - \bar{\eta}^{(i)}_{0,1,-1}}{\lambda_{0,1,-1}}.
\end{aligned} \tag{5.28}$$

Given an estimate of the integer $\hat{N}^{(i)}_{0,1,-1}$, the residual can be formed as

$$\tilde{N}^{(i)}_{0,1,-1} = \hat{N}^{(i)}_{0,1,-1} - \bar{N}^{(i)}_{0,1,-1}. \tag{5.29}$$

The mean and covariance of $\tilde{N}^{(i)}_{0,1,-1}$ are:

$$\mu_{\tilde{N}^{(i)}_{0,1,-1}} = \delta N^{(i)}_{0,1,-1}\ cycle, \tag{5.30}$$

$$\begin{aligned}\sigma^2_{\tilde{N}^{(i)}_{0,1,-1}} &= [\frac{1}{5.861\ m}, -\frac{1}{5.861\ m}] \begin{bmatrix} (0.583m)^2 & 0 \\ 0 & (0.665m)^2 \end{bmatrix} \begin{bmatrix} \frac{1}{5.861\ m} \\ -\frac{1}{5.861\ m} \end{bmatrix} \\ &= 0.0228\ cycle^2. \end{aligned} \tag{5.31}$$

Therefore, the standard deviation of $\tilde{N}^{(i)}_{0,1,-1}$ is only 0.1509 *cycle*. If we choose $\tau_{0,1,-1} = 0.45\ cycle(3 \times \sigma_{\tilde{N}^{(i)}_{0,1,-1}})$ and the criteria to be:

$$\left.\begin{aligned} |\tilde{N}^{(i)}_{0,1,-1}| \leq \tau_{0,1,-1} \rightarrow \hat{N}^{(i)}_{0,1,-1} \text{ is correct,} \\ |\tilde{N}^{(i)}_{0,1,-1}| > \tau_{0,1,-1} \rightarrow \hat{N}^{(i)}_{0,1,-1} \text{ is incorrect,} \end{aligned}\right\} \tag{5.32}$$

then we will be able to catch error in $\hat{N}^{(i)}_{0,1,-1}$ with the chance of miss detection and false alarm both less than 1%, and an error in $\bar{N}^{(i)}_{0,1,-1}$ indicates integer estimate error in either L2 or L5.

5.3.4 Comparing Phase Measurements from Triple Frequency Measurements

Following the discussion in Section 5.2.3 and given the L5 phase measurement in Eqn. (5.19) and the integer estimate for L5 be $\hat{N}^{(i)}_{L5}$, the predicted ranges are

$$\begin{aligned}\hat{R}^{(i)}_{L5} &= \lambda_5 \Delta\phi^{(i)}_{L5} - \lambda_5 \hat{N}^{(i)}_{L5} \\ &= R^{(i)} + c\delta\bar{t}_r - \lambda_1 \delta N^{(i)}_{L5} + \bar{\eta}^{(i)}_{L5}. \end{aligned} \tag{5.33}$$

Residuals can be computed from calculated predicted ranges in L1, L2 and L5.

$$\begin{aligned}
\mathbf{r} &= \begin{bmatrix} r_{12} \\ r_{15} \\ r_{25} \end{bmatrix} = \begin{bmatrix} \hat{R}_{L1}^{(i)} - \hat{R}_{L2}^{(i)} \\ \hat{R}_{L1}^{(i)} - \hat{R}_{L5}^{(i)} \\ \hat{R}_{L2}^{(i)} - \hat{R}_{L5}^{(i)} \end{bmatrix} \\
&= \begin{bmatrix} \lambda_1 \delta N_1 - \lambda_2 \delta N_2 + \bar{\eta}_{L1}^{(i)} - \bar{\eta}_{L2}^{(i)} \\ \lambda_1 \delta N_1 - \lambda_5 \delta N_5 + \bar{\eta}_{L1}^{(i)} - \bar{\eta}_{L5}^{(i)} \\ \lambda_2 \delta N_2 - \lambda_5 \delta N_5 + \bar{\eta}_{L2}^{(i)} - \bar{\eta}_{L5}^{(i)} \end{bmatrix}. \qquad (5.34)
\end{aligned}$$

The mean and covariance of $\mathbf{r}$ are:

$$\mu_{\mathbf{r}} = \begin{bmatrix} res_{12} \\ res_{15} \\ res_{25} \end{bmatrix} = \begin{bmatrix} \lambda_1 \delta N_1 - \lambda_2 \delta N_2 \\ \lambda_1 \delta N_1 - \lambda_5 \delta N_5 \\ \lambda_2 \delta N_2 - \lambda_5 \delta N_5 \end{bmatrix} meter, \qquad (5.35)$$

$$\begin{aligned}
\sigma_{\mathbf{r}}^2 &= \begin{bmatrix} 1 & -1 & 0 \\ 1 & 0 & -1 \\ 0 & 1 & -1 \end{bmatrix} \begin{bmatrix} (0.02m)^2 & 0 & 0 \\ 0 & (0.02m)^2 & 0 \\ 0 & 0 & (0.02m)^2 \end{bmatrix} \begin{bmatrix} 1 & -1 & 0 \\ 1 & 0 & -1 \\ 0 & 1 & -1 \end{bmatrix}^{\top} \\
&= \begin{bmatrix} 0.0008 & 0.0004 & 0.0004 \\ 0.0004 & 0.0008 & 0.0004 \\ 0.0004 & 0.0004 & 0.0008 \end{bmatrix} meter^2. \qquad (5.36)
\end{aligned}$$

The three components of $\mathbf{r}$ can be visualized as the distances of an integer point $z = [\delta N_1, \ \delta N_2, \ \delta N_5]^{\top}$ in the 3-D space of L1-L2-L5 to three hyper planes;

$$\lambda_1 \delta N_1 = \lambda_2 \delta N_2 \qquad (5.37)$$

$$\lambda_1 \delta N_1 = \lambda_5 \delta N_5 \qquad (5.38)$$

$$\lambda_2 \delta N_2 = \lambda_5 \delta N_5 \qquad (5.39)$$

A test such as

$$\left.\begin{array}{l} \|\mathbf{r}\|_\infty \leq \tau \rightarrow \left(\hat{N}_1 \text{ and } \hat{N}_2 \text{ and } \hat{N}_5\right) \text{ are correct,} \\ \|\mathbf{r}\|_\infty > \tau \rightarrow \left(\hat{N}_1 \text{ or } \hat{N}_2 \text{ or } \hat{N}_5\right) \text{ is incorrect.} \end{array}\right\} \tag{5.40}$$

We can draw the 95% uncertainty ellipsoid around each integer point. The projection of each corresponding hyperplane, the region satisfies $\|\mathbf{r}\|_\infty \leq \tau$ (if we choose $\tau = 0.015$) and the integer points with the 95% uncertainty ellipsoid on the plane of L1-L2, L1-L5 and L2-L5 are shown in Fig. 5.5, Fig. 5.6 and Fig. 5.7, respectively.

We should note that, an integer points will pass the test if and only if the uncertainty ellipse falls into the region between two green dash lines in all the three figures. Here, we only With $\tau = 0.015$, none incorrect integers will pass the test with probability greater than 5%. Further calculation indicates that of all the incorrect integer points that can pass the test with a chance greater than 1%, the closest ones to the origin are $\delta N = [4,\ 3,\ 3]$ and $\delta N = [-4,\ -3,\ -3]$, both of which (and any incorrect integers further to the origin than them) could be easily detected by comparing phase range with code range, as discussed in Section 5.3.3.

Therefore, with this criteria, the rate of false alarm is less than 5%, and the rate of missed detection is less than 1%, detailed analysis will also been shown in [3].

We should note that, an integer points will pass the test if and only if the uncertainty ellipse falls into the region between two green dash lines in all the three figures. Here, we only With $\tau = 0.015$, none incorrect integers will pass the test with probability greater than 5%. Further calculation indicates that of all the incorrect integer points that can pass the test with a chance greater than 1%, the closest ones to the origin are $\delta N = [4,\ 3,\ 3]$ and $\delta N = [-4,\ -3,\ -3]$, both of which (and any incorrect integers further to the origin than

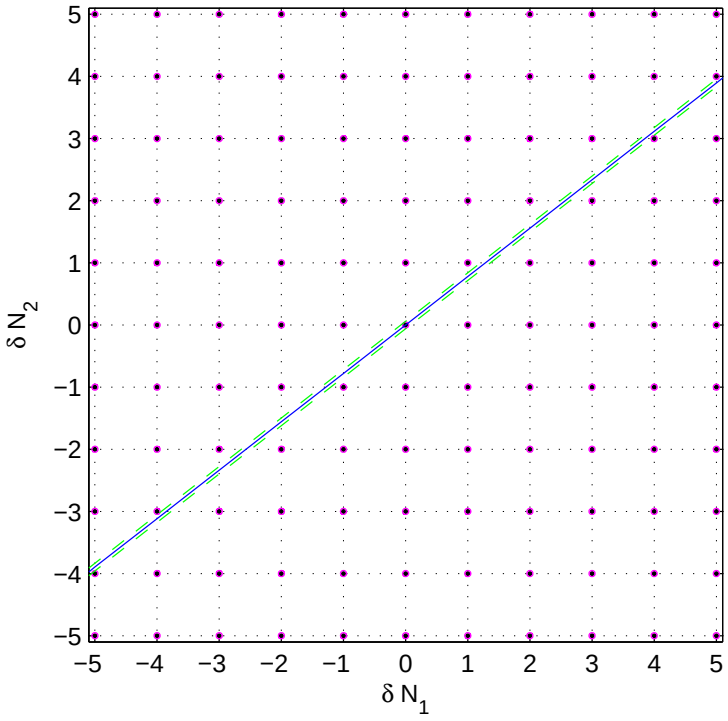

Figure 5.5: Depiction of the projection on plane L1-L2 of the integer vectors, the sections of the 95% percent ellipsoid and region of acceptance (between two green dash lines) in Eqn. (5.40) with $\tau = 0.015$.

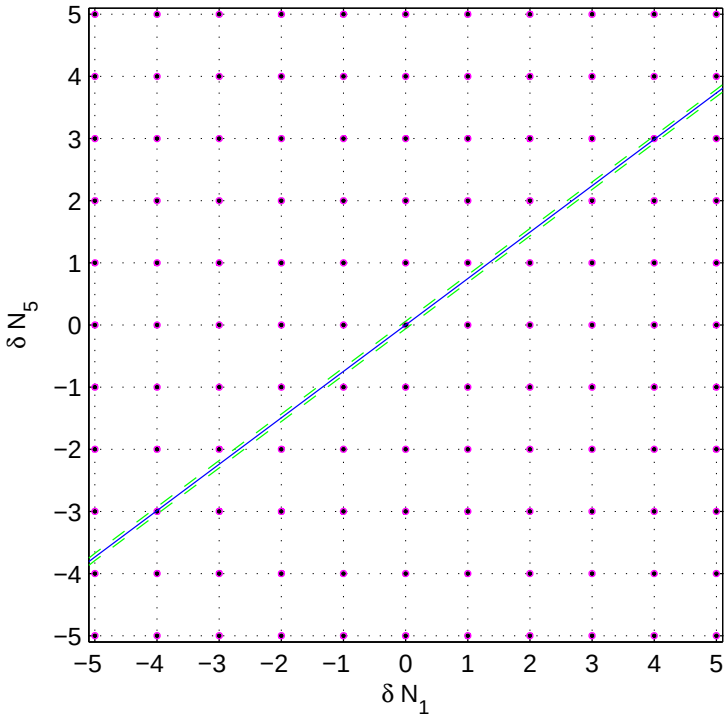

Figure 5.6: Depiction of the projection on plane L1-L5 of the integer vectors, the sections of the 95% percent ellipsoid and region of acceptance (between two green dash lines) in Eqn. (5.40) with $\tau = 0.015$.

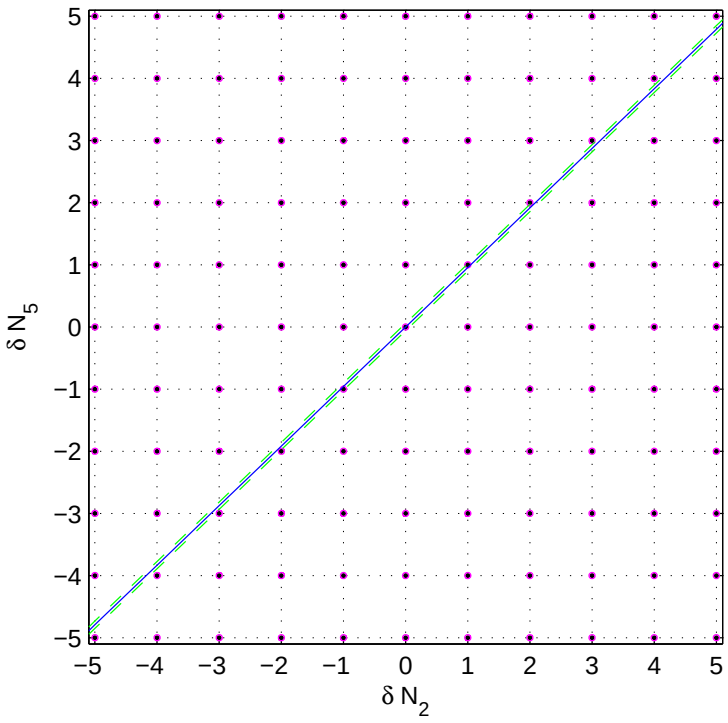

Figure 5.7: Depiction of the projection on plane L2-L5 of the integer vectors, the sections of the 95% percent ellipsoid and region of acceptance (between two green dash lines) in Eqn. (5.40) with $\tau = 0.015$.

them) could be easily detected by comparing phase range with code range, as discussed in Section 5.3.3.

Therefore, with this criteria, the rate of false alarm is less than 5%, and the rate of missed detection is less than 1%, detailed analysis will also been shown in [3].

5.4 Validation the Whole Integer Vector

The other category of integer validation validates the whole integer vector together which attracted much more research interest in the past decades. Varieties of methods have been proposed [40]. For most of the methods, the integers from all satellites are validated as a whole vector, and are accepted or refused based on certain criteria.

In [19], the integer validation is visualized by presenting the integer parameter as lattice, and the validation requires computing the integral of a Gaussian probability density function over the Voronoi cell, which is very computationally intensive. Similar discussions are given in [38, 40]. Despite all these theoretical contributions, integer validation is still an open theoretical problem as none of the available algorithms are based on the correct estimate distribution assumption or theoretical criteria [40].

However, there are some widely used tests for integer validation with satisfying performance. The well-working test criteria include Q-test [29], F-ratio test [10] and W-ratio test [41].

In this section, we will have some analytical discussion about these criteria, and present the test criteria used in our GPS/INS system.

5.4.1 Q-Test

Q-test is one of the most classical methods to decide the acceptance of integer estimates [29], the criteria for both methods are depended on the whole estimation residual vector.

Referring to Eqn. (2.13), the measurement from all the satellites can be stack up as

$$\lambda\delta\Delta\boldsymbol{\phi} \;=\; \mathbf{H}\mathbf{x} + \lambda\mathbf{N} + \bar{\boldsymbol{\eta}}$$

where $\mathbf{H}$ and $\mathbf{x}$ are also defined in the paragraph after Eqn. (2.13). As the measurements were equally weighted in traditional Q-test, the state estimate is given as

$$\hat{\mathbf{x}} = \left(\mathbf{H}^T\mathbf{H}\right)^{-1}\mathbf{H}^T\left(\delta\Delta\boldsymbol{\phi} - \lambda\hat{\mathbf{N}}\right).$$

Assume $\hat{\mathbf{N}} = \mathbf{N} + \delta\mathbf{N}$, the residual is formed as

$$\begin{aligned}
r &= \lambda\delta\Delta\boldsymbol{\phi} - \lambda\hat{\mathbf{N}} - \mathbf{H}\hat{\mathbf{x}} \\
&= \lambda\delta\Delta\boldsymbol{\phi} - \lambda\hat{\mathbf{N}} - \mathbf{H}\left(\mathbf{H}^T\mathbf{H}\right)^{-1}\mathbf{H}^T\left(\lambda\delta\Delta\boldsymbol{\phi} - \lambda\hat{\mathbf{N}}\right) \\
&= \left(\mathbf{H}\mathbf{x} + \lambda\mathbf{N} + \boldsymbol{\eta}\right) - \mathbf{H}\left(\mathbf{H}^T\mathbf{H}\right)^{-1}\mathbf{H}^T\left(\mathbf{H}\mathbf{x} + \lambda\mathbf{N} + \bar{\boldsymbol{\eta}} - \lambda\left(\mathbf{N} + \delta\mathbf{N}\right)\right) - \lambda\left(\mathbf{N} + \delta\mathbf{N}\right) \\
&= \left(\mathbf{I} - \mathbf{H}\left(\mathbf{H}^T\mathbf{H}\right)^{-1}\mathbf{H}^T\right)\left(\bar{\boldsymbol{\eta}} - \lambda\delta\mathbf{N}\right) \\
&= \mathbf{Q}\left(\bar{\boldsymbol{\eta}} - \lambda\delta\mathbf{N}\right),
\end{aligned}$$

where

$$\mathbf{Q} = \mathbf{I} - \mathbf{P},$$

$$\mathbf{P} = \mathbf{H}\left(\mathbf{H}^T\mathbf{H}\right)^{-1}\mathbf{H}^T.$$

Both $\mathbf{P}$ and $\mathbf{Q}$ are symmetric and idempotent.

Therefore, residual $r \sim \mathcal{N}\left(-\lambda\mathbf{Q}\delta\mathbf{N}, \mathbf{Q}\sigma^2\right)$ can be used to detect $\delta\mathbf{N}$, if $\delta\mathbf{N} \notin Null(\mathbf{Q})$.

Let the singular value decomposition of $\mathbf{H}$ be $\mathbf{H} = \mathbf{U}\bar{\mathbf{\Sigma}}\mathbf{V}^T$, as $\mathbf{H} \in \mathbb{R}^{K\times 4}$, $\bar{\mathbf{\Sigma}} = \begin{bmatrix} \mathbf{\Sigma} \\ \mathbf{0} \end{bmatrix}$, where $\mathbf{\Sigma} \in \mathbb{R}^{4\times 4}$ is a diagonal matrix and $\mathbf{0} \in \mathbb{R}^{(K-4)\times 4}$. $\mathbf{U} = \begin{bmatrix} \mathbf{U}_1 & \mathbf{U}_2 \end{bmatrix}$, where $\mathbf{U}_1 \in \mathbb{R}^{K\times 4}$ is a diagonal matrix and $\mathbf{U}_2 \in \mathbb{R}^{K\times(K-4)}$.

$$\begin{aligned}
\mathbf{P} &= \mathbf{H}\left(\mathbf{H}^T\mathbf{H}\right)^{-1}\mathbf{H}^T \\
&= \mathbf{U}\bar{\mathbf{\Sigma}}\mathbf{V}^T\left(\mathbf{V}\bar{\mathbf{\Sigma}}^T\mathbf{U}^T\mathbf{U}\bar{\mathbf{\Sigma}}\mathbf{V}^T\right)^{-1}\mathbf{V}\bar{\mathbf{\Sigma}}\mathbf{U}^T \\
&= \mathbf{U}\bar{\mathbf{\Sigma}}\mathbf{V}^T\left(\mathbf{V}\mathbf{\Sigma}^2\mathbf{V}^T\right)^{-1}\mathbf{V}\bar{\mathbf{\Sigma}}^T\mathbf{U}^T \\
&= \mathbf{U}_1\mathbf{\Sigma}\mathbf{V}^T\left(\mathbf{V}\mathbf{\Sigma}^{-2}\mathbf{V}^T\right)\mathbf{V}\mathbf{\Sigma}^T\mathbf{U}_1^T \\
&= \mathbf{U}_1\mathbf{U}_1^T \qquad (5.41)
\end{aligned}$$

As $\mathbf{I} = \mathbf{U}\mathbf{U}^T = \begin{bmatrix} \mathbf{U}_1 & \mathbf{U}_2 \end{bmatrix}\begin{bmatrix} \mathbf{U}_1^T \\ \mathbf{U}_2^T \end{bmatrix} = \mathbf{U}_1\mathbf{U}_1^T + \mathbf{U}_2\mathbf{U}_2^T$,

$$\mathbf{Q} = \mathbf{I} - \mathbf{P} = \mathbf{U}_2\mathbf{U}_2^T \qquad (5.42)$$

Therefore, $r \sim \mathcal{N}\left(-\lambda\mathbf{U}_2\mathbf{U}_2^T\delta\mathbf{N}, \mathbf{U}_2\mathbf{U}_2^T\sigma^2\right)$. Given the residual r, the integer errors for which $\mathbf{U}_2^T\delta\mathbf{N}$ are small will be difficult to detect. As $\mathbf{U}_1$ and $\mathbf{U}_2$ are orthogonal, these integer errors will be within the column space of $\mathbf{U}_1$.

In Q-test, the testing criteria is

$$\left.\begin{aligned}
&\|r^\top\mathbf{r}\| \le \tau \rightarrow \hat{\mathbf{N}} \text{ is correct,} \\
&\|r^\top\mathbf{r}\| > \tau \rightarrow \hat{\mathbf{N}} \text{ is incorrect.}
\end{aligned}\right\}$$

From above discussion, the integer errors that are not in the column space of $\mathbf{U}_1$ would be easily detected, but not the errors in the column space of $\mathbf{U}_1$. The matrix $\mathbf{U}_1$ is determined by satellite-user geometry and can be evaluated.

If we consider the weighting factor over satellites, the quantity we would use to determine estimate acceptance would be identical to the value of cost function $c(\mathbf{N})$, as defined in Eqn. (2.25). From the analysis in Chapter 2, the value of $c(\mathbf{N})$ follows χ^2 distribution with correct integer estimate.

5.4.2 Ratio-test

Ratio-test is another widely used testing criteria to decide the acceptance of integer estimate [29].

In ratio-test, the value of minimum cost $c(\mathbf{N})$ and second minimum cost $c(\mathbf{N})$ from all integer vector candidates are compared. The integer vector with minimum $c(\mathbf{N})$ will be accepted if the ratio κ over these two costs is smaller than some threshold. For a very long time, it has been used with satisfying performance without much theoretical discussion until recently when some underlying principles of this test were presented in [32].

5.4.3 Leave-One-Out Cross Validation and RANSAC

In another group of test criteria, part of the measurements are evaluated from the other part. Leave-one-out cross validation and RANSAC are two of the popular algorithms in this category and can be applied to GPS integer validation problem. In these tests, the measurements are put into two groups, primary group and secondary group, denoted as $\delta\Delta\boldsymbol{\phi} = \begin{bmatrix} \delta\Delta\boldsymbol{\phi}_p^T & \delta\Delta\boldsymbol{\phi}_s^T \end{bmatrix}^T$, where $\delta\Delta\boldsymbol{\phi}_s \in \mathbb{R}^M$ and $\delta\Delta\boldsymbol{\phi}_p \in \mathbb{R}^{(K-M)}$, $M \geq 4$. In leave-one-out cross validation, $M = K - 1$; and in RANSAC, $M = 4$.

Let the corresponding part of $\mathbf{H}$ for these two groups be $\mathbf{H}_p$ and $\mathbf{H}_s$, and the integer estimate being $\hat{\mathbf{N}}_p$ and $\hat{\mathbf{N}}_s$. The state estimate from the primary group of measurements

be

$$\hat{\mathbf{x}}_p = \left(\mathbf{H}_p^T \mathbf{H}_p\right)^{-1} \mathbf{H}_p^T \left(\delta\Delta\boldsymbol{\phi}_p - \lambda\hat{\mathbf{N}}_p\right) \tag{5.43}$$

Let $\hat{\mathbf{N}}_p = \mathbf{N}_p + \delta\mathbf{N}_p$ $\hat{\mathbf{N}}_s = \mathbf{N}_s + \delta\mathbf{N}_s$, then the residual for the whole measurement vector is

$$\begin{aligned}
\begin{bmatrix} \mathbf{r}_p \\ \mathbf{r}_s \end{bmatrix} &= \begin{bmatrix} \lambda\delta\Delta\boldsymbol{\phi}_p \\ \lambda\delta\Delta\boldsymbol{\phi}_s \end{bmatrix} - \begin{bmatrix} \mathbf{H}_p \\ \mathbf{H}_s \end{bmatrix} \hat{\mathbf{x}}_p - \lambda \begin{bmatrix} \hat{\mathbf{N}}_p \\ \hat{\mathbf{N}}_s \end{bmatrix} \\
&= \begin{bmatrix} \lambda\delta\Delta\boldsymbol{\phi}_p \\ \lambda\delta\Delta\boldsymbol{\phi}_s \end{bmatrix} - \begin{bmatrix} \mathbf{H}_p \\ \mathbf{H}_s \end{bmatrix} \left(\mathbf{H}_p^T \mathbf{H}_p\right)^{-1} \mathbf{H}_p^T \left(\lambda\delta\Delta\boldsymbol{\phi}_p - \lambda\mathbf{N}_p - \lambda\delta\mathbf{N}_p\right) - \lambda \begin{bmatrix} \hat{\mathbf{N}}_p \\ \hat{\mathbf{N}}_s \end{bmatrix} \qquad (5.44) \\
&= \begin{bmatrix} \left(\mathbf{I} - \mathbf{H}_p \left(\mathbf{H}_p^T \mathbf{H}_p\right)^{-1} \mathbf{H}_p^T\right) \left(\bar{\boldsymbol{\eta}}_p - \lambda\delta\mathbf{N}_p\right) \\ \left(\bar{\boldsymbol{\eta}}_s - \lambda\delta\mathbf{N}_s\right) - \mathbf{H}_s \left(\mathbf{H}_p^T \mathbf{H}_p\right)^{-1} \mathbf{H}_p^T \left(\bar{\boldsymbol{\eta}}_p - \lambda\delta\mathbf{N}_p\right) \end{bmatrix} \qquad (5.45) \\
&= \begin{bmatrix} \left(\mathbf{I} - \mathbf{H}_p \left(\mathbf{H}_p^T \mathbf{H}_p\right)^{-1} \mathbf{H}_p^T\right) \left(\bar{\boldsymbol{\eta}}_p - \lambda\delta\mathbf{N}_p\right) \\ \begin{bmatrix} \mathbf{H}_s \left(\mathbf{H}_p^T \mathbf{H}_p\right)^{-1} \mathbf{H}_p^T & -\mathbf{I} \end{bmatrix} \begin{bmatrix} \lambda\delta\mathbf{N}_p - \bar{\boldsymbol{\eta}}_p \\ \lambda\delta\mathbf{N}_s - \bar{\boldsymbol{\eta}}_s \end{bmatrix} \end{bmatrix} \qquad (5.46)
\end{aligned}$$

Let the singular value decomposition of $\mathbf{H}_p$ be $\mathbf{H}_p = \mathbf{U}_p \bar{\boldsymbol{\Sigma}}_p \mathbf{V}_p^T$ and $\mathbf{H}_s = \mathbf{U}_s \bar{\boldsymbol{\Sigma}}_s \mathbf{V}_s^T$. As $\mathbf{H}_p \in \mathbb{R}^{M\times 4}$ and $M \geq 4$, $\bar{\boldsymbol{\Sigma}}_p = \begin{bmatrix} \boldsymbol{\Sigma}_p \\ \mathbf{0} \end{bmatrix}$, where $\boldsymbol{\Sigma}_p \in \mathbb{R}^{4\times 4}$ is a diagonal matrix and $\mathbf{0} \in \mathbb{R}^{(M-4)\times 4}$. $\mathbf{U} = \begin{bmatrix} \mathbf{U}_{1p} & \mathbf{U}_2 \end{bmatrix}$, where $\mathbf{U}_{1p} \in \mathbb{R}^{M\times 4}$ is a diagonal matrix and $\mathbf{U}_{2p} \in \mathbb{R}^{M\times(M-4)}$, which does not exist in RANSAC. Therefore,

$$\begin{bmatrix} \mathbf{r}_p \\ \mathbf{r}_s \end{bmatrix} = \begin{bmatrix} \left(\mathbf{I} - \mathbf{U}_{1p}\mathbf{U}_{1p}^T\right) \left(\bar{\boldsymbol{\eta}}_p - \lambda\delta\mathbf{N}_p\right) \\ \begin{bmatrix} \mathbf{H}_s \mathbf{V}_p^T \boldsymbol{\Sigma}_p \mathbf{U}_{1p}^T & -\mathbf{I} \end{bmatrix} \begin{bmatrix} \lambda\delta\mathbf{N}_p - \bar{\boldsymbol{\eta}}_p \\ \lambda\delta\mathbf{N}_s - \bar{\boldsymbol{\eta}}_s \end{bmatrix} \end{bmatrix}.$$

Similar to Q-test, certain estimation errors will not be detectable in either of these tests.

5.5 Chapter Summary

In this chapter, we discussed the GPS integer ambiguity validation problem. First, methods for validating single integer estimate were reviewed and analytically discussed. After that, we presented the effect of GPS modernization, specifically, the launch of L5 signals, to GPS integer ambiguity validation problem. After that, we discussed methods to validate the whole integer estimate vector.

Chapter 6

Conclusions and Future Works

6.1 Conclusions

6.1.1 Conclusions

GPS integer ambiguity resolution is the key challenge for centimeter level GPS positioning. It has been a widely research problem for the past several decades.

In this dissertation, we focuses on GPS integer ambiguity problem. In Chapter 2, we studied the integer ambiguity estimation problem, which was proposed as a Weighted-Integer-least-square problem. A brief overview of pervious work on integer ambiguity resolution was presented and an improved integer ambiguity resolution method is proposed. Simulations and real-word data are presented to demonstrate the effectiveness of the method.

in Chapters 3 and 4, we presented integer ambiguity algorithms with auxiliary measurements and algorithms with multiple epoch measurements, both of which are useful in GPS challenging areas. For both problems, the measurement models were studied and reformed so that the approached proposed in Chapter 2 can be applied to find the integer estimate.

Integer ambiguity validation problem was studied in Chapter 5. We first presented methods to validate each integer estimate separately. A brief overview was presented, and then analytic discussion and test results were presented. We also presented the effect of GPS modernization on integer validation. After that, we studied the methods to validate the whole estimated integer vector. Several popular validations methods were studied, and the method we use in our GPS/INS system were presented.

6.1.2 Publications Resulting from Ph.D. Study

Following is the list of publications resulting from my Ph.D. study.

- Anning Chen, Dongfang Zheng, Arvind Ramanandan, Jay A. Farrell, "GPS Integer Ambiguity Validation with GPS Modernization". Proceedings of the 24th International Technical Meeting of the Satellite Division of the Institute of Navigation (ION GNSS 2011), In press

- Anning Chen, Dongfang Zheng, Arvind Ramanandan, Jay A. Farrell, "Near Real Time Carrier Phase GPS Aided INS". Submitted to CDC 2011

- Anning Chen, Dongfang Zheng, Arvind Ramanandan, Jay A. Farrell, "INS Aided GPS Integer Ambiguity Resolution". Proceedings of 2011 IEEE Multi-Conference on Systems and Control (MSC 2011), In press

- Anning Chen, Arvind Ramanandan, Jay A. Farrell, "High-Precision Road Map Building for Vehicle Navigation: Nodal Approach". IEEE/ION PLANS 2010, May 2010, Indiana Wells, CA

- Anning Chen, Arvind Ramanandan, Jay A. Farrell, "Improved integer ambiguity resolution by combining LAMBDA and LMS". Proceedings of the 22nd International Technical Meeting of the Satellite Division of the Institute of Navigation (ION GNSS 2009), Sept, 2009, Savannah, GA

- Anh Vu, Arvind Ramanandan, Anning Chen Jay A. Farrell and Matthew Barth, "Real-Time Computer Vision/DGPS-Aided Inertial Navigation System for Lane-Level Vehicle Navigation". Submitted to IEEE Transactions on Intelligent Transportation Systems

- Arvind Ramanandan, Anning Chen and Jay A. Farrell, "Inertial Navigation Aiding by Stationary Updates". submitted to IEEE Transactions on Intelligent Transportation Systems

- Arvind Ramanandan, Anning Chen and Jay A. Farrell, "Observability Analysis of an Inertial Navigation System with Stationary Updates". American Control Conference, In press

- Arvind Ramanandan, Anning Chen and Jay A. Farrell, "Inertial "Detection of Stationarity in an Inertial Navigation System". Proceedings of the 23rd International Technical Meeting of the Satellite Division of the Institute of Navigation (ION GNSS 2010), Sept, 2010, Portland, OR

- Arvind Ramanandan, Anning Chen and Jay A. Farrell, "Performance and Observability Analysis of a Vision and CDGPS aided Inertial Navigation System". IEEE/ION PLANS2010, May 2010, Indiana Wells, CA

6.2 Future Works

6.2.1 Integer Ambiguity Resolution for Near-Real-Time GPS/INS System

Following the discussion in Chapter 4, GPS phase measurements from multiple epoches t_1 to t_M are used for additional information to estimate integer ambiguity, in which we use GPS measurement on multiple epoches to estimate the unchanged integer and the receiver positions on these times. However, in the by proposing the problem as in eqn. (4.2), we did not consider is the correlation between the vehicle position over time, while, in GPS/INS system, the INS maintain propagating the vehicle states (includes position). Near-real-time GPS/INS system would jointly estimate the GPS integer ambiguity and INS states during t_1 to t_M.

This research will be beneficial in two aspects. First, In GPS/INS system, the INS maintain propagating the vehicle states (includes position). From time t_1 to t_M, if we consider the initial INS estimate of the vehicle position and the correlation between position at two adjacent epoch, we will have M more measurements. Having more measurements will be beneficial to GPS integer ambiguity resolution. Second, When ambiguities in measurements are resolved at time $t = t_M$, we can update the states with measurement at time t_1 to t_{M-1} by maximizing the joint a-posteriori probability density, resulting in the Maximum-A-Posteriori (MAP) estimate of the states at t_1 through t_M. Since the states at time t_1 through t_M are correlated, we automatically obtain an improved estimate of the state for the whole time interval. In effect, we have used a measurement from the past to improve the state estimate.

6.2.2 GPS Integer Ambiguity Estimation and GPS Modernization

In Chapter 5, we discussed the effect of GPS Modernization on integer validation. In addition to that, GPS Modernization will also have significant effect on integer estimation. Increased signal power at the Earth surface will decrease the measurement noises, and will increase the chance of correct integer estimation. By incorporating the signals on L5, we will have linearly combined measurements with long wavelength (5.861 meters), which can potentially decrease integer searching space. The broadcasted signals on L5 also allow civilian users with better ionospheric error estimation, which will be beneficial to long baseline integer estimation resolution. Finally, by taking advantage of other GNSS (Global Navigation Satellite System) like GLONASS, Compass and Galileo, we will have more measurements to facilitate the integer ambiguity resolution, and this will be especially beneficial in urban canyon areas.

Bibliography

[1] Geoffey Blewitt. Carrier phase ambiguity resolution for the global positioning system applied to geodetic baseline up to 2000 km. *Journal of Geophysical Research*, 94(B8):10187 – 10203, August 1989.

[2] X.W. Chang, X. Yang, and T. Zhou. MLAMBDA: A modified method for integer least-squares estimation: Implementation aspects. Technical report, School of Computer Science, McGill University, 2005.

[3] Anning Chen, Dongfang Zheng, Arvind Ramanandan, and Jay A. Farrell. GPS integer ambiguity validation with GPS modernization. In *Proceedings of the 24nd International Technical Meeting of the Satellite Division of the Institute of Navigation (ION GNSS 2011), In press*, Portland, OR.

[4] Anning Chen, Dongfang Zheng, Arvind Ramanandan, and Jay A. Farrell. INS aided GPS integer ambiguity resolution. In *Proceedings of 2011 IEEE Multi-Conference on Systems and Control (MSC 2011), In press.*

[5] Anning Chen, Dongfang Zheng, Arvind Ramanandan, and Jay A. Farrell. Near-real-time GPS integer ambiguity resolution. In *Submitted to Proceedings of 50th IEEE Conference on Decision and Control (CDC 2011).*

[6] D. Chen and G. Lachapelle. A comparison of the FASF and least-squares search algorithms for on-the-fly ambiguity resolution. *IEEE Transactions on Control Systems Technology*, 42(2):371–390, June 1995.

[7] Jingrong Cheng. *Reliable Integrated Navigation for Highway Systems.* PhD thesis, University of California, Riverside, 2005.

[8] Jingrong Cheng, Jay A. Farrell, Lu Yu, and Elmer Thomas. Aided integer ambiguity resolution algorithm. In *Position Location and Navigation Symposium*, pages 740–745, Apr 2004.

[9] J. P. Collins and R. B. Langley. Possible weighting schemes for GPS carrier phase observations in the presence of multipath. Technical Report DAAH04-96-C-0086 / TCN 98151, Final contract report for the U.S. Army Corps of Engineers Topographic Engineering Center, March 1999.

[10] Charles C. Counselman and Richard I. Abbot. Method of resolving radio phase ambiguity in satellite orbit determination. *Journal of Geophysical Research*, 94:7058–7064, June 1989.

[11] Charles C. Counselman and Sergei A. Gourevitch. Miniature interferometer terminals for earth surveying: Ambiguity and multipath with global positioning system. *IEEE Transactions on Geoscience and Remote Sensing*, GE-19(4):244–252, Oct 1981.

[12] P. de Jonge and Christian Tiberius. LAMBDA method for integer ambiguity estimation: Implementation aspects. Technical Report 12, In Delft Geodetic Computing Center, 1996. LGR-Series.

[13] Jay A. Farell, Tony D. Givargis, and Matthew J. Barth. Real-time differential carrier phase GPS-aided INS. *IEEE Transactions on Control Systems Technology*, 8(4):709 – 721, July 2000.

[14] Jay A. Farrell. *Aided Navigation, GPS with High Rate Sensors*. McGraw-Hill, 2008.

[15] E. Frei and G. Beutler. Some considerations concerning an adaptive, optimized technique to resolve the initial phase ambiguities. In *Proceedings of the Fifth International Geodetic Symposium on Satellite Positioning*, Mar 1989.

[16] Yang Gao and Zuofa Li. Cycle slip detection and ambiguity resolution algorithms for dual-frequency GPS data processing. *Marine Geodesy*, 22(3):169–181, 1999.

[17] Jr. H. W. Lenstra. Integer programming with a fixed number of variables. *Mathematics of Operations Research*, 8(4):538–548, November 1983.

[18] Shaowei Han and Chris Rizos. Comparing GPS ambiguity resolution techniques. *GPS world*, 8(10):54–61, 1997.

[19] Arash Hassibi and Stephen Boyd. Integer parameter estimation in linear models with applications to GPS. *IEEE Transactions on Signal Proceeding*, 46(11):2938–2952, Nov 1998.

[20] Ron Hatch. Instantaneous ambiguity resolution. In *Kinematic Systems in Geodesy, Surveying and Remote Sensing, IAG Symposia 107*, pages 299–308, Sept 1990.

[21] Ron Hatch and Hans-Juergen Euler. Comparison of several AROF kinematic techniques. *Proceedings of ION*, GPS:363–370, 1994.

[22] P. Henkel, V. Gomez, and C. Günther. Modified LAMBDA for absolute carrier phase positioning in the presence of biases. In *Proceedings of the International Technical Meeting of The Institute of Navigation (ION ITM 2009)*, pages 644–651, Anaheim, CA, January 2009.

[23] P. Henkel and C. Günther. Reliable integer ambiguity resolution with multi-frequency code carrier linear combinations. In *Proceedings of the 23rd International Technical Meeting of the Satellite Division of The Institute of Navigation (ION GNSS 2010)*, pages 185–195, Portland, OR, September 2010.

[24] B. Hofmann-Wellenhof, H. Lichtenegger, and J. Collins. *Global Positioning System, Theory and Practice, 4th edition.* New York: Springer-Verlag, 1997.

[25] Patrick Y.C. Hwang and R.Grover Brown. GPS navigation: Combining pseudorange with continuous carrier phase using a Kalman filter. *Navigation: Journal of The Institute of Navigation*, 37(2):175–190, 1990.

[26] Donghyun Kim and Richard B. Langley. GPS ambiguity resolution and validation: Methodologies, trends and issues. In *Proceeding of the 7th GNSS WorkshopInternational Symposium on GPS/GNSS, Seoul, Korea*, 2000.

[27] H Landau and H. J. Euler. On-the-fly ambiguity resolution for precise differential positioning. In *Proceedings of the 5th International Technical Meeting of the Satellite Division of The Institute of Navigation (ION GPS 1992)*, pages 607 – 613, Albuquerque, NM, September 1992.

[28] A. K. Lenstra, Jr. H. W. Lenstra, and L. Lovasz. Factoring pollynomials with rational coefficients. *Mathematical Annals*, 261(4):515–534, December 1982.

[29] Pratap Misra and Per Enge. *Global Positioning System: Signals, Measurements, and Performance*. Ganga-Jamuna Press, 2001.

[30] M. Pratt, B. Burke, and P. Misra. Single-epoch integer ambiguity resolution with GPS L1-L2 carrier phase measurements. *Proceedings of ION*, GPS:1737–1746, 1997.

[31] Jan Skaloud. Readucing the gps ambiguity search space by including inertial data. In *Proceedings of the 11th International Technical Meeting of the Satellite Division of The Institute of Navigation (ION GNSS 1998)*, pages 2073–2080, September 1998.

[32] Peter J.G. Teunissen and Sandra Verhagen. On the foundation of the popular ratio test for gnss ambiguity resolution. In *Proceedings of the 17th International Technical Meeting of the Satellite Division of The Institute of Navigation (ION GNSS 2004)*, pages 2529 – 2540, September 2004.

[33] P.J.G. Teunissen. Least-squares estimation of the integer GPS ambiguity. In *Invited Lecture, Section IV Theory and Methodology. IAG General Meeting*, Aug 1993.

[34] P.J.G. Teunissen. A new method for fast carrier phase ambiguity estimation. In *Position Location and Navigation Symposium*, pages 562–573, Apr 1994.

[35] P.J.G. Teunissen. The least-squares ambiguity decorrelation adjustment: a method for fast GPS integer ambiguity estimation. *Journal of Geodesy*, 70:65–82, 1995.

[36] P.J.G. Teunissen. A canonical theory for short GPS baselines. *IEEE Transactions on Signal Proceeding*, 71(9):513–525, 1997.

[37] P.J.G. Teunissen. An optimal property of the integer least-squares estimator. *Journal of Geodesy*, 73:587–593, 1999.

[38] P.J.G Teunissen and Sandra Verhagen. Integer ambiguity validation: Still an open problem? In *Proceedings Space, Aeronautical and Navigational Electronics Symposium (SANE2007), the Institute of Electronics, Information and Communication Engineers (IEICE)*, volume 107, pages 1–6, April 2007.

[39] van Emde Boas P. Another NP-complete partition problem and the complexity of computing short vectors in a lattice. Technical report, Mathmatisch Instituut, Amsterdam, The Netherlands, 1981.

[40] Sandra Verhagen. Integer ambiguity validation: an open problem? *GPS Solutions*, 8(1):36–43, April 2004.

[41] J. Wang, M. P. Stewart, and M. Tsakiri. A discrimination test procedure for ambiguity resolution on-the-fly. *Journal of Geodesy*, 72(11):1432–1394, November 1998.

[42] Peiliang Xu. Random simulation and GPS decorrelation. *Journal of Geodesy*, 75:408–423, 2001.

[43] Yunchun Yang, Richard T. Sharpe, and Ronald R. Hatch. A fast ambiguity resolution technique for RTK embedded within a GPS receiver. In *Proceedings of ION GPS 2002*, pages 945–952, September 2002.